

HENDRIK LUUK

Distribution and
behavioral effects of WfsI protein
in the central nervous system

Department of Physiology, University of Tartu, Tartu, Estonia

Dissertation is accepted for the commencement of the degree of *doctor philosophiae* in Neuroscience on February 20, 2009, by the Council of the commencement of Doctoral Degree in Neuroscience

Supervisors: Sulev Kõks, MD, PhD, Professor, Department of Physiology,
University of Tartu

Eero Vasar, MD, PhD, Professor, Department of Physiology,
University of Tartu

Reviewers: Anti Kalda, MD, PhD, Senior Research Fellow,
Department of Pharmacology and Toxicology,
University of Tartu

Ursel Soomets, PhD, Senior Research Fellow,
Department of Biochemistry, Faculty of Medicine,
University of Tartu

Opponent: Matti S. Airaksinen, MD, PhD, Docent in Neurobiology,
Neuroscience Center, University of Helsinki, Finland

Commencement: April 28, 2009

This research was supported by the European Regional Development Fund

Publication of this dissertation is granted by the University of Tartu

ISSN 1736–2792

ISBN 978–9949–19–072–0 (trükis)

ISBN 978–9949–19–073–7 (PDF)

Autoriõigus Hendrik Luuk, 2009

Tartu Ülikooli Kirjastus

www.tyk.ee

Tellimuse nr. 58

CONTENTS

LIST OF ORIGINAL PUBLICATIONS	7
ABBREVIATIONS	8
INTRODUCTION	9
REVIEW OF LITERATURE	11
1. Wolfram syndrome	11
2. WFS1 gene and protein	13
3. Mutations in WFS1	16
4. Wfs1-deficient mice	18
AIMS OF THE STUDY	20
MATERIALS AND METHODS	21
1. Cat odor-induced fear response in rats (Study 1)	21
2. Generation of Wfs1-deficient mice harboring β -galactosidase transgene (Studies 2 and 3)	21
3. Animals	22
4. cDNA representational difference analysis (Study 1)	23
5. Production of Wfs1 antibodies (Study 2)	26
6. Histochemistry (Study 2)	27
7. Drugs (Study 3)	31
8. Behavioral studies (Study 3)	31
9. Measurements of metabolic and endocrine parameters (Study 3)	37
10. Statistical analyses (Studies 1 and 3)	38
RESULTS	39
1. Study 1: Wfs1 mRNA is upregulated in amygdaloid area of rats after cat odor-induced fear response	39
2. Study 2: Distribution of Wfs1 protein in the central nervous system of the mouse	44
2.1. Forebrain	48
2.2. Diencephalon	52
2.3. Midbrain and brainstem	54
2.4. Cerebellum	56
2.5. Spinal cord	56
2.6. Circumventricular organs	58
3. Study 3: The behavioral profile of Wfs1-deficient mice	58
3.1. Reproduction and overt appearance	58
3.2. Body weight and glucose tolerance test	59
3.3. Stress-induced changes in corticosterone levels	61
3.4. Stress-induced analgesia	61
3.5. Rota-rod test	62
3.6. Locomotor activity in dim and bright environments	62
3.7. Effect of amphetamine and apomorphine on locomotor activity	63

3.8. Effect of short-term isolation on exploratory activity in light-dark test	65
3.9. The effect of diazepam in elevated plus-maze	65
3.10. Fear conditioning test	67
3.12. Hyponeophagia test	68
3.13. Forced swimming test	68
3.14. Morris water maze test	68
3.15. Active avoidance test	70
DISCUSSION	71
1. Wfs1 mRNA is induced in amygdaloid area of rats after cat odor-induced fear response	71
2. Wfs1 protein expression is enriched in basal forebrain structures involved in the regulation of behavioral adaptation	72
2.1. Technical considerations	72
2.2. Relationship of Wfs1 expression to the Extended Amygdala concept	72
2.3. Relationship of Wfs1 immunoreactive nerve fibers to known projection pathways	73
2.4. Relationship of Wfs1 expression to Wolfram Syndrome	74
3. Wfs1-deficiency results in impaired behavioral adaptation in stressful environment	76
4. Concluding remarks and future prospects	80
CONCLUSIONS	83
REFERENCES	85
APPENDIX 1	95
APPENDIX 2	107
APPENDIX 3	109
SUMMARY IN ESTONIAN	111
ACKNOWLEDGEMENTS	116
ORIGINAL PUBLICATIONS	117

LIST OF ORIGINAL PUBLICATIONS

1. Kõks S, Planken A, **Luuk H**, Vasar E. 2002. Cat odor exposure increases the expression of wolframin gene in the amygdaloid area of rat. *Neuroscience Letters*, 322(2):116–20.
2. **Luuk H**, Kõks S, Plaas M, Hannibal J, Rehfeld JF, Vasar E. 2008. Distribution of Wfs1 protein in the central nervous system of the mouse and its relation to clinical symptoms of the Wolfram syndrome. *Journal of Comparative Neurology*, 509(6):642–60.
3. **Luuk H**, Plaas M, Raud S, Innos J, Sütt S, Lasner H, Abramov U, Kurrikoff K, Kõks S, Vasar E. 2008. Wfs1-deficient mice display impaired behavioural adaptation in stressful environment. *Behavioural Brain Research*, Nov 11. [Epub ahead of print].

Contribution of the author:

1. The author performed RT-PCR.
2. The author designed the study, cloned the targeting construct for making Wfs1-deficient Wfs1^{b^{gal}/b^{gal}} mice, established breeding and genotyping strategies, performed initial genotyping, performed histological staining and analysis, wrote the manuscript and handled correspondence.
3. The author cloned the targeting construct for making Wfs1-deficient Wfs1^{b^{gal}/b^{gal}} mice, established breeding and genotyping strategies, participated in designing the study, performed the analysis of vocalizations and reproduction rates, and participated in writing the manuscript.

ABBREVIATIONS

aa	– amino acid residues
CA1	– CA1 field of Ammon's horn
cDNA	– complementary DNA
CISD2	– CDGSH iron sulfur domain 2
CS	– conditioned stimulus
DI	– diabetes insipidus
DNA	– 2-desoxyribonucleic acid
ER	– endoplasmic reticulum
GABA	– gamma-aminobutyric acid
GLP-1	– glucagon-like peptide-1
GLP-2	– glucagon-like peptide-2
HL	– hearing loss
HPA	– hypothalamic-pituitary-adrenocortical
kb	– one thousand nucleotide bases or base pairs
LFSNHL	– low frequency sensoryneural hearing loss
mRNA	– messenger RNA
RNA	– ribonucleic acid
SER	– smooth endoplasmic reticulum
UPR	– unfolded protein response
US	– unconditioned stimulus
Wfs1	– Wolfram syndrome 1 gene or protein in any species other than human
WFS1	– Wolfram syndrome 1 gene or protein in human
Wfs1 ^{bgal/bgal}	– Wfs1-deficient mouse strain expressing truncated Wfs1 protein fused to β -galactosidase reporter enzyme
Wfs2	– Wolfram syndrome 2 locus in human
Wolframin	– Wfs1 protein
WS	– Wolfram syndrome

INTRODUCTION

Identification of environmental information critical for survival and procreation is crucial for forming appropriate behavioral responses. An important psychological aspect of this process is emotion perception – the appreciation of feelings of anxiety and fear in response to danger, sadness in response to failure or loss, and joy and pleasure in response to success and naturally reinforcing stimuli. Impaired or distorted perception of emotions is characteristic of almost all psychiatric disorders and is accompanied by reduced coping with everyday life. Impaired behavioral adaptation is not specific to people with psychiatric disorders only, it is a long-term consequence of stressful life events and genetic predispositions that can affect all species with complex nervous systems. Hence, studies of emotional behavior of laboratory animals have provided important clues to understanding the neurobiology of human psychopathology (Phillips *et al.*, 2003; Quirk and Beer, 2006). Additionally, a number of methods based on animal models are available to identify genes involved in diseases with complex etiology such as schizophrenia, anxiety disorders, epilepsy, autism etc (Leonardo and Hen, 2006; Sunkin and Hohmann, 2007). For example, a screen for genes influencing anxiety-related behavioral traits in inbred mouse strains has yielded several candidates (Hovatta *et al.*, 2005).

A popular ethological paradigm for studying fear-like behavior in rodents is based on the presentation of predatory odor (Takahashi *et al.*, 2005). In rats and, to a lesser extent, in mice the presentation of a cloth impregnated with cat odor induces freezing behavior, avoidance of the cloth and an increase in plasma corticosterone. Cat odor-induced fear in rodents is an innate response hard-wired in the brain circuitry and not readily influenced by learning. In the present study, cat odor-induced fear response was used to screen the amygdaloid area of rats for transcriptionally induced genes in relation to control rats.

One of the candidates identified in the present study as involved in cat odor-induced fear response was *Wfs1* gene which became the object of subsequent studies. There are a number of considerations from the viewpoint of nervous system function that make *Wfs1* gene and protein attractive objects of research. First, disruption of both alleles of *Wfs1* gene in humans causes a rare hereditary disorder called the Wolfram syndrome (Inoue *et al.*, 1998; Strom *et al.*, 1998; Wolfram and Wagener, 1938), which is accompanied by a variety of neurological and psychiatric symptoms (Barrett *et al.*, 1995; Swift *et al.*, 1991; Swift *et al.*, 1990). Secondly, the disruption of one allele of *Wfs1* gene confers markedly increased risk of hospitalization for psychiatric illness (Swift and Swift, 2005), and, independently, is the cause of hereditary low-frequency hearing loss in approximately half of the documented cases (Bespalova *et al.*, 2001; Lesperance *et al.*, 1995; Young *et al.*, 2001, Fukuoka *et al.*, 2007). Third, *Wfs1* has been implicated in fear and anxiety-related behaviors in rodents (Kesner *et al.*, 2007; Koks *et al.*, 2002) and its polymorphisms are possibly associated with increased risk for mood disorders (Koido *et al.*, 2005). Fourth, still very little is known about the distribution and functional implications of

Wfs1 protein in the central nervous system. The present study aims to provide at least partial answers to the aforementioned research questions and to establish directions for future studies.

REVIEW OF LITERATURE

I. Wolfram syndrome

Mutations in WFS1 gene on chromosome 4p16.1 are a major cause of Wolfram syndrome (WS, OMIM #222300), a rare autosomal recessive disorder characterized by early-onset non-autoimmune insulin-dependent diabetes mellitus and progressive optic atrophy (Inoue *et al.*, 1998; Khanim *et al.*, 2001; Strom *et al.*, 1998; Wolfram and Wagener, 1938). In the remaining Wolfram syndrome cases (approximately 10%), the disease has been linked to mutations in CISD2 gene (NM_001008388) residing in Wfs2 locus on chromosome 4q22–24 (Amr *et al.*, 2007; El-Shanti *et al.*, 2000). Probably not coincidentally, the proteins encoded by these genes are localized to endoplasmic reticulum and affect intracellular calcium homeostasis (Amr *et al.*, 2007; Takeda *et al.*, 2001; Takei *et al.*, 2006). The prevalence of WS has been estimated to be 1 in 770,000 in the UK, and 1 in 100,000 in a North American population (Barrett *et al.*, 1995; Fraser and Gunn, 1977). WS carrier frequency is 1 in 345 in the UK and around 1% in the US (Barrett *et al.*, 1995; Swift *et al.*, 1991). WS is also known under the acronym DIDMOAD (Diabetes Insipidus, Diabetes Mellitus, Optic Atrophy, and Deafness) due to high incidence of diabetes insipidus and hearing loss affecting primarily higher frequencies. However, the prevalence of diabetes insipidus and hearing loss appears variable across different populations of WS patients (Table 1). In a cross-population meta-analysis of 96 WS patients, both DI and HL were reported in approximately 56% of the cases (Cano *et al.*, 2007).

Table 1. The prevalence of diabetes insipidus (DI) and hearing loss (HL) in patients with Wolfram syndrome.

	DI% of WS patients	HL% of WS patients	Sample size	Population origin	Study
	71	61	46	UK	(Barrett <i>et al.</i> , 1995)
	78	55	9	Turkey	(Simsek <i>et al.</i> , 2003)
	43	71	7	Spain	(Domenech <i>et al.</i> , 2004)
	25	75	8	Denmark	(Hansen <i>et al.</i> , 2005)
	41	52	27	France	(Cano <i>et al.</i> , 2007)
Mean	52	63	97		

In general, WS patients display considerable clinical pleiomorphism with sensory-neural deafness, hypothalamic diabetes insipidus, neurological complications (cerebellar ataxia, myoclonus, epilepsy, nystagmus), renal tract abnor-

malities, gastrointestinal dysmotility, primary gonadal atrophy, psychiatric disorders, short stature, peptic ulcers, cataract and a number of other symptoms being documented (Bardo *et al.*, 2006; Barrett *et al.*, 1995; Cremers *et al.*, 1977; Hadidy *et al.*, 2004; Hansen *et al.*, 2005; Kinsley and Firth, 1992; Medlej *et al.*, 2004; Simsek *et al.*, 2003; Swift *et al.*, 1990). For example, Barrett *et al.* (1995) have reported such neurological symptoms as truncal/gait ataxia (characterized by unsteady gait and falls), areflexia of lower limbs, central apnoeas, cerebellar dysarthria, autonomic neuropathy etc. The median age of onset for insulin-deficient diabetes mellitus and optic atrophy is in the first and second decades, respectively (Barrett *et al.*, 1995; Cano *et al.*, 2007; Hansen *et al.*, 2005). Renal-tract abnormalities appear in the third decade followed by neurological complications in the fourth decade (Barrett *et al.*, 1995). The median age of death is 30 years, with the most common causes of mortality being neurological manifestations and the complications of urinary tract atony (Barrett *et al.*, 1995; Kinsley *et al.*, 1995). Selective loss of pancreatic β -cells has been documented in WS patients (Karasik *et al.*, 1989).

Neuropathological manifestations of WS (summarized in Table 2) include atrophy of the optic nerves, chiasm and tracts that is not secondary to retinal pathology, atrophy of the hypothalamic region (especially paraventricular and supraoptic nuclei) and posterior pituitary (neurohypophysis), and ponto-cerebellar and brain stem pathology. Post-mortem studies of single patients have revealed widespread axonal pathology (Shannon *et al.*, 1999), loss of neurons from the lateral geniculate nuclei (Genis *et al.*, 1997; Shannon *et al.*, 1999), atrophy of olfactory bulbs and tracts (Genis *et al.*, 1997), atrophy of corpus callosum and septum pellucidum (Kinsley and Firth, 1992), atrophy of the cochlear nerve, cochlear nuclei and inferior colliculus, and demyelination of the pyramidal tracts (Genis *et al.*, 1997). A recent study reported an almost complete absence of retinal ganglion cells, and inner and outer hair cells in the basal turn of the cochlea as likely reasons for blindness and high frequency hearing loss in a WS patient (Justin B. Hilson, personal communication). Psychiatric findings in Wolfram syndrome patients include progressive dementia, severe depression, attempted suicides, paranoid delusions, auditory or visual hallucinations, violent and assaultative behavior, learning disabilities, mental retardation, anorexia, and insomnia (Bretz *et al.*, 1970; Kellner *et al.*, 1994; Kinsley and Firth, 1992; Nanko *et al.*, 1992; Paley and Tunbridge, 1956; Rose *et al.*, 1966; Swift *et al.*, 1990). Swift *et al.* (1990) investigated the medical histories of 68 WS patients in the US and reported that 60% of them had experienced psychiatric manifestations. In several patients, antidepressants alone or in combination with antipsychotics were effective in controlling the symptoms. In some patients, benzodiazepines were used to decrease aggression.

Table 2. Neuropathologic manifestations of Wolfram syndrome

Pathology	Reported in studies
Atrophy of the optic nerves, chiasm and tracts	1, 3, 4, 10, 11, 12, 16
Atrophy of the hypothalamic region and/or posterior pituitary	2, 3, 4, 12, 15
pontocerebellar and/or brain stem pathology	1, 5, 6, 7, 8, 9, 10, 12, 13, 14, 15, 16
wide-spread axonal pathology	15
loss of neurons from the lateral geniculate nuclei	4, 15
Atrophy of corpus callosum and septum pellucidum	17
Atrophy of olfactory bulbs and tracts	4
loss of neurons in the cochlear nuclei and inferior colliculus	4
loss of fibers in the cochlear nerve	4
demyelination of the pyramidal tracts	4
1 – Barrett <i>et al.</i> (1997); 2 – Gabreels <i>et al.</i> (1998); 3 – Galluzzi <i>et al.</i> (1999); 4 – Genis <i>et al.</i> (1997); 5 – Hadidy <i>et al.</i> (2004); 6 – Hattori <i>et al.</i> (1998); 7 – Ito <i>et al.</i> (2007); 8 – Leiva-Santana <i>et al.</i> (1993); 9 – Mathis <i>et al.</i> (2007); 10 – Medlej <i>et al.</i> (2004); 11 – Mtanda <i>et al.</i> (1986); 12 – Pakdemirli <i>et al.</i> (2005); 13 – Saiz <i>et al.</i> (1995); 14 – Scolding <i>et al.</i> (1996); 15 – Shannon <i>et al.</i> (1999); 16 – Yang <i>et al.</i> (2005); 17 – Kinsley and Firth (1992)	

According to Swift *et al.* (1998) and Swift & Swift (2005), the prevalence of WFS1 mutation carriers (WS heterozygotes) is around 1% in the general population, and they have a 7-fold increased risk of hospitalization for psychiatric illness. In the latter study, 8 out of 11 individuals with a history of psychiatric hospitalization from a total of 25 WS families were heterozygous for WFS1 mutations. Notably, all eight mutation-positive subjects had been hospitalized for a major depression. WS carriers have also been reported with post-traumatic stress disorder, general anxiety disorder and suicide attempts (Swift *et al.*, 1998).

In summary, the frequent occurrence of primary neurodegeneration in WS patients, and the high prevalence of psychiatric disorders in WS patients and WS carriers suggests a marked role for WFS1 protein in the human brain function.

2. WFS1 gene and protein

In humans and mice, *Wfs1* gene (ENSG00000109501 – see Figure 1, and ENSMUSG00000039474, respectively) is located on chromosomes 4p16.1 and 5qB3, respectively. Interestingly, a number of hereditary diseases with neurological complications, and psychiatric disorders have been mapped to the 4p16 region in humans: Huntington's disease (HD, OMIM #143100; 4p16.3 – caused

by the accumulation of CAG repeats in the Huntingtin gene ENSG00000197386), low-frequency sensoryneural hearing loss (DFNA6, OMIM #600965; 4p16.1 – caused by mutations in WFS1 gene), autosomal dominant congenital stationary night blindness (CSNBAD2, OMIM #163500; 4p16.3), Wolf-Hirschhorn syndrome (WHS, OMIM #194190; 4p16.3), putative association of attention deficit-hyperactivity disorder (ADHD, OMIM #143465) with dopamine receptor 5 gene (Kustanovich *et al.*, 2004), bipolar disorder (Asherson *et al.*, 1998; Blackwood *et al.*, 1996; Christoforou *et al.*, 2007; Ewald *et al.*, 2002), a suggestive linkage of 4p16.1 with food-related obsessions in patients with eating disorders (Bacanu *et al.*, 2005), and schizophrenia (Asherson *et al.*, 1998; Christoforou *et al.*, 2007). WFS1 gene is composed of eight exons spanning approximately 30 kilobases (kb) of genomic DNA. WFS1 transcript (the messenger RNA) is approximately 3.6 kb long with the translation start-site located in the beginning of the second exon, and around 60% of the 2.6 kb of coding sequence is located in exon eight which is by far the largest exon (2.6 kb).

A characterization of WFS1 gene promoter has mapped the minimal promoter to the region -49 to +104 bp relative to the transcription start site (average reporter activity was 25% of the 2 kb full length promoter activity in two cell lines), and has identified a strong activating region between -49 and -233 bp (addition of the region to the minimal promoter resulted in approx. 210% of full-length promoter activity) and a negative regulatory region between -233 to -327 (addition of the region to the hyperactive promoter decreased its activity to the level of the full-length promoter) (Ricketts *et al.*, 2006). Chromatin immunoprecipitation and luciferase reporter assay demonstrated the binding of Sp1 and Sp3 transcription factors to the minimal WFS1 promoter and the regulation of WFS1 transcriptional activity by these proteins (Ricketts *et al.*, 2006). Additionally, Kakiuchi *et al.* (2006) have identified an ER-stress response element-like conserved motif in WFS1 promoter as critical for its regulation by XBP1, which is a key transcription factor in the ER stress response pathway. However, XBP1 was found not to interact directly with this motif.

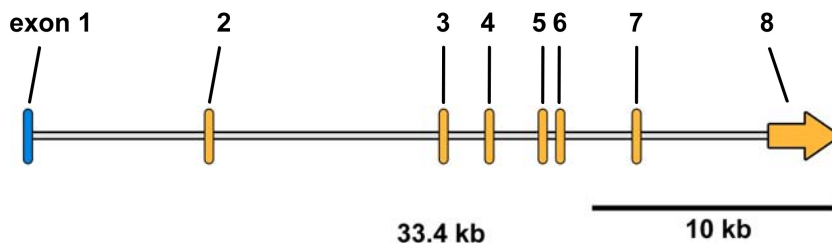


Figure 1. Genomic layout of WFS1 gene. Orange and blue represent protein coding and non-coding exons, respectively.

Northern blot analyses of commercial human tissue RNA panels have indicated high WFS1 expression in the heart, intermediate expression in placenta, lung, brain and pancreas, weak expression in liver, skeletal muscle and kidney, and negligible expression in exocrine pancreas (Inoue *et al.*, 1998; Strom *et al.*, 1998). On the other hand, western blot analysis of Wfs1 protein in mouse tissues has indicated high expression in the heart and the brain, intermediate expression in the liver, skeletal muscle and pancreas, and low expression in the spleen and kidney (Hofmann *et al.*, 2003). To my knowledge, no analysis of WFS1 protein levels in human tissues has been performed, yet.

WFS1 protein is composed of 890 amino acids and has a molecular weight of approximately 100 kDa. It is embedded in the endoplasmic reticulum (ER) membrane by 9 transmembrane segments with its aminoterminal domain located in the cytoplasm and carboxyterminal domain in the ER lumen (Hofmann *et al.*, 2003). The maturation of WFS1 protein involves N-glycosylation but no proteolytical processing or phosphorylation (Hofmann *et al.*, 2003). In native conditions Wfs1 protein is found in 400 kDa, presumably homotetrameric, complexes (Hofmann *et al.*, 2003). The predicted half-life of WFS1 protein is approximately 48 hours in transiently transfected COS-7 cells (Hofmann *et al.*, 2003). Although the precise function of Wfs1 protein is unknown, it has been shown to be involved in maintaining Ca^{2+} homeostasis in the endoplasmic reticulum (Osman *et al.*, 2003; Takei *et al.*, 2006). Importantly, WFS1 protein has been shown to positively modulate Ca^{2+} levels in the ER by increasing the rate of Ca^{2+} uptake (Takei *et al.*, 2006), and to have a dose-dependent positive effect on insulin secretion from isolated pancreatic islets upon stimulation with 15 mM glucose or 1 mM carbachol (carbachol releases Ca^{2+} from the ER by an inositol (1,4,5)-trisphosphate-dependent mechanism) (Ishihara *et al.*, 2004). Several studies of Wfs1-deficient pancreatic β -cells have demonstrated impairments in glucose-stimulated insulin secretion and cell cycle progression accompanied by the activation of ER-stress/unfolded protein response (UPR) pathways and enhanced susceptibility to apoptosis (Ishihara *et al.*, 2004; Riggs *et al.*, 2005; Yamada *et al.*, 2006). The UPR coordinates the temporary downregulation of protein translation, the upregulation of ER chaperones, folding machinery, and ER-associated degradation in order to reduce the workload on the ER protein processing and folding machinery, and prevent the accumulation of misfolded proteins (Hampton, 2000). Wfs1 expression is increased in the pancreatic β -cells in response to various ER stress-inducing compounds as well as in diabetic Akita mice harboring a dominant negative mutation in the insulin 2 gene (Fonseca *et al.*, 2005; Kakiuchi *et al.*, 2006; Ueda *et al.*, 2005; Yamaguchi *et al.*, 2004). Additionally, the sodium-potassium ATPase 1 subunit has been shown to interact with WFS1 transmembrane and ER lumenal domains (Zatyka *et al.*, 2007). In light of the common symptoms of Wolfram syndrome patients, pancreatic β -cells and neurons appear to be the most susceptible to the loss of WFS1 function. In line with this suggestion, a recent study reported no increase in the expression level of ER-stress marker genes in heart, skeletal muscle, and brown adipose tissue in

Wfs1-deficient mice (Yamada *et al.*, 2006). By using immunohistology Wfs1 expression has been detected in retinal ganglion cells and optic nerve glia (astrocytes) of cynomolgus monkey (*Macaca fascicularis*) (Yamamoto *et al.*, 2006), in a variety of inner ear cells (Cryns *et al.*, 2003), and various retinal cell types and optic nerve glia (astrocytes) of the mouse (Kawano *et al.*, 2008). In the mouse central visual system Wfs1 expression has been detected in suprachiasmatic nucleus, superior colliculus, and primary and secondary visual cortices (Kawano *et al.*, 2008). A study of rat brain has reported high expression of Wfs1 mRNA and protein in selected areas of the limbic system including the amygdaloid area, CA1 region of hippocampus, olfactory tubercle, and superficial layer of piriform cortex (Takeda *et al.*, 2001).

3. Mutations in WFS1

In WS patients mutations are distributed across the length of the coding sequence concentrating in the largest exon, exon 8, and include deletions, insertions, nonsense and missense mutations (see Khanim *et al.* (2001), for a review). Many of the patients have at least one mutation, missense or truncation, which alters the hydrophilic carboxy tail of the protein. A substantial proportion of WS patients are compound heterozygotes carrying two different WFS1 mutant alleles (Cano *et al.*, 2007). According to an online WFS1 mutation database (Lesperance, 2008) and recently published reports, the number of reported base substitutions, small deletions and small insertions in WS patients is 114, 75, and 30, respectively. Additionally, there are 40 reports of WFS1 base substitutions in autosomal dominant low frequency sensory-neural hearing loss, 21 reports of base substitutions in psychiatric patients, and 3 reports of base substitutions in diabetic patients. Appendix 1 summarizes the mutations found in WFS1 gene.

In order to highlight the structurally and functionally most susceptible regions in WFS1 protein I plotted all single amino acid changes (substitutions and deletions) against the predicted transmembrane topology of WFS1 protein (Figure 2). Prediction of the transmembrane topology of WFS1 was done using <http://www.cbs.dtu.dk/services/TMHMM> application. In total, 101 different mutations were included in the plot. If the mutations were distributed uniformly across the entire protein their median distance would be 8.8 amino acid residues (aa). The actual median distance between the mutations was 5 aa and the standard deviation from the expected median for uniform distribution was 15 aa suggesting a non-uniform distribution. The functionally most susceptible regions were identified by clusters of at least three mutations occurring in different positions and spaced less than 8.8 aa. This criterion yielded 14 clusters, one of which was located in the cytoplasmic N-terminal domain, 8 of which were located in the transmembrane regions or in the transition regions between a transmembrane domain and a hydrophilic loop, and 5 of which were located in the ER lumenal C-terminal domain. Thus, from the viewpoint of

functional integrity, the transmembrane regions and the C-terminal domain of WFS1 protein are the most sensitive. This conclusion underscores the possible role of WFS1 as a channel the permeability of which is highly dependent on the topology of the transmembrane regions.

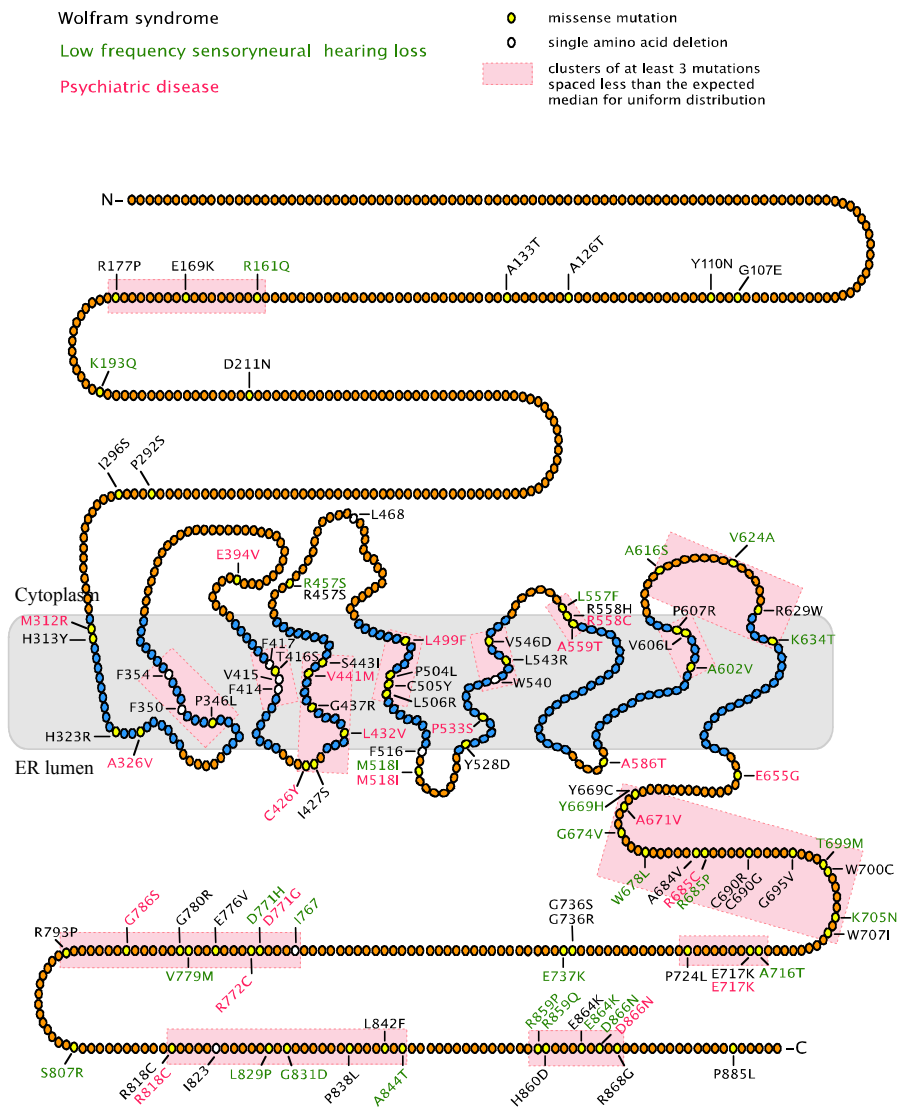


Figure 2. Mutations causing single amino acid changes in WFS1 protein. Only mutations producing single amino acid substitutions or deletions are indicated. Mutations written in black, green and red have been identified in Wolfram Syndrome patients, low frequency sensoryneural hearing loss patients, and psychiatric patients, respectively. In the mutation definition, the first letter denotes the original amino acid, the number denotes its position in the WFS1 protein primary sequence, and the last letter denotes the mutated form. In case of deletions, the last letter is absent.

4. Wfs1-deficient mice

There are three publications on Wfs1-deficient mice, two of which describe the metabolic (Ishihara *et al.*, 2004) and behavioral phenotype (Kato *et al.*, 2008) of mice lacking the second exon of Wfs1 gene, and the third which describes the metabolic phenotype of mice lacking the eighth exon of Wfs1 in the pancreatic β -cells only (Riggs *et al.*, 2005). Importantly, in the mice generated by Ishihara *et al.* (2004) and also studied by Kato *et al.* (2008), Wfs1 mRNA lacking exon 2 was still detectable. However, no Wfs1 immunoreactivity was detected in the brain lysates using an antibody that recognized a truncated Wfs1 protein lacking the first 80 amino terminal amino acids. The presence of carboxy terminal Wfs1 immunoreactivity has not been investigated in these mice. Thus, there remains a possibility that the mice express amino terminally truncated Wfs1 protein which has been translated from one of the internal methionines (located at positions 184, 230, 299).

According to Ishihara *et al.* (2004), the homozygous Wfs1-deficient mice constituted the expected 25% of the total population and were normal in appearance, growth and fertility. No motor disturbances were apparent, and the urine osmolality was normal. It was noted that impairments in glucose homeostasis were more severe in the male than female Wfs1-deficient mice, and in the [(129SV x C57BL/6) x C57BL/6]F2 hybrid background in relation to the F5 generation C57BL/6 backcross. By 9 months of age, 60% of the male F2 mice (8 out of 13) displayed abnormally high blood glucose levels while in the F5 males the measure was normal. In order to reduce phenotypic variations arising from genetic heterogeneity the subsequent study was conducted only in male F5 mice. The principal findings in homozygous Wfs1-deficient mice are summarized in Appendix 2. Taken together, the mice investigated by Ishihara *et al.* (2004) displayed decreased non-fasting plasma insulin and higher sensitivity to insulin concomitant with normal blood glucose levels, grossly reduced number of islets, mildly reduced insulin content per islet, and decreased stimulus secretion coupling of insulin arising from markedly reduced cytosolic Ca^{2+} reponse in β -cells. Additionally, the study showed that apoptosis is triggered in Wfs1-deficient pancreatic β -cells by an ER-stress-dependent pathway, and not by tumor necrosis factor β and interferon γ -dependent pathway. Together, the results suggest that Wfs1-deficiency results in impaired insulin secretion from pancreatic β -cells and apoptotic degeneration of pancreatic islets via an ER-stress-dependent mechanism.

The homozygous pancreatic Wfs1-deficient mice generated by Riggs *et al.* (2005) were created in the 129SvJ genetic background. They were born in expected Mendelian ratios and only male mice were used for the experiments. The results are summarized in Appendix 2. The mice displayed glucose intolerance by 4 months of age, lower body weight by 6 months, they had normal fasting blood glucose and plasma insulin levels, increased non-fasting blood glucose concomitant with decreased plasma insulin, impaired glucose-stimulated plasma insulin response, lower pancreatic β -cell mass and increased

expression of apoptotic and ER-stress markers. Most of the disturbances became evident or statistically significant at 6 months of age. In general, the mice exhibited an earlier on-set of metabolic disturbances in relation to the mice investigated by Ishihara *et al.* (2004), but the spectrum of disturbances was very similar. In contrast to Ishihara *et al.* (2004), the mice created by Riggs *et al.* (2005) had lower body weight by 6 months of age, displayed lower non-fasting plasma insulin by 4 months (in Ishihara *et al.* the same was noted at 9 months of age), and the number of activated caspase 3-positive islet cells was increased at 6 months. The reduction of β -cell mass and intolerance to glucose appear to be the characteristic effects of Wfs1-deficiency in mice.

Recently, Kato *et al.* (2008) conducted a behavioral study of Wfs1-deficient mice created by Ishihara *et al.* (2004). All mice were males backcrossed to the C57BL/6 genetic background for at least 8 generations. Studies of circadian behavior did not reveal obvious disturbances. Next, a battery of tests consisting of open-field test, startle response and prepulse inhibition test, elevated plus-maze, Morris water maze, passive avoidance learning, active avoidance learning and forced swimming test was administered to mice aged 3 months at the beginning of the battery. Homozygous Wfs1-deficient mice displayed longer escape latency in the conditioning phase of the passive avoidance test and first block of trials on day 3 in the active avoidance test. In the second phase of the study, home cage motor activity test, open field test, light-dark box test, elevated plus-maze, startle response and prepulse inhibition, Morris water maze and fear conditioning tests were administered to 8-month old mice. Homozygous Wfs1-deficient mice were found to display longer time of freezing during the presentation of the conditioned stimulus in the fear conditioning test. In the last phase of the study, social interaction test, rotarod, sucrose preference test, tail suspension test, forced swimming, marble burying, hot plate and tail flick tests were performed on mice 9 weeks old at the beginning of the battery. The only notable finding was that homozygous Wfs1-deficient mice displayed an overall non-significant tendency for lower social interaction. Together, these results support the notion that Wfs1-deficient mice in that study had subtle impairments in behavioral activation in demanding situations. In addition to the almost negligible behavioral differences, no alterations in the body weight or other phenotypic parameters were reported.

AIMS OF THE STUDY

The general aim of the present study was to reveal genes associated with anxiety response due to cat odor exposure, and to study the functional implications of one of the identified candidates in the regulation of emotional behavior.

1. Identify genes involved in the regulation of anxiety response in the amygdaloid area of rats after exposure to cat odor (Study 1).
2. Identify the distribution of *Wfs1* gene – one of the identified candidate genes from Study 1 – in the mouse central nervous system (Study 2).
3. Create a *Wfs1* gene knock-out mouse model and study the behavioral phenotype of *Wfs1*-deficient mice (Study 3).

MATERIALS AND METHODS

I. Cat odor-induced fear response in rats (Study I)

For rodents, cat odor is an innate fear-inducing stimulus. Laboratory rats and mice, reared for generations without any contact to alive predators, display clear avoidance response towards a cloth rubbed on a cat, cat feces, cat urine and TMT (2,5-dihydro-2,4,5-trimethylthiazoline – the major component of the anal gland secretions of the red fox) (Blanchard *et al.*, 2003; Hebb *et al.*, 2002; Raud *et al.*, 2007; Roy *et al.*, 2001). Berton and colleagues have demonstrated that the anxiety-like response of mice to cat feces is lower if the cat has been kept on a vegetarian diet (Berton *et al.*, 1998). A number of studies have indicated the contribution of different amygdalar nuclei and the bed nucleus of stria terminalis in modulating predator odor-induced fear (Takahashi *et al.*, 2005). In the present study, rats were exposed to a cloth worn by a free-ranging cat around its collar. Two groups of rats (12 rats in each) were exposed either to a cloth impregnated with cat odor (fear group) or to a clean cloth (control group). As our aim was not to detect immediate early genes, which are rather unspecific, the exposure to cat odor and simultaneous video recording lasted 30 min. The exposure was performed in two separate but similar rooms (lighting conditions, humidity, ventilation, etc.) and animals were habituated to these rooms 3 days before the experiment. Videotaped behavioral responses were analyzed by an observer who was unaware of the manipulations performed with rats. At the end of each minute, the videotape was paused and the number of animals sniffing the cloth, in the proximity of the cloth, or touching the cloth were recorded. We also counted the number of grooming animals in each group. These behavioral measures have been shown to reflect avoidance and fear of an unpleasant object (Belzung *et al.*, 2001; Dielenberg *et al.*, 2001).

2. Generation of Wfs1-deficient mice harboring β -galactosidase transgene (Studies 2 and 3)

Wfs1 targeting construct (Figure 3) was created by subcloning a 8.8 kb BamHI fragment from 129SvEv/TacfBr mouse genomic PAC clone 391-J24 (RPCI21 library, MRC UK HGMP Resource Centre, UK) including introns 6–7 and exons 7–8 of Wfs1 gene into pGem11 cloning plasmid (Promega). A 3.7 kb NcoI fragment was replaced by an in-frame NLSLacZNeo cassette, deleting more than 90% of the 8th exon and 60% of the total coding sequence including 8 of the 9 predicted transmembrane domains. A pgk-TK negative selection cassette was cloned upstream of 5' genomic arm. NotI-linearized targeting construct was electroporated into W4/129S6 embryonic stem (ES) cells (Taconic) which were selected for resistance to Neomycin and Gancyclovir. ES cell colonies were tested for homologous recombination by PCR using

recombination-specific primer pair NeoR1 5' GACCGCTATCAGGACA TAGCG and Wfs1_WTR1 5' AGGACTCAGGTTCTGCCTCA. PCR-product was sequenced to verify the integration site. ES cell clone 8A2 was injected into C57BL/6 blastocysts and heterozygous F1 mice were established by mating male chimeras with C57BL/6 female mice. F2 generation homozygous Wfs1-deficient animals were obtained by crossing heterozygous F1 mice. Mice were genotyped by multiplex PCR for both alleles using primers WfsKO_wtF2 5' TTGGCTTGATTTGTCTCGCC, NeoR1 5' GACCGCTATCAGGACATAGCG and WfsKO_uniR2 5' CCCATCCTGCTCTCTGAACC.

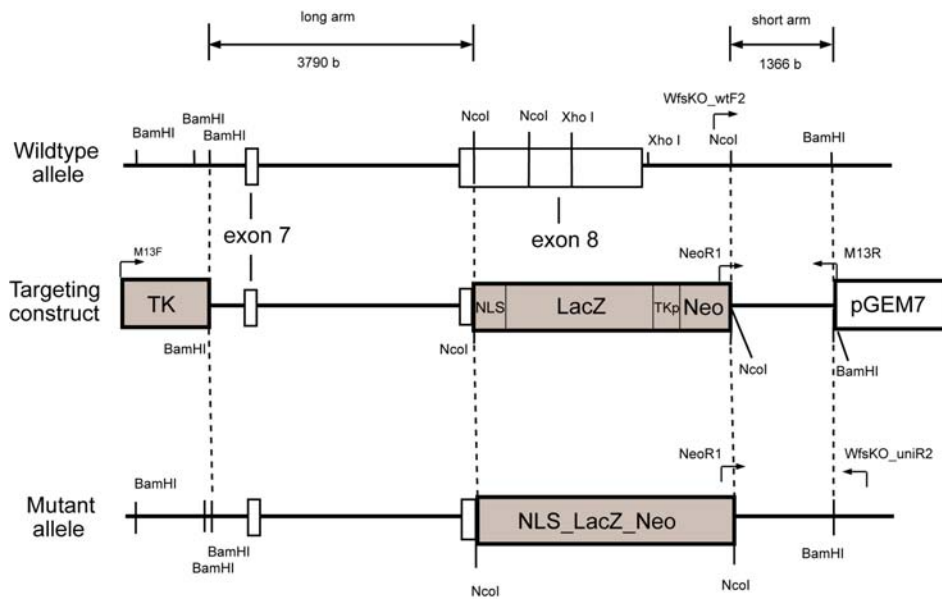


Figure 3. Targeting construct for creating Wfs1^{bga/bga} mice.

3. Animals

In Study 1 the subjects were 24 male rats (Han/Kuo: WIST) weighing 250–280 g at the time of testing. They were housed in groups of six in a temperature-controlled (21 ± 2 °C) facility under a 12/12 h light/dark cycle (lights on at 07:00 h). Tap water and food pellets were freely available. All animal procedures were approved by the University of Tartu Animal Care Committee in accordance with the European Communities Directive of 24 November 1986 (86/609/EEC).

In Study 2 the subjects were adult mice with C57BL/6 (Scanbur, Karlslunde, Denmark) and 129S6/SvEvTac F2 hybrid genetic background [(129S6/SvEvTac x C57BL/6) x (129S6/SvEvTac x C57BL/6)] (age 3–6 months). F2 hybrids are frequently used for initial phenotypic characterization of mutant

mice when genetic homogeneity of the population is not required (Wolfer *et al.*, 2002). F2 hybrids are obtained by a two-step procedure. First, mice from two different inbred strains are mated to produce F1 heterozygous mice who are heterozygous for genetic variants derived from both of the original strains at all loci (i.e. for each pair of homologous chromosomes, one is derived from one inbred strain while the other is derived from the other inbred strain). Second, F1 heterozygous mice are mated to produce F2 hybrids who are more or less random mixes of the genetic material derived from the original strains due to meiotic crossing-over events between the F1 chromosomes which result in mosaicism of the F2 chromosomes in relation to the two parental strains. Thus, F2 hybrids constitute a genetically heterogeneous population derived from two ancestral inbred strains, and they can be used to study the effects of targeted genetic alterations that manifest across a genetically heterogeneous background. Mice were housed under standard laboratory conditions on a 12-hour light/dark cycle (lights on at 07:00 hours) with free access to food and water. Eight mice homozygous for β -galactosidase knockin ($Wfs1^{bgal/bgal}$) were used for X-Gal staining experiments (4 males and 4 females) and, for immunohistochemistry, 1 male $Wfs1^{bgal/bgal}$ mouse, 10 wild-type littermates (8 males and 2 females), and 2 male $Wfs1^{+/bgal}$ mice were used. Permission (No. 39, 7 October 2005) for Study 2 was given by the Estonian National Board of Animal Experiments in accordance with the European Communities Directive (86/609/EEC).

In Study 3 the subjects were female F2 hybrids [(129S6/SvEvTac x C57BL/6) x (129S6/SvEvTac x C57BL/6)] of $Wfs1$ β -galactosidase knockin mice 2 to 4 months old at the time of testing. Mice were housed in groups of ten to twelve at $20\pm 2^\circ\text{C}$ under a 12-h/12-h light/dark cycle (lights on at 07:00 hours). All tests were performed between 10 a.m. and 18 p.m. Tap water and food pellets were freely available. The permission (No. 39, 7 October 2005) for Study 3 was given by the Estonian National Board of Animal Experiments in accordance with the European Communities Directive of 24 November 1986 (86/609/EEC).

4. cDNA representational difference analysis (Study I)

After the behavioral testing, the rats were decapitated, the brains were rapidly removed from the skull and sliced. Amygdala dissection was performed using a round-shape puncher (Figure 4). The tissue samples included the basolateral, central and medial nuclei of amygdala. Thereafter, mRNA was purified from the tissue samples of amygdala (QIAGEN RNeasy and Oligotex mRNA kit) and cDNA was synthesized (GIBCO BRL Superscript Choice System for cDNA Synthesis). cDNA representational difference analysis (cDNA RDA) was performed according to the protocol of Hubank and Schatz (1999) with minor modifications (O'Neill and Sinclair, 1997; Pastorian *et al.*, 2000). Briefly, double-stranded cDNA derived from purified RNA by reverse transcription

PCR with oligo(dT₁₈) primers was digested with DpnII (New England Biolabs) and ligated to annealed R-Bgl-24 adaptors (see Table 4, for primer sequences). Amplicons for both “tester” and “driver” were generated with Vent DNA Polymerase (New England Biolabs) using self-complementary R-Bgl-24 primers. For tester 5 and for driver 20 200- μ l PCRs were performed. DpnII digestion was used to remove the R-adaptors from both driver and tester amplicons followed by ligation of J-24-Bgl adaptors to the tester amplicons only. Subtractive hybridizations were performed in 5- μ l reactions at 67 °C for 24 hours in a thermocycler. To generate difference product 1 (DP1), 0.4 μ g of tester cDNA amplicon was mixed with 40 μ g of driver cDNA amplicon at a ratio of 1:100 followed by PCR amplification with self-complementary J-Bgl-24 primers. Such procedure is expected to exponentially amplify only tester:tester hybrids (i.e. transcripts over-represented in the tester cDNA amplicon). DP1 was digested with DpnII to remove J-adaptors before ligation of N-Bgl-24-adaptors. To generate DP2 50 ng of N-ligated DP1 was mixed with 40 μ g of driver cDNA amplicon at a ratio of 1:800 and amplified by PCR with self-complementary N-Bgl-24 primers. DP2 was digested with DpnII to remove N-adaptors before ligation of J-adaptors. To generate a third difference product (DP3), 100 pg J-ligated DP2 was mixed with 40 μ g driver cDNA amplicon (stringency 1:400 000). Another experiment was performed where 4 ng of J-ligated DP2 was mixed with 40 μ g of driver cDNA to get a ratio of 1:10 000 for DP3. DP3 was digested with DpnII to obtain BamHI compatible ends. For removal of digested adaptors spin column purification with Qiagen PCR purification kit was applied. The subtracted library was fractionated by 1.5% low-melting agarose gel electrophoresis. Fractions were cut out of the gel and QIAEX II Gel Extraction was performed. Fractions were ligated into the BamHI site of vector pGEM-7 and transformed into DH5- α competent cells. Transformed competent cells were plated onto LB-agar plates supplemented with 50 μ g/ml ampicillin, 8 μ g/ml X-Gal and 0.1 mM IPTG followed by incubation at 37 °C overnight. After brief incubation at 4°C the blue/white staining became clearly distinguishable. The plasmids were purified from 2-ml cultures of the white colonies by alkaline lysis protocol. 300 ng of each plasmid DNA was used to perform cycle sequencing on ABI310 sequencer (Perkin-Elmer) with M13 forward primers according to the manufacturer’s instructions.

After sequencing and alignment, only clones containing different inserts were used for dot blot analysis to confirm the results of RDA. 100 ng of plasmid DNA in 5 μ l of 0.4 M NaOH and 10 mM EDTA was denatured (10 min at 100 °C) and dotted onto a Hybond N⁺ nylon membrane, followed by UV cross-linking. Each set of clones was dotted onto two identical membranes. DIG High Prime DNA Labeling and Detection Starter Kit I (Roche) was used to generate hybridization probes and for hybridization of membranes. Equal amount of cDNA from cat odor-exposed and control rats was used for the synthesis of DIG-labeled probes. One membrane was hybridized with labeled cDNA from “fear” group; another was hybridized with labeled cDNA from

“control” group. Two membranes containing different set of clones (one from “fear” and the other from “control” group) were hybridized with a single population of labeled cDNA in one hybridization tube in identical conditions. Each experiment was repeated twice to control for experimental variation. Dot blots were scanned and analyzed with Quantity One Software (GS 710 Calibrated Imaging Densitometer, BioRad). Identical dots (representing a single clone) from membranes hybridized with different probes were compared for intensity. To correct for the gray value, a small area in between dots was measured as a local reference. Each gray value of the measured areas was corrected for this local reference. Resulting optical densities of dots were compared to the membrane hybridized with different probe in the same experiment. Results are expressed as fold changes of respective dots.

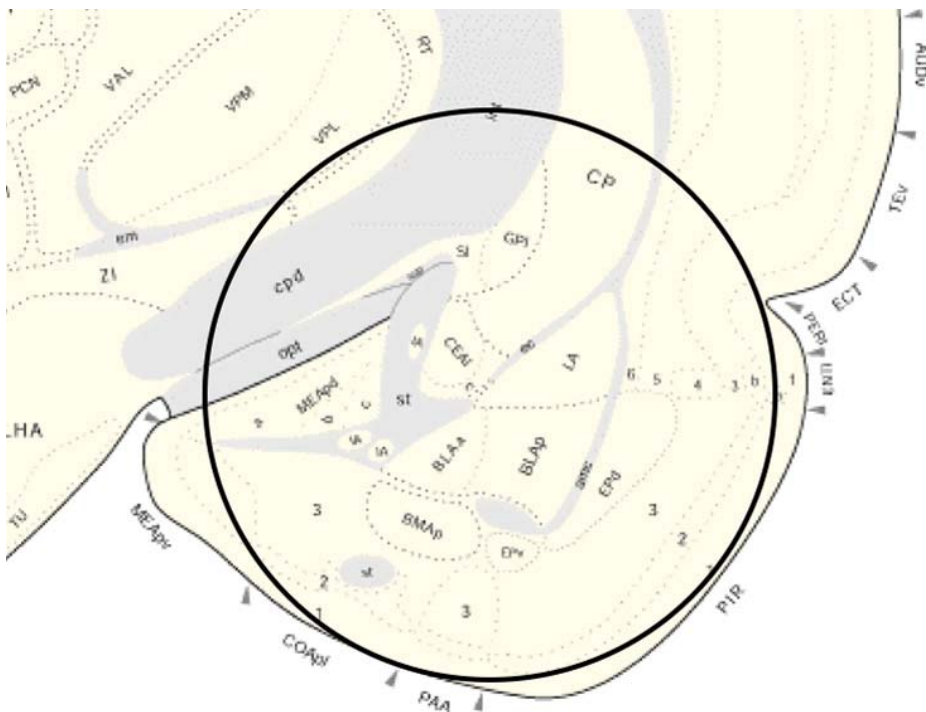


Figure 4. Schematic illustration of the brain slice used for punching out the amygdaloid area.

To further validate the differences obtained during subtractive hybridization, we performed a PCR analysis from starting-cDNA and cDNA amplicons (not used for differential cloning). Total RNA was extracted, DNase-treated and subjected to reverse transcription-polymerase chain reaction (RT-PCR) using specific primers for cyclophilin (a house-keeping gene used as internal reference for RNA quantity) and Wfs1 (Table 4). First-strand synthesis was performed by

Superscript II (GIBCO BRL) according to the manufacturer's guidelines. Briefly, 2 pmol of gene specific primers and 500 ng DNase-treated RNA were used. To exclude possible genomic DNA contamination, we performed a parallel reaction lacking Superscript II revertase. PCR was performed from 10% of the first-strand reaction mix and products were separated by agarose gel electrophoresis. Results were compared by densitometric analysis using Quantity One Software (GS 710 Calibrated Imaging Densitometer, BioRad).

Table 4. Sequences of primers used for RDA and RT-PCR

Name	Sequence of primer
R-Bgl-24	5'-AGCACTCTCCAGCCTCTCACCGCA
R-Bgl-12	5'-GATCTGCGGTGA
J-Bgl-24	5'-ACCGACGTCG-ACTATCCATGAACA
J-Bgl-12	5'-GATCTGTTCATG
N-Bgl-24	5'-AGGCAACTGTGCTATCCGAGGGAA
N-Bgl-12	5'-GATCTTCCCTCG
Wfs1F	5'-CCAAGCAGGGCAGGCGGGAG
Wfs1R	5'-GGCAGCCTTGCGCACTGCCC
CfosF	5'-GAGTGGTGAAGACCATGTCA
CfosR	5'-TCTCTTTCAGTAGATTGGCA

5. Production of Wfs1 antibodies (Study 2)

Two series of eight rabbits were immunized with 100 mg of synthetic peptide corresponding to either amino acids 1–11 (MNSGT PPPSPSC) or 877–890 (FAFDFFF PFLSAA) of mouse Wfs1 protein (Cambridge Research Biochemicals, Billingham, UK), termed Wfs1N and Wfs1C peptides, respectively. The peptides were coupled to bovine serum albumin (BSA) and administered with complete Freund's adjuvant. Five or more booster injections using Freund's incomplete adjuvant were administered at 8-week intervals, using one-half of the initial dose of antigen per immunization. Rabbits were bled from an ear vein 10 days after the last immunization. In order to demonstrate the presence of intact Wfs1 protein in the wild-type mice and the absence of Wfs1 C-terminal immunoreactivity in Wfs1^{bga/bgal} mice with a single antibody, sera from rabbits immunized with Wfs1C peptide were screened. Serum 05149/4, specific to Wfs1C peptide (referred to as Wfs1C antibody), was selected for Wfs1 immunostaining.

6. Histochemistry (Study 2)

6.1. Perfusion and tissue processing

Mice were deeply anesthetized with a 150- μ L intraperitoneal injection of a mixture containing Hypnorm® (fentanyl citrate 0.315 mg/mL and fluanisone 10 mg/mL, Janssen Animal Health, Buckinghamshire, UK), Dormicum® (midazolam 1.25 mg/mL, Roche, Mannheim, Germany), and water (dilution 1:1:2). Mice were perfused transcardially with 15 mL phosphate-buffered saline (PBS) and 15 mL of either 2% paraformaldehyde (PFA; X-Gal staining) or 4% PFA (immunohistochemistry) in 0.1M sodium phosphate buffer (PB), pH 7.4. Next, the brains were cut in two halves to facilitate penetration of the solution, incubated overnight in 20% sucrose 1% PFA in PB, frozen, and cut into sections of either 100 μ m (X-Gal staining) or 40 μ m (immunohistochemistry, X-Gal staining with ethidium bromide counterstain). After staining the sections were transferred to gelatinized glass slides and mounted with Pertex (Histolab, Malmö, Sweden). Digital images were adjusted for brightness, contrast, evenness of illumination, and sharpness by using Adobe Photoshop CS 2 (San Jose, USA).

6.2. X-Gal staining

For X-Gal staining, 100 μ m thick free-floating sections were stained overnight in 5 mM $K_3Fe(CN)_6$, 5 mM $K_4Fe(CN)_6$, 1 mg/ml X-Gal, 0.125% Triton X-100 in PB at room temperature in the dark. Alternatively, whole brains were incubated in X-Gal staining solution immediately after fixation. After X-Gal staining, tissue was incubated in 2% PFA solution in PB to give it a pale white appearance. Sections were photomicrographed with a Sensicam CCD camera (PCO, Kelheim, Germany) attached to an Olympus SZX12 microscope (Olympus, Hamburg, Germany). Whole mount brains were submerged in water and photographed with a Pentax K100D digital photocamera (Pentax, Hamburg, Germany).

6.3. Ethidium bromide staining

For fluorescent counterstaining with ethidium bromide, slides were incubated in the following solutions (incubation time was 3 minutes unless stated otherwise): 100% xylene, 100% methanol, 96% ethanol, 70% ethanol, 50 % ethanol, PB, 0.001% ethidium bromide in PB (1 minute), and PB. They were then dehydrated through ascending graded alcohols and cleared in xylene. Ethidium bromide staining was visualized with RITC filter.

6.4. Immunohistochemistry

6.4.1. Antibody characterization

All primary antibodies, except Wfs1 antibody (in-house) and β -galactosidase antibody (Sigma, USA), were obtained from Chemicon (Temecula, USA). Omission of the primary antisera abolished all specific staining for the antibodies used in the present study (data not shown).

For labeling of striatal efferents, a polyclonal rabbit antiserum directed against a synthetic Met5-enkephalin peptide (H-Tyr-Gly-Gly-Phe-Met-OH) was used (cat. no. AB5026). On immunoblots, it has been shown to possess minimal crossreactivity with Leu5-enkephalin (5.8%), β -endorphin and β -Lipotropin (both <0.01%) (Millipore, 2008b). The antibody staining has been reported to overlap with preproenkephalin promoter-driven GFP fluorescence in lateral globus pallidus after lentiviral delivery (Jakobsson *et al.*, 2006). In agreement with the above, we detected strongly immunoreactive nervefibers and neuropil in lateral globus pallidus and ventral pallidum, which are the terminal- as well as way stations for dorsal and ventral striatal efferents, respectively.

For labeling of dopaminergic neurons in substantia nigra and ventral tegmental area, a mouse monoclonal antibody clone LNC1 (cat. no. MAB318) specific for tyrosine hydroxylase was used. The antibody has been raised against tyrosine hydroxylase purified from PC12 cells and recognizes an epitope on the outside of the regulatory N-terminus (Millipore, 2008a). The antibody has been used extensively for labeling of catecholaminergic neurons. In western blot of human brain samples, the antibody recognizes an intensive 60 kDa band corresponding to the tyrosine hydroxylase monomer (Wolf *et al.*, 1991). In the ventral midbrain, the antibody labels perikarya and processes of dopaminergic neurons located in the compact part of substantia nigra and ventral tegmental area.

For labeling of neurons, mouse monoclonal antibody NeuN clone A60 was used (cat. no. MAB377). The antibody has been raised against purified cell nuclei from mouse brain and typically labels nuclei and, to a lesser degree, perinuclear cytoplasm of various post-mitotic neuronal cell types of all vertebrates tested (Mullen *et al.*, 1992). No immunoreactivity has been observed in oligodendrocytes in the white matter of the spinal cord and brain, and Bergmann glia in the cerebellum. Similarly, robust NeuN immunoreactivity is seen after retinoic acid treatment that induces neuronal differentiation of the P19 embryonal carcinoma cell line, but no staining is evident in unstimulated P19 cells.

In order to establish immunohistochemical borders between the subdivisions of the amygdaloid complex, goat polyclonal anti-vesicular acetylcholine transporter (VACHT) antibody was used (cat. no. AB1578). The antibody has been raised against a synthetic peptide (CSPPGPFDDGCEDDYNYYSRS) corresponding to amino acids 511–530 of the carboxy terminus of the rat VACHT and labels nerve terminals and fibers, and, to a lesser degree, dendrites and perikarya of mouse and rat cholinergic neurons in a fashion similar to

histochemical staining of acetylcholine esterase (Arvidsson *et al.*, 1997). Preabsorption of the antisera with the peptide antigen was shown to abolish all specific staining.

For immunolabeling of β -galactosidase reporter enzyme in $Wfs1^{+/bgal}$ mice, we used a biotin conjugate of mouse monoclonal antibody clone GAL-13 (cat. no. B0271) raised against purified β -galactosidase from *Escherichia coli* bacterium. The tissue distribution of the antibody staining overlapped extensively with X-Gal staining in $Wfs1^{bgal/bgal}$ mice and with endogenous $Wfs1$ expression pattern in $Wfs1^{+/bgal}$ mice (see results of Study 2), indicating that it specifically labeled the β -galactosidase reporter enzyme that had been genetically targeted into the coding sequence of mouse $Wfs1$ gene. No β -galactosidase immunostaining or X-Gal staining was detected in wildtype mice (data not shown).

6.4.2. Staining procedures

For $Wfs1$ immunostaining with rabbit polyclonal $Wfs1C$ antibody (diluted 1:500), free-floating sections were incubated for 1 hour at room temperature on a shaker followed by overnight incubation at 4 degrees celsius. Incubation at room temperature was found to be essential to ensure the reproducibility of $Wfs1$ staining especially in regions with low $Wfs1$ expression. It was also found that treatment with 1% H_2O_2 masks the antigen for $Wfs1C$ antibody, and thus incubation with $Wfs1C$ antibody was always performed prior to the 1% H_2O_2 treatment. Incubations with biotinylated or fluorescently labelled secondary antibodies were performed for 1 hour at room temperature on a shaker, all other incubations were performed for 30 minutes. For double immunostaining with mouse monoclonal antibody NeuN clone A60 (diluted 1:1000), sections were blocked with 5% normal goat serum (Dako, Copenhagen, Denmark) and incubated with a mix of $Wfs1C$ and NeuN antibodies followed by goat anti-mouse IgG antibody coupled to Alexa Fluor 488 (cat. no. A11001, Molecular Probes, Leiden, The Netherlands, diluted 1:500) and goat anti-rabbit IgG antibody coupled to Alexa Fluor 568 fluorescent dye (cat no. A11011, Molecular Probes, diluted 1:1000). For double immunostaining with mouse monoclonal antibody to tyrosine hydroxylase (diluted 1:2000), sections were blocked with 5% normal donkey serum (Jackson Immunoresearch Laboratories, West Grove, USA) and incubated with a mix of $Wfs1C$ and tyrosine hydroxylase antibodies followed by biotin-SP-conjugated $F(ab')_2$ fragment of donkey anti-mouse IgG antibody (cat. no. 715-066-151, Jackson Immunoresearch Laboratories, diluted 1:1600), followed by goat anti-rabbit IgG antibody coupled to Alexa Fluor 488 (cat no. A11008, Molecular Probes, diluted 1:1000) and streptavidin Texas Red (cat. no. RPN1233V, Amersham Biosciences, UK, diluted 1:50). For double immunostaining with Met-enkephalin rabbit polyclonal antibody (diluted 1:20,000) we used a modification of the method described by (Shindler and Roth, 1996). In order to avoid the masking of

antigen from Wfs1C antibody by 1% H₂O₂ treatment, incubation with Wfs1C antibody was performed after reacting sections with Met-enkephalin primary antibody and biotinylated donkey anti-rabbit IgG secondary antibody. After incubation with Wfs1C, sections were treated with 1% H₂O₂ and processed further using the conventional method for tyramide signal amplification. According to this scenario, by the time a high concentration of Wfs1C antibody was added, the very small amount of Met-enkephalin antibody had already been reacted with biotinylated secondary antibody and the two immunoreactions could proceed independently (Met-enkephalin reaction by streptavidin and biotinyl-tyramide mediated amplification, and Wfs1C reaction by fluorescence-labeled anti-rabbit IgG secondary antibody staining). For double immunostaining with Met-enkephalin, sections were blocked with 5% normal donkey serum and incubated overnight with anti-Met-enkephalin antibody, followed by biotin-SP-conjugated F(ab')₂ fragment of donkey anti-rabbit IgG antibody (cat. no. 711-066-152, Jackson ImmunoResearch Laboratories, diluted 1:1600), followed by incubation with Wfs1C antibody as indicated above, 1% H₂O₂ treatment for 10 minutes, incubation with ABC complex (Vectastain Elite ABC Kit, cat. no. PK-6100, Vector Laboratories, USA), incubation with biotinylated tyramide (TSA Indirect KIT, cat. no. NEL700001KT, PerkinElmer, USA, diluted 1:50), and finally by streptavidin Texas Red and goat anti-rabbit IgG antibody coupled to Alexa Fluor 488 (both as indicated above). For double immunostaining with goat anti-vesicular acetylcholine transporter polyclonal antibody (diluted 1:20,000), sections were blocked with 5% normal donkey serum and incubated overnight with a mix of anti-vesicular acetylcholine transporter and Wfs1C antibodies, followed by biotin-SP-conjugated F(ab')₂ fragment of donkey anti-goat IgG antibody (cat. no. 705-066-147, Jackson ImmunoResearch Laboratories, diluted 1:1600), followed by the same procedures as described for the doublestaining with anti-Met-enkephalin antibody starting from the H₂O₂ treatment step. For double immunostaining with biotin conjugate of mouse monoclonal antibody to E. Coli β -galactosidase clone GAL-13 (diluted 1:5000), sections were blocked with 5% normal donkey serum and incubated overnight with a mix of anti- β -galactosidase and Wfs1C antibodies, followed by the above procedures starting from the H₂O₂ treatment step. After staining, sections were transferred to gelatinized glass-slides and mounted in a 1:1 mix of glycerol and PBS and stored at -20 degrees. Photomicrographs were recorded using Olympus BX61 microscope equipped with Olympus DX70 CCD camera (Olympus, Hamburg, Germany). Confocal microscopy was performed with Olympus Fluoview FV1000 and Zeiss LSM 510 laser scanning confocal microscopes. Image processing was performed as indicated above. Control of the specificity of Wfs1C antiserum was performed by staining of brain sections from Wfs1^{bgal/bgal} mouse lacking C-terminal domain of Wfs1 protein which indicated complete absence of Wfs1 immunoreactivity (see results of Study 2).

7. Drugs (Study 3)

All injections were performed intraperitoneally (i.p.) in a volume of 10 ml/kg which is a generally approved standard for laboratory mice (<http://www.uku.fi/vkek/ohjeistusta/annostelujanaytteenotto.shtml>). Amphetamine (2.5, 5, 7.5 mg/kg, Sigma, U.S.A.), a compound increasing the release of dopamine from the presynaptic terminals, and apomorphine (3 mg/kg, Sigma, U.S.A.), an unselective dopamine D1 and D2 receptor agonist, were dissolved in saline. Ascorbic acid was added to the final concentration of 0.1 % to prevent the oxidation of apomorphine. Diazepam (1 mg/kg, Grindex, Latvia), an anxiolytic GABAA receptor agonist, was diluted in saline.

8. Behavioral studies (Study 3)

8.1. Capturing and analysis of vocalizations

Since the most peculiar aspect of the overt phenotype of homozygous *Wfs1*-deficient population was the presence of individuals producing spontaneous audible vocalizations we decided to characterize these sounds. AT803b omnidirectional condenser microphone (Audio-Technica, Japan) with a working frequency response range of 100 Hz -10 kHz was attached above the Plexiglas chamber used for monitoring locomotor activity of single mice. Audio recordings (44.1 kHz sampling frequency, 16 bit depth) were captured on computer hard disc using US122 digital audio interface (Tascam, U.S.A.) and adjusted for volume using CoolEdit Pro 2.0 (Syntrillium, U.S.A.). Sonogram was generated with SasLab Light application (Avisoft, Germany).

8.2. Rota-rod test

Motor performance was assessed by rota-rod. A 1-min training session was given to each mouse on the rotarod (diameter 8 cm, 9 rpm) 5 min before the first measurement. Motor performance (time until the first fall) was registered during a 2-min session.

8.3. Stress-induced analgesia

Stress was induced by electric foot-shocks (0.2, 0.4, 0.6 mA, alternating current) during 3 minutes in the apparatus used for active and passive avoidance testing (TSE Systems, Germany). Each group of mice received electric foot-shocks of a single intensity only. Withdrawal latencies in the radiant-heat tail flick test were measured before (baseline) and after stress treatment. Removal

of the tail from the heat source terminated the application of thermal stimulation. Ceiling tail-flick latencies were 30 s. Restraint tubes (opaque plastic cylinders, inner diameter 28 mm, length 90 mm, the closed end of the tube had a small hole for breathing) were used for the immobilization of mice during the measurement. Mice were habituated with the tubes for 5 days prior to the measurements.

8.4. Locomotor activity

Locomotor activity of single mice was measured for 30 minutes in sound-proof photoelectric motility boxes (448 mm×448 mm×450 mm) connected to a computer (TSE, Technical & Scientific Equipment GmbH, Germany). In the first study we investigated the effect of illumination on locomotor activity of *Wfs1*-deficient mice. The experiment was performed in dimly (20 lx) and brightly (450 lx) lit conditions on two consecutive days. Half of the animals were first exposed to brightly lit motility boxes and the second half to dimly lit motility boxes. On the second day the treatments were reversed so that each animal experienced both conditions. The results from the two experiments were collapsed. In the second study we investigated the effects of amphetamine (2.5–7.5 mg/kg) and apomorphine (3 mg/kg) on locomotor activity. Amphetamine and apomorphine were injected intraperitoneally at 30 and 15 minutes, respectively, prior to the measurement of locomotor activity in a bright environment (450 lx). The schedule of experiments is presented in Table 4. For each individual, the effect of amphetamine was compared to the mean effect of saline treatments performed in the same individual on days 4 and 20. Similarly, the effect of apomorphine was compared to the mean effect of saline treatments performed on days 20 and 28.

Table 4. Pharmacological treatment schedule in locomotor activity experiment (Study 3)

Day	Treatment
1–3	Habituation with the motility boxes
4	Treatment with saline
8	Treatment with amphetamine (2.5 mg/kg)
12	Treatment with amphetamine (5 mg/kg)
16	Treatment with amphetamine (7.5 mg/kg)
20	Treatment with saline
24	Treatment with apomorphine (3 mg/kg)
28	Treatment with saline

The floor of the testing apparatus was cleaned with damp towels and dried thoroughly after each mouse. Computer registered the distance travelled, the

number of rearings and corner entries, and time spent in the central part of the motility boxes.

8.5. Light-dark exploration test

Light-dark exploration test is an unconditioned test of anxiety-like behavior designed for mice (Crawley and Goodwin, 1980). Since social isolation is known to affect exploratory activity (Abramov *et al.*, 2004), the effect of short-term isolation on the behavior of *Wfs1*-deficient mice was tested explicitly. One group of animals was exposed to the exploration test without previous isolation (non-isolated animals), the second group was isolated for 15–20 minutes before the experiment. The experiments were carried out in a dim room (illumination ~20 lx). Plexiglas box (45x20x20 cm) was divided into two parts: 2/3 was brightly illuminated (~270 lux) and 1/3 was painted black, covered by a lid and separated from the white compartment with a partition containing an opening (13x5 cm). A mouse was placed in the centre of the light compartment facing away from the opening between the two compartments, and, during 5 minutes, latency to move into the dark compartment, time spent in the light compartment and number of transitions between the two compartments were recorded.

8.6. Elevated plus-maze test

The test employs a naturalistic conflict in mice between the tendency to explore a novel environment and aversive properties of a brightly lit, open area (Handley and Mithani, 1984; Lister, 1987; Pellow *et al.*, 1985). The plus-maze consisted of two opposite open arms (17.5x5 cm) without sidewalls and two enclosed arms of the same size with 14-cm-high sidewalls and an end wall. The arms extended from a common central square (5x5 cm) and were perpendicular to each other, making the shape of a plus sign. The entire plus-maze apparatus was elevated to a height of 30 cm and placed in a dim room (illumination level ~20 lx). In order to encourage open arm exploration, a slightly raised edge (0.25 cm) was put around the perimeter of the open arm, providing a grip for animals. The open arms were divided into three equal parts by lines. The anxiolytic effect of diazepam, a GABA_A receptor agonist, on exploratory activity was studied in *Wfs1*-deficient mice and their wild-type littermates isolated for 30 minutes before the experiment. Diazepam was administered 30 minutes before the study. The control group received vehicle containing a few drops of Tween-80 in saline. Testing began by placing an animal on the central platform of the maze facing an open arm. An arm entry was counted only when all four limbs were within a given arm. Standard 5-minutes test duration was employed (Lister, 1987; Pellow *et al.*, 1985), and the maze was wiped clean with damp and dry towels between the subjects. Test sessions were video-recorded and the videotapes were subsequently blind-scored by a trained observer. The following

measures were registered by the observer: 1) time spent on open arms; 2) number of closed and open arm entries (entries into the most distant part of open arms were counted separately); 3) number of line crossings; 4) ratio between open and total arm entries; 5) number of head dips; 6) number of attempts to enter the central platform located between open and closed arms.

8.7. Fear conditioning test

This is a form of classical conditioning which investigates the establishment of a simple association between a conditioned stimulus (10 kHz tone, CS) with an unconditioned aversive stimulus (0.5 mA electric foot-shock with a duration of 2 s, US). The study was performed according to the method described by Paylor *et al.* (1998) with some modifications. Experiments were carried out with a computer-controlled fear conditioning system (TSE). Context and tone-dependent experiments took place in a lit room. During the training period and on the day of the experiment, mice were kept in their home-cages. Training was conducted in a transparent acrylic chamber (110x160x160 mm/110x135x155 mm) containing 3 mm stainless steel rod floor, spaced 0.5 cm, through which electric foot shocks could be administered. The test chamber was placed inside a sound-attenuated chamber and was constantly illuminated (~132 lux). Mice were observed through a window in the front wall of the sound-attenuated chamber. Animals were placed in the conditioning context for 120 s and were then exposed to a CS for 30 s. The CS was terminated by a US. 120 s later another CS-US pairing was presented. The mouse was removed from the chamber 15–30 s later and returned to its home cage.

The mice were tested for contextual memory twenty-four hours later by placing them back into the test chamber for 5 min with no CS applied. Total time of freezing (defined as the absence of any movements for more than 3 s) was measured using the standard 10 s interval sampling procedure. Four hours later the mouse was tested for freezing behavior to the auditory CS. Testing was performed in a different acrylic chamber (220x160x160 mm/220x135x155 mm) the floor of which was covered with white cardboard. The background color was black. Duration of the test was 6 minutes: 3 minutes without the tone (pre-CS phase) and 3 minutes with the tone (CS phase). Freezing was counted during the CS phase. Additionally, the number of rearings in pre-CS and CS periods was recorded.

8.8. Hyponeophagia test

The experiment was carried out in a brightly lit (400 lux) room. The mice, food-deprived for 24 h, were taken from their home-cage and placed singly in a translucent plastic box (18x22x14 cm) filled with a single layer of food pellets (Lactamin AB, Sweden; weighing 1.5–3.5 g) to a depth of ca 1 cm. To avoid

social transmission of behavior, mice that had already been tested were placed in a separate box. The latency to start eating was measured from the time a mouse was placed in the box. Eating was defined as eating for at least 3 s consecutively. A cut-off score of 180 s was used.

8.9. Forced swimming test

Mice were placed for 6 min into a glass cylinder (diameter 12 cm, height 24 cm, water depth 15 cm) filled with $25\pm0.5^{\circ}\text{C}$ fresh tap water. A 5 second standard interval sampling technique was used for rating behavior (Cryan *et al.*, 2002) during the last 4 min of the test. Specific behavioral components were distinguished: (1) climbing behavior, defined as upward-directed movements of the forepaws along the side of the swim chamber; (2) swimming behavior, the horizontal movement throughout the swim chamber; (3) immobility, defined as no activity other than that required to keep the animal's head above water.

8.10. Morris water maze test

Spatial memory was studied in Morris water maze (TSE Technical & Scientific Equipment GMBH, Germany). The pool (150 cm in diameter, 50 cm in depth) was filled with $22\text{--}24^{\circ}\text{C}$ water to a depth of 38 cm. Water surface was made opaque with the addition of non-toxic fine-grained white putty. The invisible white escape platform (16 cm in diameter, submerged 1 cm under water) was positioned in the centre of the imaginary Southwest quadrant, 20 cm from the wall. It remained in a fixed position during the training. Subjects' movements were recorder by a computer connected to the video camera placed above the pool. The experimental room was lighted with four symmetrically placed lamps with 25W light-bulbs and also a table lamp, which filled the room with dim light (ca 20 lux). Colored flyers and figures on the walls served as spatial cues. During each trial, a mouse was released into the water facing the wall of the pool from pseudo-randomly chosen cardinal compass points (North, East, South and West). Randomization ensured that all positions were sampled before a given position was repeated. The acquisition phase of the experiment consisted of a series of 20 initial training trials, lasting up to 60 s each with inter-trial interval of approximately 1 hour (5 trials per day on 4 consecutive days) and 12 reverse training trials (6 trials per day on 2 days). A 60 s probe trial without the platform was performed at the end of each training cycle, one hour after the last training trial. In probe trials, mice were released at a location on the opposite side of where platform had been located (on day 4 from Northeast, on day 6 from Southwest). For statistical purposes, the reversal training sessions were divided into 4 blocks of 3 trials. In all trials, mice were allowed to swim until they landed on the platform or until 60 s had elapsed. Mice failing to find the

platform within 60 s were gently placed on the platform with a metal escape sieve and left there about 15 s to orient. Mice that found the platform were also left there for about 15 s. After each trial mice were put to their home cage with the escape sieve. Mice quickly learned to associate the sieve with escaping from the pool and consistently oriented to or followed the sieve on its appearance. The ability of mice to orient to or follow the escape sieve represented independent measures of vision and attention. The latency to find the submerged platform, the distance travelled, swim velocity and time spent in the periphery were registered with water maze software (TSE Technical & Scientific Equipment GMBH, Germany).

8.11. Active avoidance test

Active avoidance is a fear-motivated associative avoidance task providing a simple way to assess associative learning and memory. In this task the mouse has to learn to predict the occurrence of an aversive event (electric foot shock) based on the presentation of a specific stimulus (tone or light), in order to avoid the aversive event by moving to a different compartment.

Active avoidance learning was carried out in a rectangular two-way automated shuttle-box (TSE), consisting of two similar chambers (14 cm x 11 cm x 16 cm) connected by an arched opening (4 cm x 4 cm). The box was surrounded by a soundproof chamber. The apparatus was located in a quiet, very dimly (5 lux) illuminated room. The shuttle-boxes had a cover with a lightbulb (10 W) attached above each compartment. Foot shocks could be administered through a stainless steel rod floor (diameter 3 mm, spaced 5 mm). Mice were placed in the dark compartment facing the wall of the chamber and submitted to an active avoidance test for four consecutive days, 30 trials a day. The test started with a habituation time of 10 s. The conditioned stimulus (CS) was a 10 kHz tone with a maximum duration of 20 s accompanied by lighting up of the target compartment (light and sound signal). The unconditioned stimulus (US; 0.3 mA electrical foot shock for 5 s) was switched on 5 s after CS and was followed by a stronger US (by a 0.6 mA foot shock for a maximum of 10 s) in case the mouse failed to move to the target compartment. Intertrial interval was 10 s. After 30 trials, mice were taken back to their home cage.

8.12. Testing order of animals

Only experimentally naïve animals were subjected to the experiments marked as first in the testing order (Table 5). We tested all mice several times to reduce the number of animals used. Behavioral tests were divided into two categories, either sensitive or insensitive to previous experimental experience. Plus-maze, forced swimming test, locomotor activity, fear conditioning and hyponeophagia were considered as sensitive, whereas stress-induced analgesia, rota-rod test,

Morris water maze test, active avoidance test and dopamine agonist induced hyperlocomotion as insensitive tests (McIlwain *et al.*, 2001; Voikar *et al.*, 2004).

Table 5. The order of behavioral tests (Study 3)

Behavioral test	Number in order
Elevated plus-maze	1
Locomotor activity test	1, 2
Forced swimming test	1
Hyponeophagia	1
Fear conditioning	1
Light-dark exploration test	2
Amphetamine-induced hyperlocomotion	2
Apomorphine-induced hyperlocomotion	3
Rota-rod test	3
Active avoidance test	3
Stress-induced analgesia	3
Morris water-maze test	3

9. Measurements of metabolic and endocrine parameters (Study 3)

9.1. Blood glucose measurement and glucose tolerance test

Non-fasted experimentally naïve animals were used for this experiment. The injection of D(+)-glucose (Sigma, 2 g/kg, dissolved in saline) was given intraperitoneally. Blood was collected from the tail vein before the injection (at 0 minutes), and 30, 60 and 120 minutes after the injection. Blood glucose concentration was measured using Accu-Check GO portable glucometer (Roche, Mannheim, Germany).

9.2. Corticosterone response to stress

The study was performed between 12:00 and 14:00. An equivalent number of group-housed experimentally naïve animals received either an intraperitoneal injection of saline (stress treatment group) or were left undisturbed in their home cage until decapitation in a separate room after 30 minutes. Blood from the trunk was collected into heparinized tubes and centrifuged for 10 min at $1500 \times g$. Sera were stored at $-20\text{ }^{\circ}\text{C}$ until the assay using corticosterone HS ELISA kit Octeia from Immunodiagnostic Systems (U.K.) according to

manufacturer's instructions. Briefly, 400 µl of buffer was added to 100 µl of calibrator, control or sample serum, followed by 30 min incubation at 80 °C and cooling to the room temperature. 100 µl of heat-treated calibrator, control or sample were transferred to antibody-coated plates and 100 µl of enzyme conjugate was added. Plate was covered and incubated at 22 °C for 4 hours, then washed three times with wash buffer. Next, 200 µl of TMB substrate was added and incubated at 22 °C for 30 min. Absorbance was measured at 450 nm after adding 100 µl of stop solution.

10. Statistical analyses (Studies 1 and 3)

Statistica for Windows 7.0 software was used for statistical analyses. In study 1, anxiety-like behavior of rats was analyzed using the non-parametric Mann-Whitney U-test. In Study 3, most behavioral experiments and corticosterone measurements were analysed using one-way or two-way analysis of variance (ANOVA). Two-way mixed design ANOVA was applied to data from glucose tolerance test (genotype, between-subjects x time, within subjects) and fear conditioning studies (genotype, between subjects x tone, within subjects). Data from studies of locomotor activity as well as the learning curves in active avoidance and Morris water maze tests were analyzed by repeated measures ANOVA. Genotype was a between-subjects variable in all ANOVA analyses. *Post hoc* comparisons between individual groups were performed with Newman-Keuls test. Data from forced swimming test were analysed with non-parametric Mann-Whitney U-test. Data from rota-rod, hyponeophagia and context-dependent experiments in fear conditioning paradigm were analyzed with Student's t-test. Results are expressed as mean values \pm S.E.M in the text and figures.

RESULTS

I. Study I: WfsI mRNA is upregulated in amygdaloid area of rats after cat odor-induced fear response

The cloth impregnated with cat odor induced a robust fear-like behavior in rats (Fig. 5). The rats exposed to the cat odor spent less time in the proximity of the cloth, and their exploratory and grooming behaviors were suppressed.

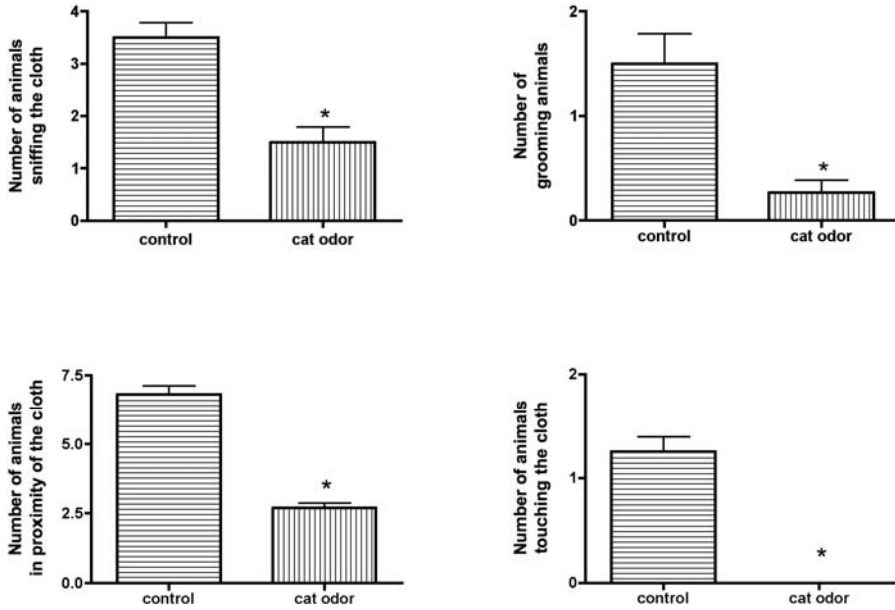


Figure 5. Behavioral changes in rats during the exposure to cat odor. Rats were exposed to the cloth impregnated with cat odor for 30 min and their behavior was recorded. At the end of each minute, the videotape was paused and the number of animals performing certain behavioral patterns was evaluated. (* $p < 0.01$, Mann–Whitney U-test).

cDNA RDA was performed to find differentially expressed genes in the amygdaloid area in response to the cat odor exposure. The starting material from six animals was pooled to minimize the fluctuations arising from individual differences. At the end of differential cloning (differential product III), clearly distinguishable bands were observed (Fig. 6).

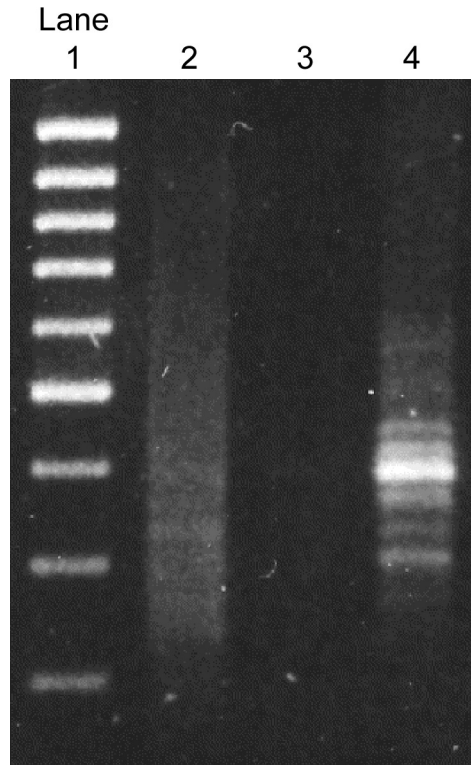


Figure 6. Result of cDNA RDA. Differential product I (DPI) shows very faint bands within a prominent smear while DPIII has clearly distinguishable bands. Lane 1, ladder (fragments 1000, 900, 800, 700, 600, 500, 400, 300, 200, 100, 80 bp); lane 2, DPI; lane 4, DPIII.

We were able to isolate 288 clones that were sequenced and identified with the NIX software (Tables 6 and 7). Database search revealed several genes with different functions. There were transcription factors (basic transcription element binding protein), transporter molecules (dynein), enzymes (carboxypeptidase E), receptors (GABA-B1a), expressed sequence tags and recently cloned proteins with unknown function. One of the most intriguing findings was the up-regulation of *Wfs1* gene (GenBank accession #AF136378) in response to the cat odor exposure. *Wfs1*-specific PCR reaction confirmed the presence of *Wfs1* transcripts in the cDNA amplicons and starting-cDNA (Fig. 7). RT-PCR and subsequent densitometric analysis of RNA samples not involved in the subtractive hybridization revealed a 1.5-fold up-regulation of *Wfs1* expression after cat odor exposure (Fig. 8).

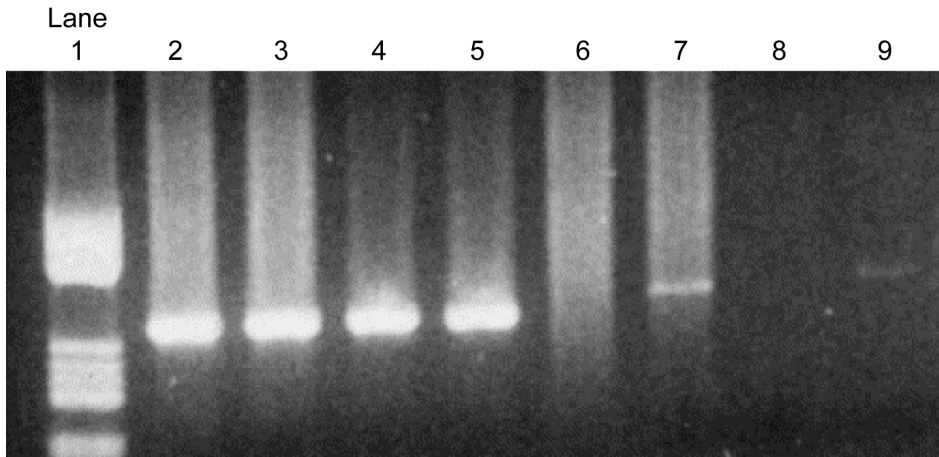


Figure 7. PCR analysis of the starting material. No or very low Wfs1 expression is detectable in the amygdala of control rats, whereas a distinct product is seen in the amygdala of cat odor-exposed animals. Lane 1, ladder (fragments 587, 540, 458, 434, 267, 234, 213, 192, 184, 124, 104 bp); lane 2, control cDNA amplicon with cyclophilin primers; lane 3, cat odor cDNA amplicon with cyclophilin primers; lane 4, starting-cDNA from control amygdala with cyclophilin primers; lane 5, cat odor starting-cDNA with cyclophilin primers; lane 6, control cDNA amplicon with Wfs1 primers; lane 7, cat odor cDNA amplicon with Wfs1 primers; lane 8, starting-cDNA from control amygdala with Wfs1 primers; lane 9, cat odor starting-cDNA with Wfs1 primers.

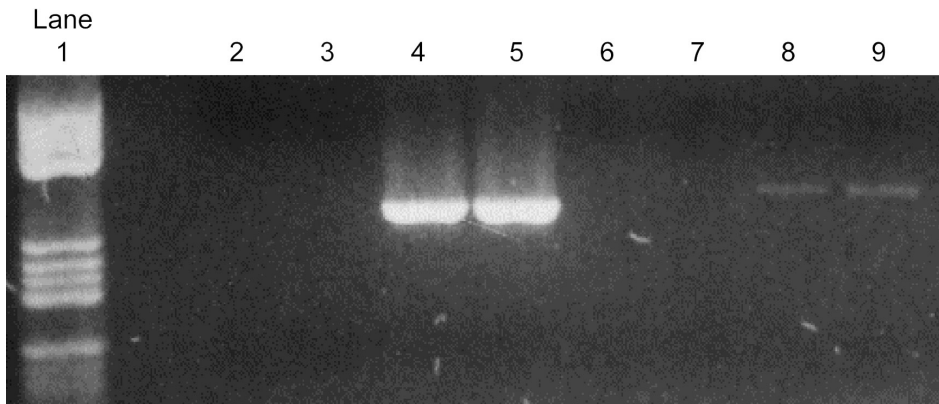


Figure 8. Results from the reverse transcription PCR (RT-PCR) of RNA extracted from rats not involved in the subtractive hybridization. Lane 1, ladder (fragments 587, 540, 458, 434, 267, 234, 213, 192, 184, 124, 104, 89, 64 bp); lanes 2 (control) and 3 (cat odor), RT-PCR lacking reverse transcriptase with cyclophilin primers; lanes 4 (control) and 5 (cat odor), RT-PCR with cyclophilin primers; lanes 6 (control) and 7 (cat odor), RT-PCR lacking reverse transcriptase with Wfs1 primers; lanes 8 (control) and 9 (cat odor), RT-PCR with Wfs1 primers.

Table 6. Transcripts with relatively higher expression in the amygdaloid area of rats exposed to cat odor.

Gene name	GenBank No.	Increase
GAMM1 M. musculus protein, Myg-1	AF252871	1.8
CDCrel-1A	AB027143	1.5
KIAA0337 protein, Rho-specific guanine-nucleotide exchange factor 164 kDa	NM_014786	1.5
Rattus norvegicus Rho GTPase activating protein 4 (Arhgap4)	NM_144740	1.5
Neural F box protein NFB42	AF098301	1.4
Putative transmembrane protein 2c	AF282981	1.4
BEC1 protein	AF035814	1.3
Ca/calmoduline-dependent protein kinase alpha	AB023658	1.3
KIAA0408 protein	AL096711	1.3
Mus musculus expressed sequence AI428855	AI428855	1.3
Na ⁺ ,K ⁺ -ATPase alpha(+) isoform catalytic subunit	M14512	1.3
NADH-ubiquinone oxidoreductase B17 subunit	XM_204158	1.3
NIR1	AF334586	1.3
Rattus norvegicus calmodulin III (Calm3)	AF231407	1.3
Rattus norvegicus CaM-kinase II inhibitor alpha	AF271156	1.3
Rattus norvegicus neurochondrin, norbin	NM_053543	1.3
Apolipoprotein E gene	J02582	1.2
Carboxypeptidase E (EC 3.4.17.10.)	X51406	1.2
DXImx39e, M. musculus	AF229636	1.2
Homeobox protein HOX-4.4 and HOX-4.5	X62669	1.2
Limbic system associated membrane protein (LsAMP)	NM_017242	1.2
Myelin-associated glycoprotein precursor (I-MAG/S-MAG)	M14871	1.2
NCI-CGAP-Lu29, M. musculus cDNA clone 601102606F1	BE305755	1.2
ODZ3	AF195418	1.2
T-type calcium channel alpha-1 subunit	AF051947	1.2
WFS1, wolframin	AF136378	1.2
Beta-spectrin III	AB008551	1.1
EST 196451 Normalized rat kidney, cDNA clone RKIAV31	AA892648	1.1
EST349530 Rat gene index, cDNA clone RGIEO08	AW918226	1.1
Gelsolin (actin-depolymerizing factor – ADF), brevin	J04953	1.1
Homo sapiens cDNA clone IMAGE:2813462	AW303350	1.1
KIAA0429 protein	XM226503	1.1
KIAA0771 protein	AB018314	1.1
Mus musculus cDNA clone IMAGE:575778	AA120430	1.1
NCI-CGAP-Lu29, M. musculus cDNA clone IMAGE: 3989880, 601770406F1	BF161425	1.1
NIH_MGC_71 Homo sapiens cDNA clone	BE889795	1.1
Rattus norvegicus Tyrosine 3-monooxygenase/tryptophan 5-monooxygenase activation protein, theta polypeptide	NM_013053	1.1
Transketolase (EC 2.2.1.1.)	U09256	1.1
Rattus norvegicus similar to hypothetical protein MGC25696	XM229276	1.1
KIAA0014 protein	NM_014665	1.1

Table 7. Transcripts with relatively higher expression in the amygdaloid area of control rats.

Gene name	GenBank No.	Increase
Similar to general control of amino acid synthesis-like 2, LOC303540	XM220979	1.4
Rattus norvegicus heat stable antigen CD24, nectadrin	U49062	1.4
2,3-cyclic nucleotide 3-phosphodiesterase (CNPII)	L16532	1.3
Mus musculus signal recognition particle receptor beta subunit	U17343	1.3
Neural membrane protein 35	AF044201	1.3
Testican-3 protein	AJ278998	1.3
G protein gamma subunit (gamma7 subunit)	L23219	1.2
MAP kinase kinase	Z16415	1.2
Mus musculus, clone IMAGE:3987018	BC019714	1.2
Mus musculus, Similar to hypothetical protein clone MGC:7259 IMAGE:3484751	BC002144	1.2
Nischarin	AF315344	1.2
Plectin	X59601	1.2
Rattus norvegicus voltage-dependent anion channel	AF268469	1.2
rELO1 mRNA for fatty acid elongase 1	AB071985	1.2
Rev-Erb-alpha protein	AF291821	1.2
Sequence specific single-stranded DNA-binding protein 2	AY037837	1.2
Similar to stress-associated endoplasmic reticulum protein 1	BC029067	1.2
Cyclin-dependent kinase homologue	L37092	1.1
EST293447 Normalized rat brain cDNA clone RGIBE57	AW143151	1.1
Mus musculus, predicted gene ICRFP703B1614Q5.3	BC002208	1.1
NCI_CGAP_Mam2 Mus musculus cDNA clone IMAGE:5374091, 603346543F1	BI697150	1.1
Non-histone chromosomal protein HMG-14	X53476	1.1
Rab geranylgeranyl transferase component B beta	S62097	1.1
SIR2L2	AF299337	1.1
Splicing factor U2AF 65 kDa subunit	X64587	1.1
ZnBP gene for zinc binding protein	X64053	1.1

2. Study 2: Distribution of Wfs1 protein in the central nervous system of the mouse

Immunostaining of wild-type mice with Wfs1C antibody revealed a distinct expression pattern in the cortex and basal forebrain (Fig. 9). The specificity of antibody staining was confirmed by complete absence of the signal in Wfs1^{bgal/bgal} mice, who lack 531 C-terminal amino acids of Wfs1 protein and express, instead, an in-frame fusion of bacterial β -galactosidase reporter enzyme (Fig. 9A-D). Double immunostaining of β -galactosidase reporter enzyme and Wfs1 protein in heterozygous Wfs1^{bgal/bgal} mice revealed a virtually complete overlap of immunoreactivity in terms of cellular distribution and expression level, indicating that the expression of both proteins was indeed controlled by the same promoter (Fig. 9E-M). On the subcellular level, however, distribution of β -galactosidase immunoreactivity diverged from endogenous Wfs1 protein (this was expected as the Wfs1- β -galactosidase fusion protein lacks at least 7 of the 9 transmembrane domains and C-terminal portion of endogenous Wfs1 protein) and was often found in large perinuclearly located, presumably cytoplasmic, aggregates (arrowheads in Fig. 9I, J, L, M). In accordance with the distribution of β -galactosidase immunoreactivity, X-Gal staining of Wfs1^{bgal/bgal} mice was almost identical to Wfs1 immunostaining on wild-type littermates with the only detectable difference being that immunostaining consistently revealed neuronal perikarya, processes and nerve fibers while X-Gal staining of β -galactosidase was usually confined to cell bodies and proximal processes only (see Fig. 10, for high power micrographs illustrating the relationship of Wfs1-immunostaining and X-Gal staining). In some cases, X-Gal staining was also detected in areas containing Wfs1-positive nerve fibers such as the alveus, dorsal hippocampal commissure, reticular part of substantia nigra (Fig. 11K) and ventral part of lateral globus pallidus (data not shown). X-Gal staining was also observed in a few brain structures that consist only of glial cells such as the subcommissural organ and the superficial glial layer of cochlear nucleus (Fig. 11J, K, O).

Based on the evidence presented above, we concluded that β -galactosidase activity in Wfs1^{bgal/bgal} mice reflects endogenous Wfs1 promoter activity accurately, and proceeded to map Wfs1 expression pattern in the mouse nervous system by X-Gal staining method (Table 8). For the sake of clarity, X-Gal staining results are referred to as Wfs1 expression, in the following paragraphs. Unless stated otherwise, the term Wfs1 expression refers to Wfs1-positive neuronal cell bodies as determined by X-Gal staining and Wfs1 NeuN double-label immunohistochemistry. Wfs1-positive nerve fibers were identified on the basis of immunostaining only, because β -galactosidase activity was rarely observed there.

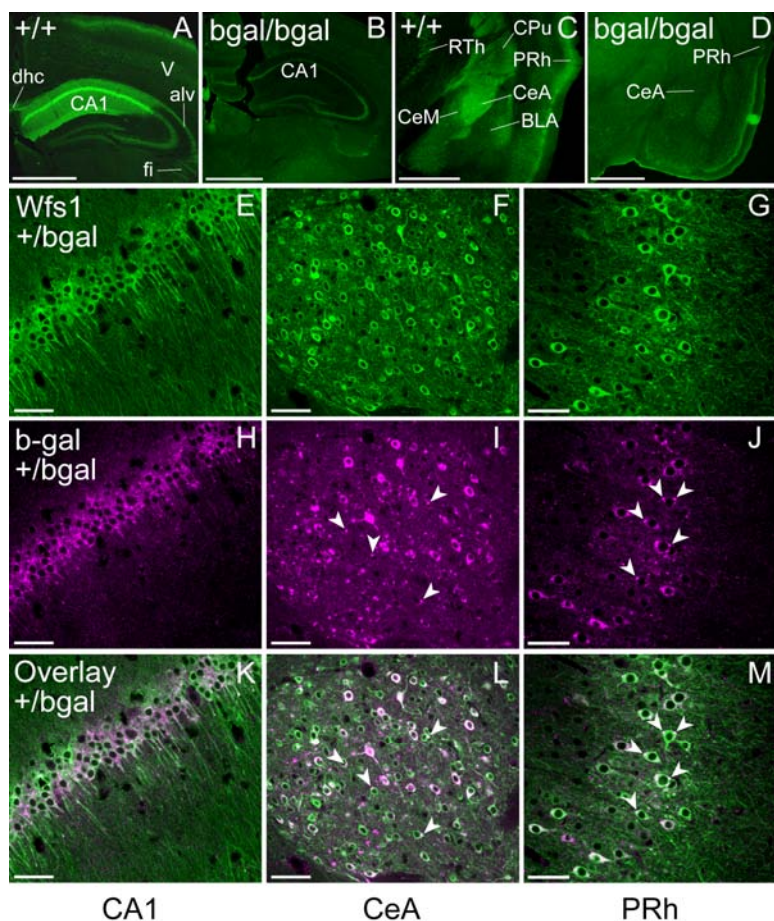


Figure 9. Single- (A–D) and double-label (E–M) immunofluorescent stainings of coronal sections illustrating Wfs1 immunoreactivity (green) in normal (+/+) and Wfs1-deficient mice expressing β -galactosidase reporter enzyme (bgal/bgal), and Wfs1 (green) and β -galactosidase (magenta) immunoreactivities in heterozygous (+/bgal) mice. **A, B:** Unlike normal mice (A), Wfs1-deficient mice (B) display no immunostaining of superficial part of layer 2/3 of neocortex, CA1 field of hippocampus, alveus, fimbria and dorsal hippocampal commissure. In addition, weak punctate Wfs1 staining is seen in neocortical layer V of normal mice (A; for corresponding high power confocal image see Fig. 4B). **C, D:** Unlike normal mice (C), Wfs1-deficient mice (D) display no immunostaining of central amygdaloid nucleus, perirhinal cortex, lateral part of basolateral amygdala, reticular thalamic nucleus and caudal caudate putamen. Weak unspecific staining of piriform cortex is seen in the Wfs1-deficient mice. **E–M:** Confocal images of double immunofluorescent staining of Wfs1 (green) and β -galactosidase (magenta) on coronal brain sections from heterozygous Wfs1^{+/bgal} mice (overlapping of the two signals appears white). There is an almost complete overlap of Wfs1 and β -galactosidase immunoreactivities in Wfs1-positive neurons in hippocampal CA1 region (E, H, K), central amygdaloid nucleus (F, I, L) and perirhinal cortex (G, J, M). Arrowheads mark large aggregates with high β -galactosidase immunoreactivity that are likely due to the cytoplasmic aggregation of Wfs1- β -galactosidase fusion protein. For abbreviations, see Appendix 3. Scale bar = 1 mm in A–D; 50 μ m in E–M.

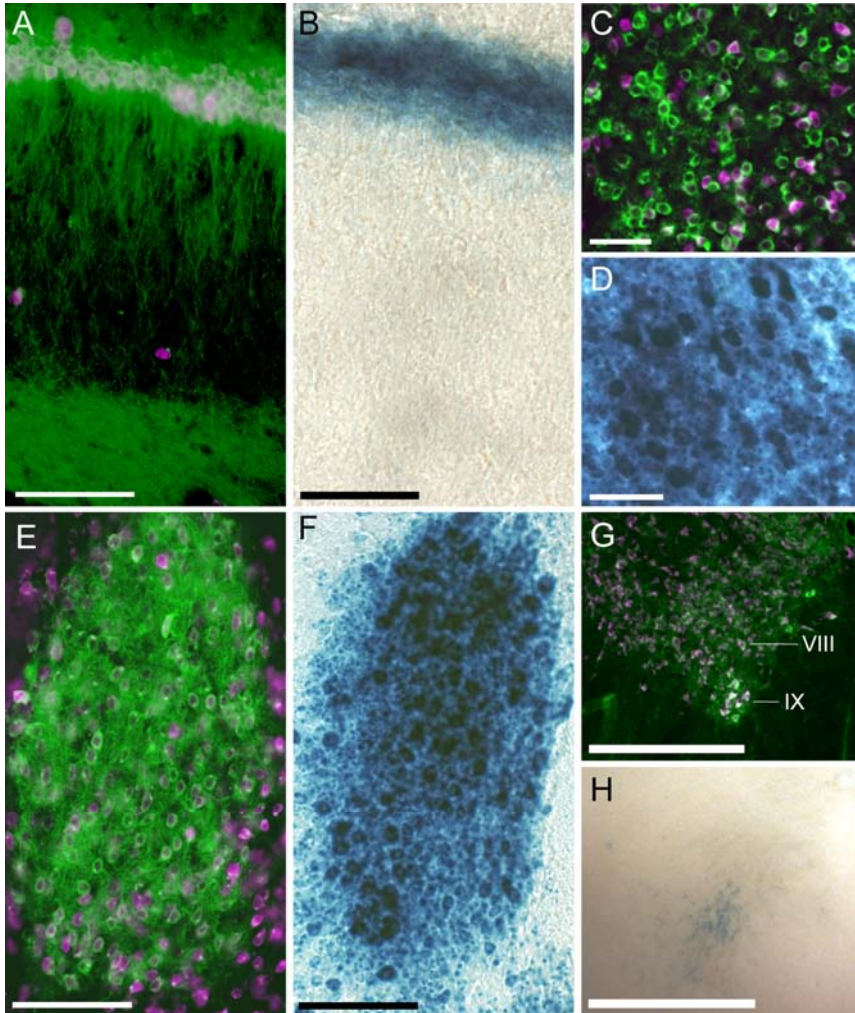


Figure 10. High power micrographs of coronal brain sections illustrating the relationship of Wfs1 immunoreactivity in normal mice and X-gal staining in Wfs1^{bgal/bgal} mice. **A, C, E, G:** Double immunofluorescence micrographs of Wfs1 (green) and NeuN (magenta) immunoreactivity in normal mice. For corresponding X-gal sections of Wfs1^{bgal/bgal} mice see B, D, F, H. **A:** Strong Wfs1 immunoreactivity is present in perikarya, as well as apical and basal dendrites of CA1 pyramidal neurons of hippocampus. A dense plexus of Wfs1 immunoreactive fibers is seen in the stratum lacunosum moleculare, corresponding to terminal arborizations of apical dendrites or incoming fibers from the perforant pathway. **B:** X-gal staining is prominent in pyramidal cell layer and proximal processes only. **C–D:** Very high Wfs1 expression is seen in neuronal perikarya of the central nucleus of amygdala with weaker staining in proximal processes. Note the relatively lower intensity of NeuN staining in highly Wfs1-positive neurons (a similar tendency was observed in other parts of the central extended amygdala). **E–F:** Very high Wfs1 expression is seen in neuronal perikarya and proximal processes of the dorsal part of lateral bed nucleus of stria terminalis. **G–H:** Weak Wfs1 expression is seen in ventral horn neurons corresponding to laminae VIII and IX of a cervical spinal cord segment. Scale bar = 50 μm in A–F; 500 μm in G–H.

Table 8. Distribution of Wfs1 Protein Expressing Cells in the Mouse Central Nervous System¹

Area	Level	Area	Level
Forebrain		Presubiculum	–
<i>Olfactory bulb</i>	–	Parasubiculum	++++
<i>Septum</i>		Diencephalon	
Lateral septal nucleus, dorsal	+++	<i>Hypothalamus</i>	
Lateral septal nucleus, ventral	–	Periventricular nucleus	+
<i>Cerebral cortex</i>		Supraoptic nucleus	+
Orbital cortex	+++	Suprachiasmatic nucleus	+
Prelimbic cortex	+++	Paraventricular nucleus	++
Infralimbic cortex	+++	Dorsomedial hypothalamus,	
Cingulate cortex	+++	compact	++
Insular cortex	++++	Ventromedial hypothalamus	(+) ²
Perirhinal cortex	++++	Arcuate nucleus, ventromedial	+
Postrhinal cortex	++++	Ventral tuberomammillary	
Ectorhinal cortex	+++	nucleus	+
Lateral entorhinal cortex	+++	<i>Thalamus</i>	
Medial entorhinal cortex	+++	Paraventricular thalamic nucleus,	
Auditory cortex	++	anterior	(+) ²
Somatosensory cortex	++	Reticular thalamic nucleus	(+) ²
Motor cortex	++	Zona incerta	(+) ²
Piriform cortex	++	Midbrain	
<i>Basal ganglia and striatum</i>		Inferior colliculus, central nucleus	++
Olfactory tubercle	++++	Substantia nigra, reticular	–
Nucleus accumbens, core	+++	Substantia nigra, compact	–
Nucleus accumbens, shell	+++	Periaqueductal gray	–
Caudate putamen, anterior	–	Ventral tegmental area	–
Caudate putamen, posterior	++	Brainstem	
Marginal zone	+	<i>Sensory nuclei</i>	
Lateral globus pallidus	–	Lateral lemniscus	++
Medial globus pallidus	–	Paralemniscal nucleus	+
Ventral pallidum	–	Rostral periolivary region	++
Lateral stripe of striatum	++	Lateral superior olive	++
<i>Extended amygdala</i>		Superior paraolivary nucleus	++
Central amygdaloid n., lateral		Nucleus of the trapezoid body	+
div.	++++	Principal trigeminal nucleus	+
Central amygdaloid n., capsular div.	++++	Mesencephalic trigeminal nucleus	(+) ²
Central amygdaloid n., medial div.	+	Ventral cochlear nucleus	+
Dorsal part of lateral bed n. of stria		Superficial glial layer of the	
terminalis	++++	cochlear nucleus	+++
Ventral part of lateral bed n. of stria		Vestibular nucleus, medial	+
terminalis	+	Vestibular nucleus, lateral	+
Lateral bed n. of stria terminalis,		<i>Motor nuclei</i>	
posterior	+	Oculomotor nucleus	++
Supracapsular bed n. of stria		Pontine reticular nucleus, oral	+
terminalis	+	Motor trigeminal nucleus	+
Interstitial n. of posterior limb of ant.		Facial nucleus	+
commissure	+++	Inferior olivary nucleus, medial	+
Medial amygdaloid n., posterodorsal	+	Lateral reticular nucleus	+
Medial amygdaloid n., posteroventral	(+) ²	Red nucleus	+
Medial bed n. of stria terminalis	(+) ²		
Sublenticular extended amygdala	–		

Area	Level	Area	Level
<i>Cortical-like amygdala</i>		<i>Other</i>	
Lateral amygdaloid nucleus	(+) ²	Locus coeruleus	(+) ²
Basolateral amygdaloid nucleus, lateral	+	Parabrachial nucleus	–
Basomedial amygdaloid nucleus	(+) ²	Nucleus of the solitary tract	–
Intercalated nuclei of amygdala	+	Cerebellum	
Posterolateral cortical amygdaloid nucleus	+	Medial (fastigial) cerebellar nucleus	+
Cortex-amygdala transition zone	+++	Purkinje cells	(+) ²
Amygdalopiriform transition area	++	Medulla spinalis	
Amygdalostriatal transition area	++	Lamina VIII	+
<i>Hippocampal formation</i>		Lamina IX	+
CA1	++++	Circumventricular organs	
CA2	–	Subfornical organ	(+) ²
CA3	–	Vascular organ of the lam. terminalis	–
Dentate gyrus	–	Subcommissural organ	+++
Subiculum	–	Area postrema	+++

¹ –, not detected; +, low expression; ++, moderate expression; +++, high expression; +++++, very high expression

² low expression level detected by immunohistochemistry only

2.1. Forebrain

Olfactory bulb. No Wfs1 expression was detected in the olfactory bulb (Fig. 11A).

Cerebral cortex. Wfs1-positive cells formed a laminar distribution in the most superficial part of the second and third layers of neocortex and second layer of piriform cortex (Figs. 9A and 11). Very high Wfs1 expression was detected in insular, peri- and postrhinal cortices where it formed a continuous band that progressed along the rhinal fissure and terminated in the postrhinal cortex (Figs. 9C, 11 and 13B). High to moderate Wfs1 expression was detected in ecto- and entorhinal cortices and in the prefrontal cortex including orbital, prelimbic, infralimbic and cingulate cortices. X-Gal staining of medial and lateral entorhinal cortices revealed a dotted pattern of highly Wfs1-positive cell clusters separated by cells with lower Wfs1 expression (Fig. 13H, I). Moderate Wfs1 expression was detected in primary and secondary motor cortices, somatosensory cortex, auditory cortex and piriform cortex. Wfs1 immunoreactive puncta, reminiscent of axo-somatic contacts, were detected in the layer V of the neocortex (Figs. 9A, 12B).

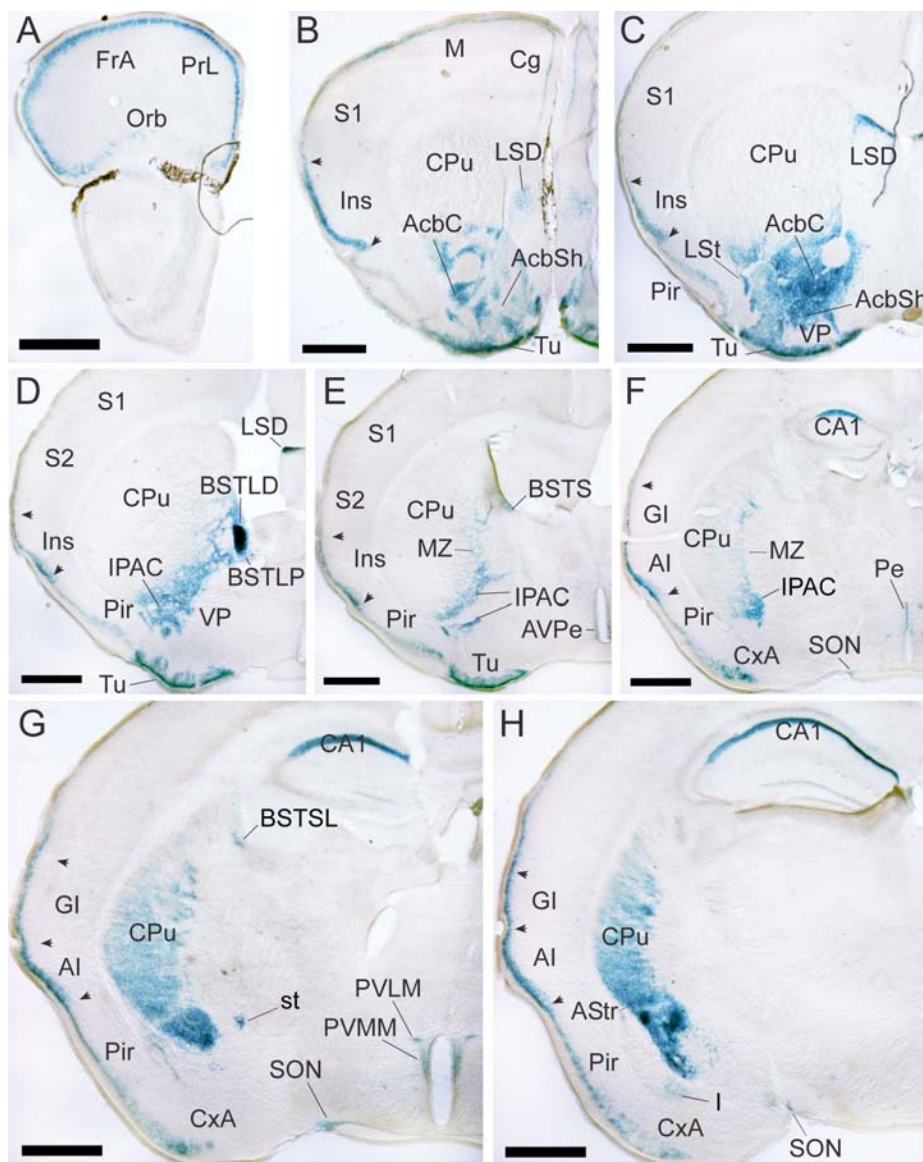


Figure 11. Low power micrographs of X-Gal-stained coronal brain sections illustrating *Wfs1* protein expression pattern in *Wfs1^{bgal/bgall}* mice. In general, blue color indicates the presence of *Wfs1*-positive cell bodies (for exceptions, see section Technical considerations). For abbreviations, see Appendix 3. Scale bar = 1 mm.

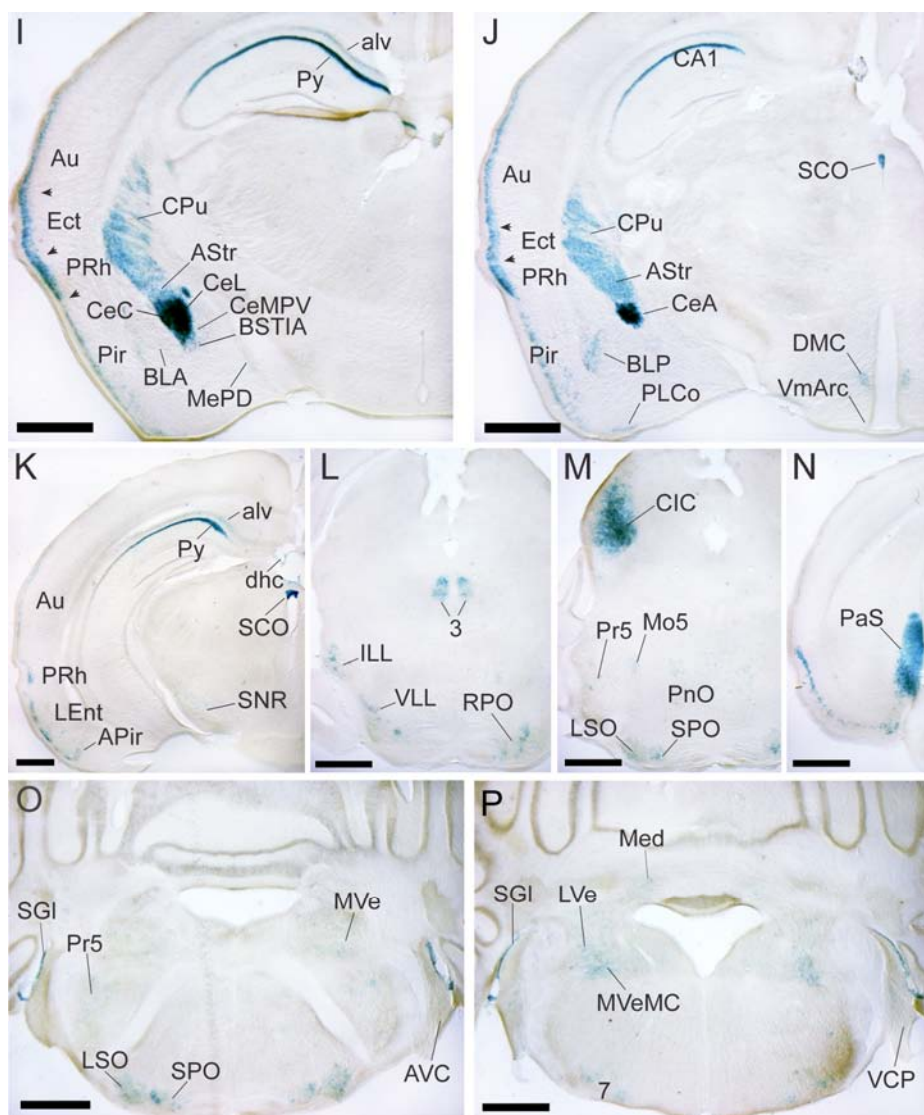


Figure 11 (continued).

Basal ganglia and striatum. Densely distributed, highly Wfs1-positive neurons were detected in the nucleus accumbens, olfactory tubercle and dorsal nucleus of lateral septum (Figs. 11B–C, 12A, 13D). Moderate Wfs1 expression was detected in caudal caudate putamen (Figs. 9C, 11G–J) and lateral stripe of striatum (Fig. 11C). Weak Wfs1 expression was seen in the marginal zone between caudate putamen and lateral globus pallidus (Fig. 11E–F). No Wfs1-expressing cells were found in ventral pallidum, lateral and medial globus pallidus (Fig. 11C–H). Wfs1 immunoreactive fibers were seen in subcommissural ventral pallidum (Figs. 12E and 14G–I), ventral part of rostral lateral globus pallidus (Fig. 12F), posterior caudate putamen (Fig. 14C), and throughout the entire extent of the posterior part of lateral globus pallidus (Fig. 14J–L). In order to verify the localization of Wfs1 positive fibers in the subcommissural ventral pallidum (VP), double staining with pallidal marker Met-enkephalin was used (data not shown). Wfs1 staining overlapped extensively with Met-enkephalin immunoreactivity, but unlike Wfs1 immunoreactivity, which was rather uniform across the extent of VP and appeared slightly more pronounced ventrolaterally, Met-enkephalin staining was the highest in the dorsal and medial aspects of VP and less pronounced in the ventrolateral aspect.

Unlike Met-enkephalin immunoreactivity, Wfs1-positive fibers were not found to extend ventrally into the horizontal diagonal band and magnocellular preoptic area. Wfs1 immunoreactivity in the ventral aspect of the rostral part of lateral globus pallidus (LGP) was also investigated in relation to the pallidal marker Met-enkephalin. An overlap of Wfs1 immunoreactivity with the pallidal marker was only apparent in the ventral aspect of rostral LGP. Low Wfs1 immunoreactivity was also seen in the ventrally adjacent central sublentiform extended amygdala (see below).

Amygdaloid complex and extended amygdala. Very high Wfs1 expression was seen in the lateral and, to a slightly lesser degree, capsular divisions of central amygdaloid nucleus and dorsal part of lateral bed nucleus of stria terminalis (Figs. 9C,F, 10C–F, 11D, I, J, 12H, I and 13F, G). Strong to moderate expression was found in the interstitial nucleus of the posterior limb of the anterior commissure and cortex amygdala transition zone (Figs. 11D–H and 14G). Moderate to weak Wfs1 expression was observed in posterior part of lateral bed nucleus of stria terminalis (Fig. 11D), in a cell-group located rostral to the central amygdaloid complex near the stria terminalis (Fig. 11G), lateral part of basolateral amygdala (Figs. 9C, 11I, J, 12H, I), amygdalostratial and amygdalopiriform transition areas and posterolateral cortical amygdaloid nucleus (Fig. 11H, J, K). Wfs1 expression in basolateral amygdala was verified by double immunostaining with respective marker vesicular acetylcholine transporter (VAcHT), which indicated that the distribution of Wfs1-positive neurons in basolateral amygdala appears to follow a mediolateral gradient that is inverse to that of the VAcHT immunoreactive nerve fibers. Thus the density of Wfs1 immunoreactive neurons was higher along the lateral and dorsolateral borders of anterior and posterior parts of basolateral amygdala where the density of

VACHT immunoreactive fibers was relatively lower (Fig. 12H, I). Weak Wfs1 expression was detected in the medial division of central amygdaloid nucleus (Figs. 9C, 11I), supracapsular bed nucleus of stria terminalis (Fig. 11E), medial amygdaloid nucleus (Fig. 11I), intercalated nuclei of amygdala, posterolateral cortical amygdaloid nucleus (Fig. 11H, J), and ventral part of lateral bed nucleus of stria terminalis (data not shown). Additionally, weakly Wfs1 immunoreactive neurons were detected in the ventral part of lateral amygdaloid nucleus, dorsal part of basomedial amygdaloid nucleus and posterior medial bed nucleus of stria terminalis (data not shown). While X-Gal staining indicated the absence of Wfs1-positive cells in sublenticular extended amygdala (Fig. 11E–F), immunohistochemistry revealed fine Wfs1-positive nerve fibers in the central sublenticular extended amygdala (Fig. 12E–G).

Hippocampal formation. Very high Wfs1 expression was observed in CA1 pyramidal cell layer and parasubiculum (Figs. 10B, 11G–K, N) with considerably weaker staining in alveus and dorsal hippocampal commissure that was found to correspond to Wfs1-positive nerve fibers (see below). Wfs1 immunostaining in wild-type mice revealed strong Wfs1 immunoreactivity in pyramidal cell bodies as well as apical and basal dendritic trees that extend into stratum radiatum and stratum oriens, respectively (Figs. 9A, E and 10A). Prominent Wfs1 immunoreactivity was also seen in stratum lacunosum moleculare corresponding to distal apical dendrites of CA1 pyramidal cells or incoming fibers from the perforant pathway (Witter and Amaral, 2004). Wfs1 immunoreactive nerve fibers were detected in alveus, fimbria, dorsal hippocampal commissure (Fig. 9A) and subiculum (data not shown). No Wfs1 expression was detected in CA2, CA3, dentate gyrus and presubiculum (Fig. 11I, N).

2.2. Diencephalon

Hypothalamus. Moderate Wfs1 expression was detected in the medial and lateral magnocellular divisions of paraventricular nucleus and compact part of the dorsomedial hypothalamic nucleus (Fig. 11G, J). Weak Wfs1 expression was evident in periventricular, supraoptic, ventromedial arcuate and ventral tuberomammillary nuclei (Figs. 11E–G, J, 12E, 13D) and suprachiasmatic nucleus (Fig. 12J). Immunostaining revealed weakly Wfs1 immunoreactive neurons in the ventromedial hypothalamic nucleus (data not shown). Strongly immunoreactive nerve fibers were detected in the medial forebrain bundle (Figs. 12E, F, 14J, M), which likely represent striatofugal axons originating from the nucleus accumbens.

Thalamus. Weak Wfs1 immunoreactivity was found in the reticular thalamic nucleus (Fig. 9C, 12E), zona incerta and anterior paraventricular thalamic nucleus (data not shown).

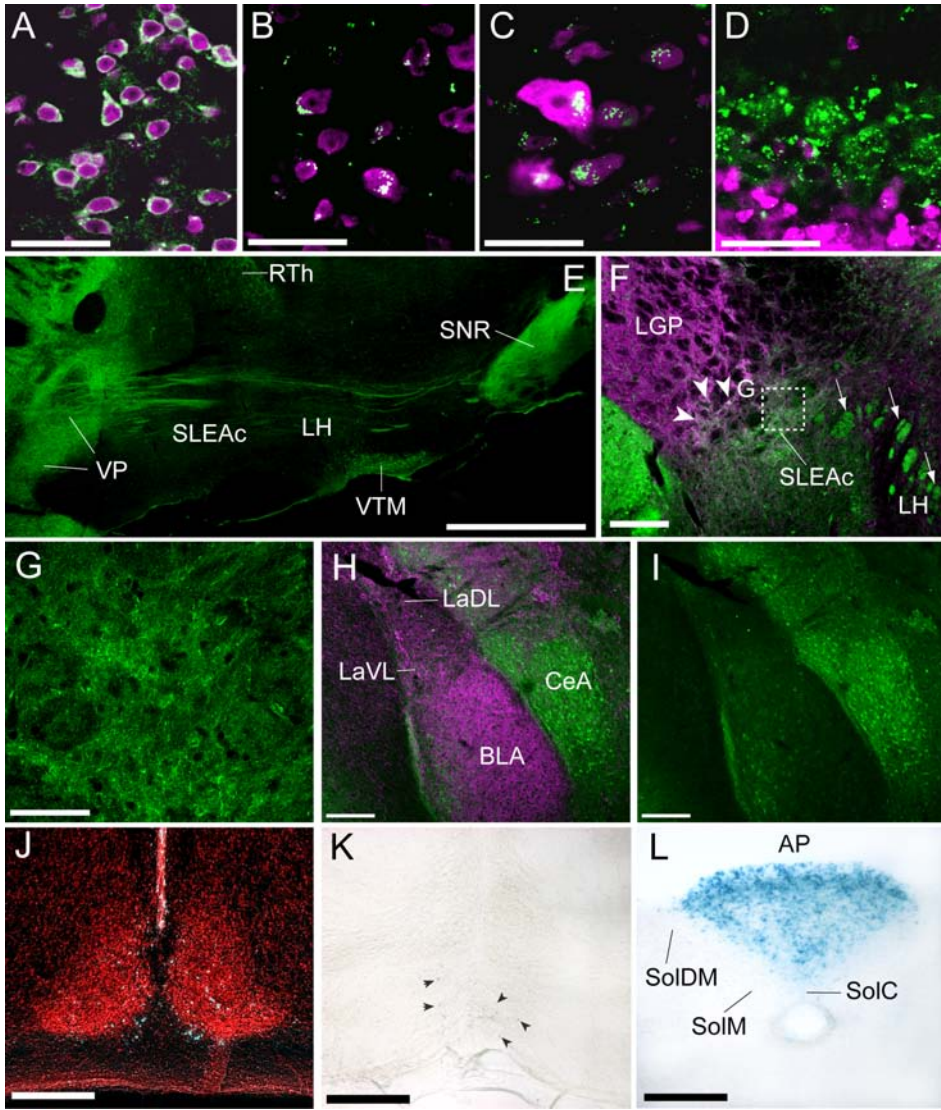


Figure 12. Wfs1 expression in selected regions of the mouse brain. **A–D:** High power confocal images illustrating the distribution of Wfs1 immunoreactivity (green) in relation to neuronal marker NeuN (magenta; overlapping areas appear white). **A:** Extensive overlap of Wfs1 and NeuN immunoreactivity is seen in the neuronal perikarya of nucleus accumbens. **B:** Wfs1 immunoreactive puncta are located on NeuN-positive neurons in layer V of the neocortex. No Wfs1 expression is detectable in layer V neurons. **C:** Wfs1 immunoreactive puncta are located on large NeuN-positive neurons in the mesencephalic trigeminal nucleus. Low level of Wfs1 expression was also detected in these cells. **D:** Wfs1 immunoreactive puncta are seen on cerebellar Purkinje cells and weak staining in the perikarya. Note the absence of NeuN staining in Purkinje cells. **E:** Wfs1 immunoreactive fibers, continuous between ventral pallidum and substantia nigra, are seen in the lateral hypothalamus on a sagittal section through

the basal forebrain cut approximately at 1.20 mm in lateral stereotaxic coordinates. Based on their arrangement, the fibers likely represent striatofugal axons originating from the nucleus accumbens. Low Wfs1 expression is seen in reticular thalamic and ventral tuberomammillary nuclei. **F:** Low power confocal image of Wfs1 (green) and pallidal marker Met-enkephalin (magenta) double immunofluorescent staining on a coronal section through the rostral part of lateral globus pallidus (lateral is to the left, medial to the right; the section corresponds to Fig. 3F). An overlap of Wfs1 and Met-enkephalin immunoreactive nerve fibers is seen in the ventral part of lateral globus pallidus (marked with arrowheads) while not being evident in the rest of the globus pallidus at this level. Fine Wfs1-positive nerve fibers are seen in the central sublentiform extended amygdala (below lateral globus pallidus). Strongly immunoreactive fascicles representing bundles of Wfs1-positive nerve fibers are seen in the lateral hypothalamus (arrows). **G:** High power confocal image of Wfs1 immunoreactive nerve fibers in the central sublentiform extended amygdala from the boxed area in F. **H–I:** Low power confocal image of Wfs1 (green in H, I) and basolateral amygdala marker vesicular acetylcholine transporter (VACHT, magenta in H) double immunofluorescent staining on a coronal section approximately midway through the rostro-caudal extent of the amygdaloid complex (lateral is to the left, medial to the right; the section corresponds to Fig. 3I). High Wfs1 expression is seen in the central amygdaloid nucleus and to a lesser degree in the posterior caudate putamen. Weakly Wfs1-positive cells are seen in the lateral part of the basolateral amygdaloid nucleus. The distribution of Wfs1-positive neurons in the basolateral amygdala appears to follow a mediolateral gradient that is inverse to that of the VACHT immunoreactive nerve fibers. **J:** Weak Wfs1 expression is seen in the suprachiasmatic nucleus. Pseudo color inverted X-Gal staining (cyan) with ethidium bromide counterstain (red). **K:** Coronal section of caudal brainstem showing weak Wfs1 expression in pyramidal decussation by X-Gal staining (arrowheads). **L:** Coronal section of caudal brainstem showing high Wfs1 expression in the area postrema by X-Gal staining. No Wfs1 expression is seen in the solitary nuclear complex. For abbreviations, see Appendix 3. Scale bar = 50 μ m in A–D, G; 1 mm in E; 200 μ m in F, H–L.

2.3. Midbrain and brainstem

Moderate to low Wfs1 expression was found in the central nucleus of inferior colliculus (Fig. 11M). While X-Gal staining indicated weak Wfs1 expression in the reticular part of substantia nigra (Fig. 11K), immunostaining revealed a thick plexus of Wfs1-positive fibers that were directly continuous with Wfs1 immunoreactive fibers in the ventral pallidum and lateral hypothalamus (Fig. 12E). The density of Wfs1-positive fibers was the highest in the dorsomedial and dorsolateral parts of reticular substantia nigra (Fig. 14A, D). A much lower density of Wfs1-positive fibers was detected in the compact part of substantia nigra and ventral tegmental area (Fig. 14A–F). No Wfs1-positive neuronal somata were detected in the substantia nigra, ventral tegmental area and periaqueductal gray.

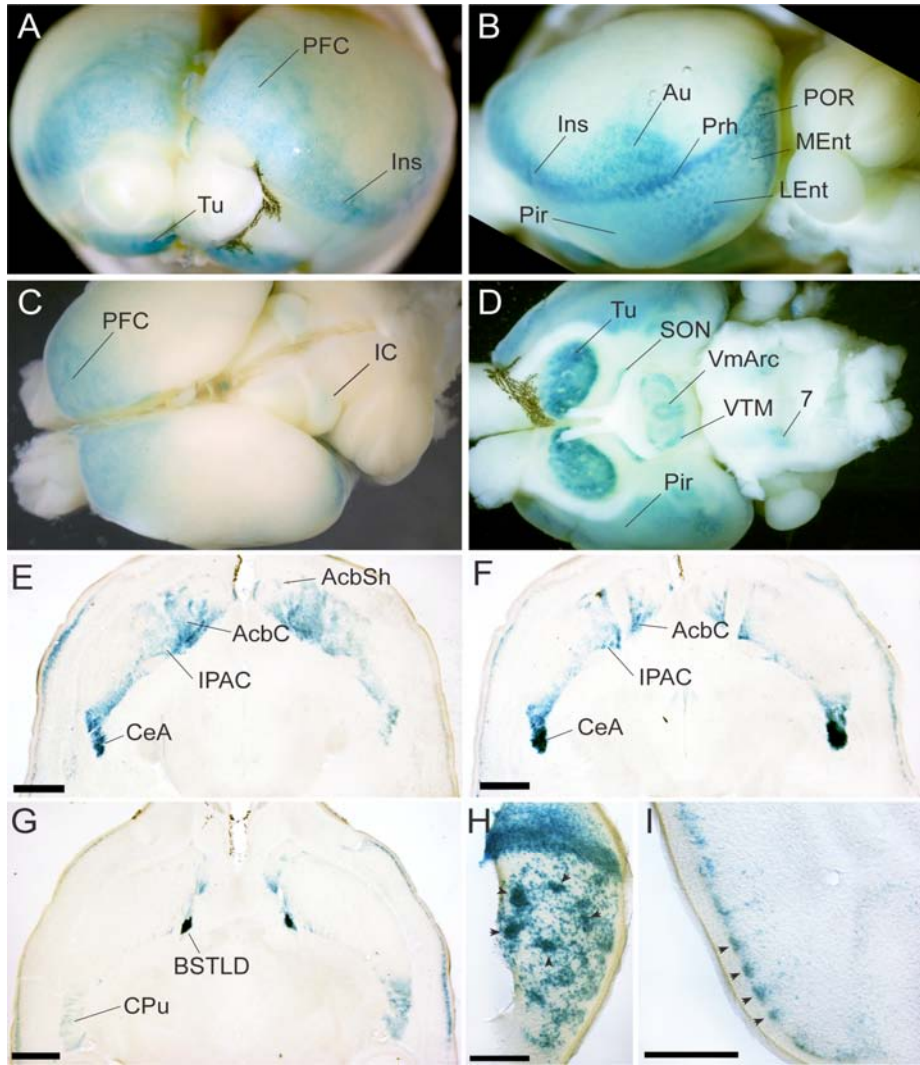


Figure 13. X-Gal staining of β -galactosidase in $Wfs1^{bgal/bgal}$ mice. **A-D:** Rostral, lateral, dorsal and ventral views, respectively, of whole mount brains. **A:** High $Wfs1$ expression is seen in the olfactory tubercle, prefrontal cortex and insular cortex. **B:** High $Wfs1$ expression is seen in insular, perirhinal and postrhinal cortices. Distinct $Wfs1$ expression in auditory cortex is also evident. In lateral and medial entorhinal cortices, a dotted pattern of highly $Wfs1$ -positive cell clusters is seen. **D:** Low $Wfs1$ expression is seen in the hypothalamic supraoptic, ventromedial arcuate and ventral tuberomammillary nuclei and in the facial nucleus. **E-G:** Horizontal sections demonstrating the selective enrichment of $Wfs1$ expression in the central extended amygdala at three levels of the ventral-dorsal axis. Note the continuity of $Wfs1$ expression in the central extended amygdala with nucleus accumbens and posterior caudate putamen. **H-I:** Arrangement of $Wfs1$ -positive neuronal clusters (arrowheads) in the medial (caudal view) and lateral (coronal section) entorhinal cortices, respectively. For abbreviations, see Appendix 3. Scale bar = 1 mm in E-H; 500 μ m in I.

In the upper brainstem, moderate to low Wfs1 expression was detected in oculomotor nucleus, lateral lemniscus including ventral, intermediate and dorsal nuclei (Fig. 11L), in paralemniscal nucleus and red nucleus (data not shown). Wfs1 immunoreactive fibers were found in the lateral lemniscus (data not shown). High Wfs1 expression was detected in the superficial glial layer of the cochlear nucleus (Fig. 11O, P). Moderate expression was observed in the rostral periolivary region, lateral superior olive and superior paraolivary nuclei (Fig. 11L, M, O). Weak Wfs1 expression was found in the oral pontine reticular nucleus, trigeminal motor nucleus, principal trigeminal nucleus (Fig. 11M), medial vestibular nucleus, ventral cochlear nucleus, facial nucleus, lateral vestibular nucleus, mediocaudal medial vestibular nucleus (Fig. 11O, P), and nucleus of the trapezoid body (data not shown). Weak Wfs1 immunoreactivity was seen in the neurons of the mesencephalic trigeminal nucleus, which also appeared to carry prominent Wfs1 immunoreactive puncta (Fig. 12C). Weakly Wfs1 immunoreactive neurons were found in the locus coeruleus, no Wfs1 expression was detected in the parabrachial nucleus (data not shown). In the caudal brainstem, weak Wfs1 expression was seen in the pyramidal decussation (Fig. 12K), lateral reticular nucleus and medial nucleus of the inferior olive (data not shown). No Wfs1 expression was detected in the solitary nuclear complex (data not shown).

2.4. Cerebellum

Weak Wfs1 expression was seen in the medial cerebellar nucleus (Fig 11P). No Wfs1 expression was detected in cerebellar cortex by X-Gal staining (Fig. 11O, P). However, immunohistochemistry revealed prominent Wfs1 immunoreactive puncta on Purkinje cells and low immunoreactivity in the perikarya (Fig 12D).

2.5. Spinal cord

In cervical spinal cord, low Wfs1 expression was seen in the ventral horn neurons corresponding to laminae VIII and IX (Fig. 10G, H). Wfs1 expression in lower segments of the spinal cord was not investigated.

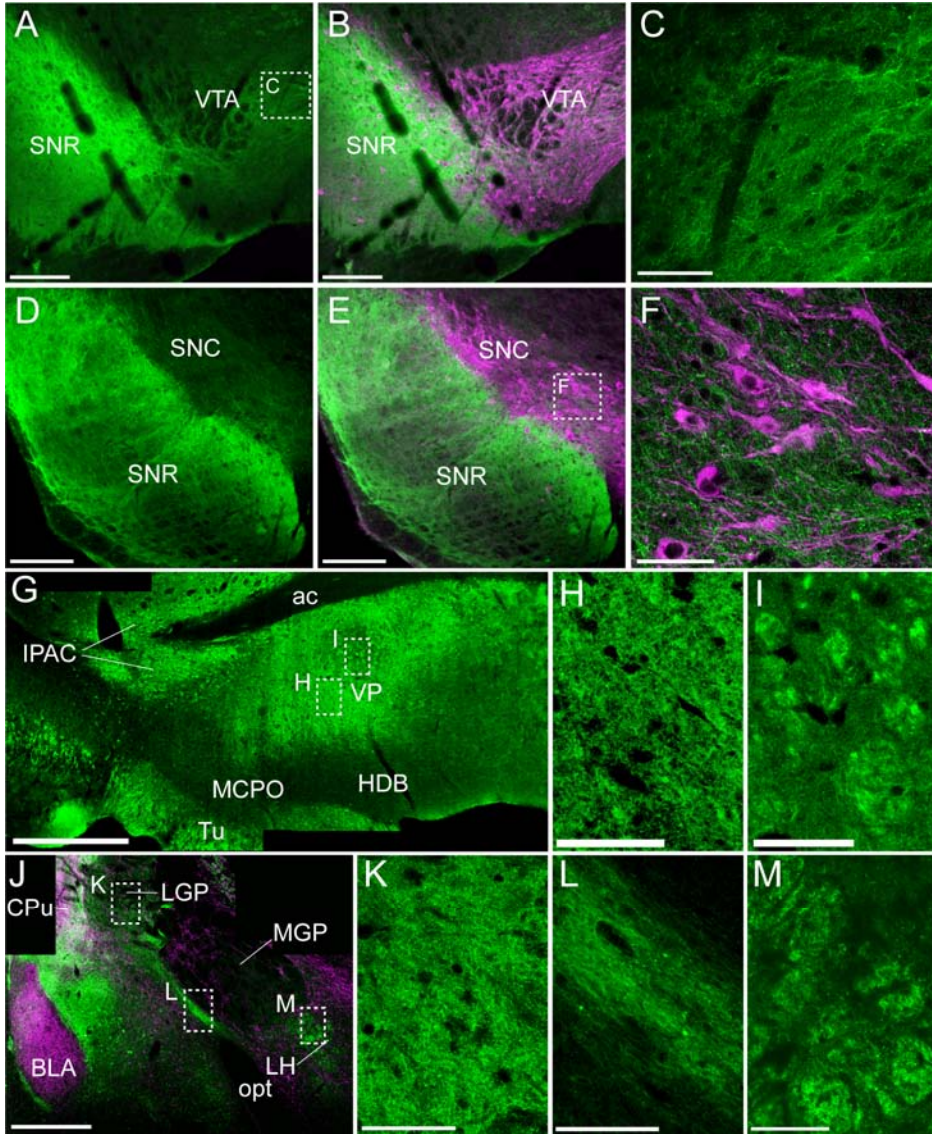


Figure 14. Distribution of Wfs1 immunoreactive nerve fibers in the midbrain (A–F) and basal forebrain (G–M). Confocal images of double immunofluorescent staining of Wfs1 (green) and dopaminergic neuron marker tyrosine hydroxylase (TH; magenta in B, E, F), or vesicular acetylcholine transporter (VACHT; magenta in J) on coronal sections of normal mouse brain (lateral is to the left, medial to the right). **A–B:** A high density of Wfs1 immunoreactive nerve fibers is seen in the reticular substantia nigra, especially in the dorsomedial part. Substantially lower amount of Wfs1 immunoreactivity is located in the nerve fibers found in the ventral tegmental area. **C:** High power confocal image of the boxed area in B, showing Wfs1 immunoreactive nerve fibers in the ventral tegmental area. **D–E:** High Wfs1 immunoreactivity is seen in the nerve fibers located in the dorsomedial and dorsolateral parts of the reticular substantia nigra, and to a lesser degree ventrally. Wfs1 immunoreactivity in the compact part of substantia nigra

is much lower. **F:** High power confocal image of the boxed area in E, showing a network of Wfs1-positive nerve fibers among the TH immunoreactive neurons in the compact part of substantia nigra. **G:** Composite image of low power confocal images demonstrating the arrangement of Wfs1 immunoreactive nerve fibers in the sub-commissural ventral pallidum. This coronal section through the basal forebrain is cut at the level where the limbs of the anterior commissure meet (the section is located slightly caudally from the one depicted in Fig. 3D). Very fine Wfs1 immunoreactive fibers are dispersed throughout the ventral pallidum (see inset H). Dorsomedially in the ventral pallidum, a circular area with a diameter of roughly 100 μm was found to contain Wfs1 immunoreactive fascicles (see inset I). No Wfs1-positive neuronal somata were found in the ventral pallidum. **H:** High power confocal image of the boxed area in the ventral aspect of ventral pallidum showing a high density of very fine Wfs1 immunoreactive nerve fibers. **I:** High power confocal image of the boxed area in the dorsomedial part of ventral pallidum showing Wfs1 immunoreactive fascicles. **J:** Composite image of double immunofluorescent confocal images demonstrating the localization of Wfs1 immunoreactivity (green) in the caudal part of lateral globus pallidus. VACHT staining (magenta) is used to indicate the location of the basolateral amygdaloid nucleus and caudate putamen. The coronal section through the basal forebrain is cut approximately at -1.34 mm from the bregma. A dorsoventral gradient of Wfs1 immunoreactivity is apparent in the lateral globus pallidus as nerve fibers converge ventrally to form a large Wfs1 immunoreactive bundle. Most likely, these fibers represent axons of Wfs1-positive neurons in the caudal caudate putamen. **K:** High power confocal image of the boxed area in the dorsal part of lateral globus pallidus in J, demonstrating a dense network of fine Wfs1 immunoreactive fibers. **L:** High power confocal image of the boxed area in J representing a large Wfs1-positive fiber bundle that emerges ventrally from the lateral globus pallidus. **M:** High power confocal image of the boxed area in the lower right part of J representing large Wfs1 immunoreactive fascicles in the lateral hypothalamus. For abbreviations, see Appendix 3. Scale bar = 250 μm in A, B, D, E; 50 μm in C, F, H, I, K-M; 500 μm in G, J.

2.6. Circumventricular organs

Strong Wfs1 expression was seen in subcommissural organ and area postrema (Figs. 11J, K and 12L). Weak Wfs1 immunoreactivity was evident in subfornical organ, no Wfs1 immunoreactivity was detected in vascular organ of lamina terminalis (data not shown).

3. Study 3: The behavioral profile of Wfs1-deficient mice

3.1. Reproduction and overt appearance

Analysis of reproduction rates of Wfs1-deficient mice during 5 months in late 2007 and early 2008 (a total of 526 births was recorded during the period) indicated an approximately 5 % lower birthrate of homozygous Wfs1-deficient

mice than expected (20.8 % of all females, 21.8 % of all males). In general, homozygous *Wfs1*-deficient mice were normal in overt appearance, but occasionally very small individuals (weighing around 15 grams at 3 months of age) were present in the male population. The most peculiar aspect of the overt phenotype of homozygous *Wfs1*-deficient population was the presence of individuals producing spontaneous audible vocalizations in the 10 kHz range. The proportion of such individuals varied across different batches from around 15 to 50 percent, and was comparable in males and females. The vocalizations can be described as "chirps" with a fundamental frequency of 3.1 kHz and prominent harmonics at 6.2 and 9.3 kHz (Figure 15). It was noted that the number of mice producing audible vocalizations was higher under stressful conditions (bright light, handling/ injection stress), that the temporal frequency of these calls could get as high as 5 times per second, and that the calls could vary in loudness. Additionally, in most individuals, calling was blocked by the administration of diazepam (1 mg/ml).

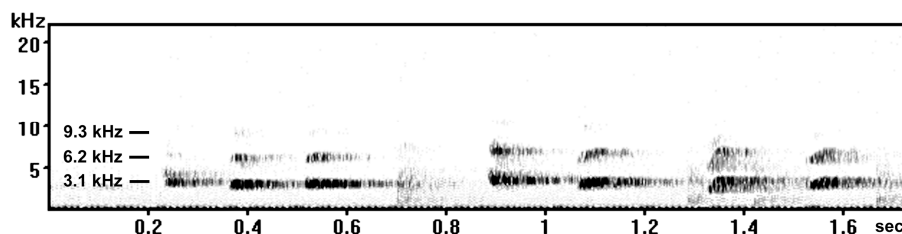


Figure 15. Sonogram of spontaneous audible vocalizations produced by homozygous *Wfs1*-deficient mice.

3.2. Body weight and glucose tolerance test

In the first batch of 2- and 3-month-old mice, significantly lower body weight was found in homozygous *Wfs1*-deficient mice when compared to wild type littermates (Figure 16A) ($F(1, 105) = 60.8, p < 0.001$ (genotype); $F(1, 105) = 7.9, p < 0.01$ (age, between-subjects); $F(1, 105) = 2.46, p = 0.12$ (genotype x age)). In contrast to wild-types, there was no significant body weight difference between 2- and 3-month-old *Wfs1*-deficient mice. In a different batch of mice, significant body weight difference between homozygous *Wfs1*-deficient and wild-type mice was established only at four months of age (Figure 16B). Weight gain between 2 and 4 months of age was more pronounced in wild-type and heterozygous *Wfs1*-deficient mice when compared to homozygous mice ($F(2, 27) = 6.7, p < 0.01$ (genotype); $F(1, 27) = 11.9, p < 0.01$ (age, within-subjects); $F(2, 27) = 0.54, p = 0.59$ (genotype x age)).

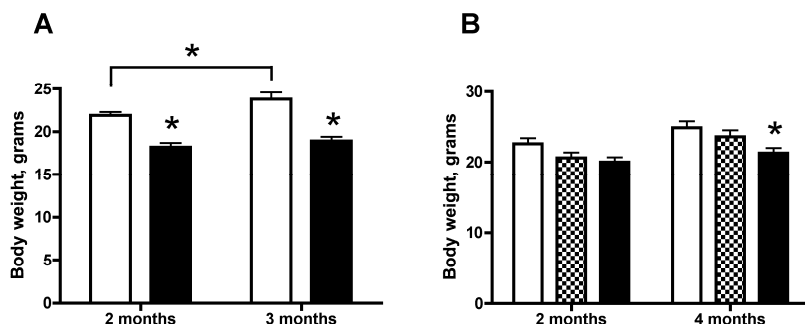


Figure 16. Lower body weight in homozygous Wfs1-deficient mice. **A.** Body weight of wild-type (white bars) and homozygous Wfs1-deficient mice (black bars) at two and three months of age. (*) $p < 0.05$ (unless indicated otherwise, compared to wild-type mice of respective age; Newman-Keuls test after significant two-way ANOVA). Number of mice in groups ranged from 22 to 30. **B.** Weight gain in wild-type (white bars), heterozygous (hatched bars) and homozygous (black bars) Wfs1-deficient mice. (*) $p < 0.05$ (compared to wild-type mice of respective age; Newman-Keuls test after significant repeated measures ANOVA). Number of mice in each group was 10.

Baseline blood glucose levels did not differ between non-fasted wild-type, heterozygous and homozygous Wfs1-deficient mice (Figure 17). Intraperitoneal administration of glucose elevated blood glucose levels only in heterozygous and homozygous Wfs1-deficient mice ($F(2, 27) = 1524.4$, $p < 0.001$ (genotype); $F(3, 27) = 81.5$, $p < 0.001$ (time, within-subjects); $F(6, 27) = 23.5$, $p < 0.001$ (genotype x time)). Compared to the baseline, in homozygous mice, the concentration of blood glucose was significantly higher at 30 and 60 minutes ($p < 0.001$), and in heterozygous mice at 30 minutes ($p < 0.001$) after the administration of glucose.

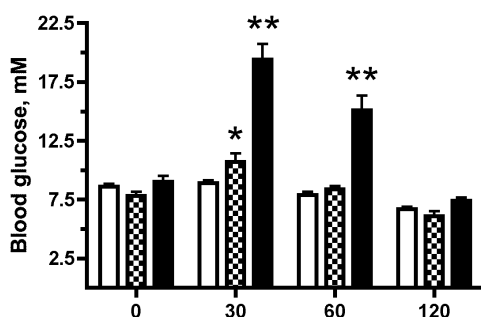


Figure 17. Intolerance to intraperitoneal glucose in non-fasted Wfs1-deficient mice. Blood glucose concentration after i.p. administration of glucose (2 g/kg). White bars – wild-type mice, hatched bars – heterozygous Wfs1-deficient mice, black bars – homozygous Wfs1-deficient mice. (*) $p < 0.05$ (compared to wild-type mice at respective time point; Newman-Keuls test after significant repeated measures ANOVA); (**) $p < 0.001$. Number of mice in each group was 10.

3.3. Stress-induced changes in corticosterone levels

No differences in mean blood plasma corticosterone levels were detected in unstressed individuals of different genotypes (Figure 18). Stress induced by handling and injection of saline induced a significantly larger increase in the plasma corticosterone concentration in homozygous *Wfs1*-deficient mice ($p < 0.05$) when compared to their wild-type littermates ($F(1, 12) = 30.9, p < 0.001$ (genotype); $F(1,12) = 128.8, p < 0.001$ (injection, between-subjects); $F(1,12) = 26.6, p < 0.001$ (genotype x injection)).

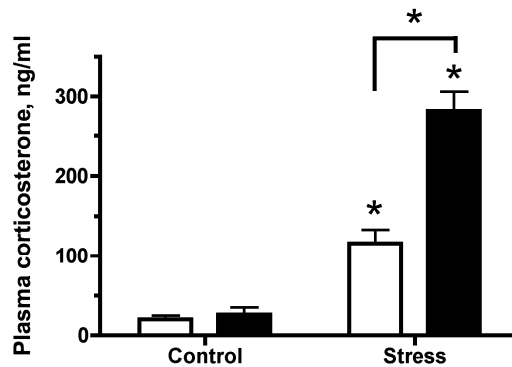


Figure 18. Stress induces higher levels of plasma corticosterone in *Wfs1*-deficient mice. White bars – wild-type mice, black bars – homozygous *Wfs1*-deficient mice. (*) $p < 0.05$ (unless indicated otherwise, compared to unstressed individuals of respective genotype; Newman-Keuls test after significant two-way ANOVA). Number of mice in each group was 4.

3.4. Stress-induced analgesia

In both, wild-type and homozygous *Wfs1*-deficient mice, the degree of analgesia was dependent on the intensity of electric footshocks (Figure 19) ($F(3, 77) = 54.4, p < 0.001$ (stress, between-subjects)). Footshocks of intermediate intensity (0.4 mA) induced a significantly stronger analgetic response in homozygous *Wfs1*-deficient mice compared to their wild-type littermates ($F(1, 77) = 5.5, p < 0.05$ (genotype); $F(3, 77) = 3.3, p < 0.05$ (genotype x stress)).

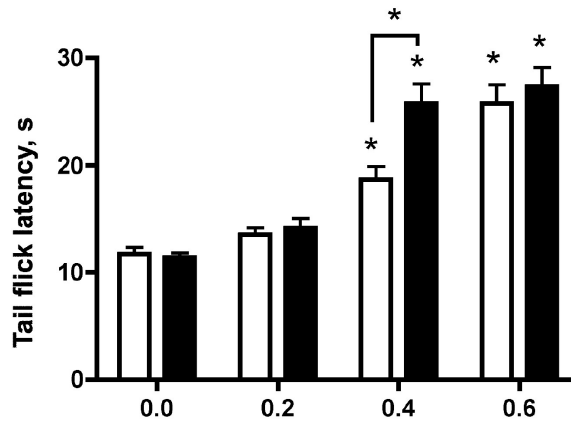


Figure 19. Stress-induced analgesia in Wfs1-deficient mice. White bars – wild-type mice, black bars – homozygous Wfs1-deficient mice. (*) $p < 0.05$ (unless indicated otherwise, compared to unstressed littermates of respective genotype; Newman-Keuls test after significant two-way ANOVA). Number of mice in groups ranged from 10 to 12.

3.5. Rota-rod test

Performance of wild-type (119 ± 1 s; $n = 14$) and homozygous Wfs1-deficient mice (110 ± 7 s; $n = 21$) was statistically not different in the rota-rod test.

3.6. Locomotor activity in dim and bright environments

Locomotor activity of wild-type and homozygous Wfs1-deficient mice was compared in a dimly (~ 20 lx) and brightly (~ 450 lx) lit room (Figure 20). Exposure of mice to bright light decreased all locomotor activity parameters in both genotypes in relation to the dim environment (time in locomotion: $F(1, 37) = 116.1$, $p < 0.001$ (environment, within-subjects)); distance travelled: $F(1, 37) = 93.4$, $p < 0.001$; time spent in the centre: $F(1, 37) = 39.5$, $p < 0.001$; number of rearing: $F(1, 37) = 17.1$, $p < 0.001$). In the dark room, homozygous Wfs1-deficient mice made significantly less rearings ($p < 0.05$) while the other parameters were similar in the genotypes. Locomotor activity was significantly lower in Wfs1-deficient mice under bright light (time in locomotion: $F(1, 37) = 10.6$, $p < 0.01$ (genotype); $F(1, 37) = 1.87$, $p = 0.18$ (genotype x environment); distance travelled: $F(1, 37) = 8.1$, $p < 0.01$ (genotype); $F(1, 37) = 1.70$, $p = 0.20$ (genotype x environment); time spent in the centre: $F(1, 37) = 2.66$, $p = 0.11$ (genotype), $F(1, 37) = 0.19$, $p = 0.62$ (genotype x environment); number of rearing: $F(1, 37) = 7.3$, $p < 0.05$ (genotype), $F(1, 37) = 0.02$, $p = 0.90$ (genotype x environment)).

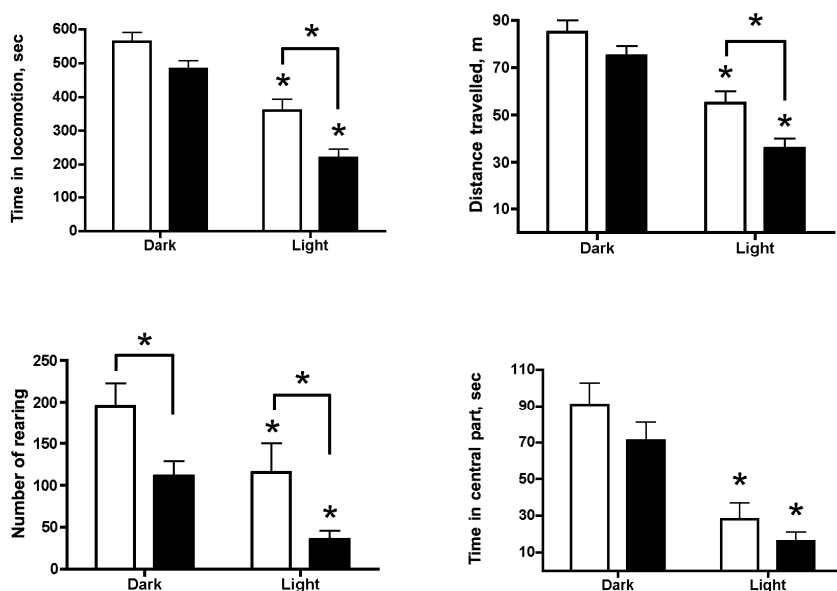


Figure 20. Lower exploratory activity in *Wfs1*-deficient mice at high illumination levels. White bars – wild-type mice ($n = 20$), black bars – homozygous *Wfs1*-deficient mice ($n = 19$). (*) $p < 0.05$ (unless indicated otherwise, compared to respective genotype in the dark environment; Newman-Keuls test after significant repeated measures ANOVA).

3.7. Effect of amphetamine and apomorphine on locomotor activity

Administration of amphetamine (2.5, 5, 7.5 mg/kg) induced a dose-dependent activation of locomotor behavior in wild-type mice (Figure 21). The stimulatory effect of amphetamine was weaker in heterozygous and homozygous *Wfs1*-deficient mice than in wild-type littermates (time in locomotion: $F(2, 27) = 5.78$, $p = 0.008$ (genotype), $F(3, 81) = 109.2$, $p < 0.001$ (treatment, within-subjects), $F(6, 81) = 0.57$, $p = 0.76$ (genotype x treatment); distance travelled: $F(2, 27) = 4.1$, $p < 0.05$ (genotype), $F(3, 81) = 59.3$, $p < 0.001$ (treatment, within-subjects), $F(6, 81) = 1.12$, $p = 0.36$ (genotype x treatment); number of corner entries: $F(2, 27) = 3.1$, $p = 0.06$ (genotype); $F(3, 81) = 34.7$, $p < 0.001$ (treatment, within-subjects); $F(6, 81) = 1.05$, $p = 0.40$ (genotype x treatment)).

The stimulatory effect of intermediate dose of amphetamine (5 mg/kg) on locomotor activity was significantly weaker in homozygous *Wfs1*-deficient mice than in wild-type littermates in terms of distance travelled and number of corner entries ($p < 0.05$). By contrast, treatment of the same mice with apomorphine (3 mg/kg) induced significantly higher locomotor activation in homozygous *Wfs1*-deficient mice when compared to the other genotypes (time

in locomotion: $F(2, 27) = 5.62, p < 0.01$ (genotype), $F(1, 27) = 29, p < 0.001$ (treatment, within-subjects), $F(2, 27) = 0.89, p = 0.42$ (genotype x treatment); distance travelled: $F(2, 27) = 5.62, p < 0.01$ (genotype), $F(1, 27) = 27.3, p < 0.001$ (treatment, within-subjects), $F(2, 27) = 0.54, p = 0.59$ (genotype x treatment); number of corner entries: $F(2, 27) = 3.74, p < 0.05$ (genotype), $F(1, 27) = 44.6, p < 0.001$ (treatment, within-subjects), $F(2, 27) = 0.18, p = 0.83$ (genotype x treatment)). A gene dose effect of *Wfs1* was apparent for all parameters presented in Figure 21.

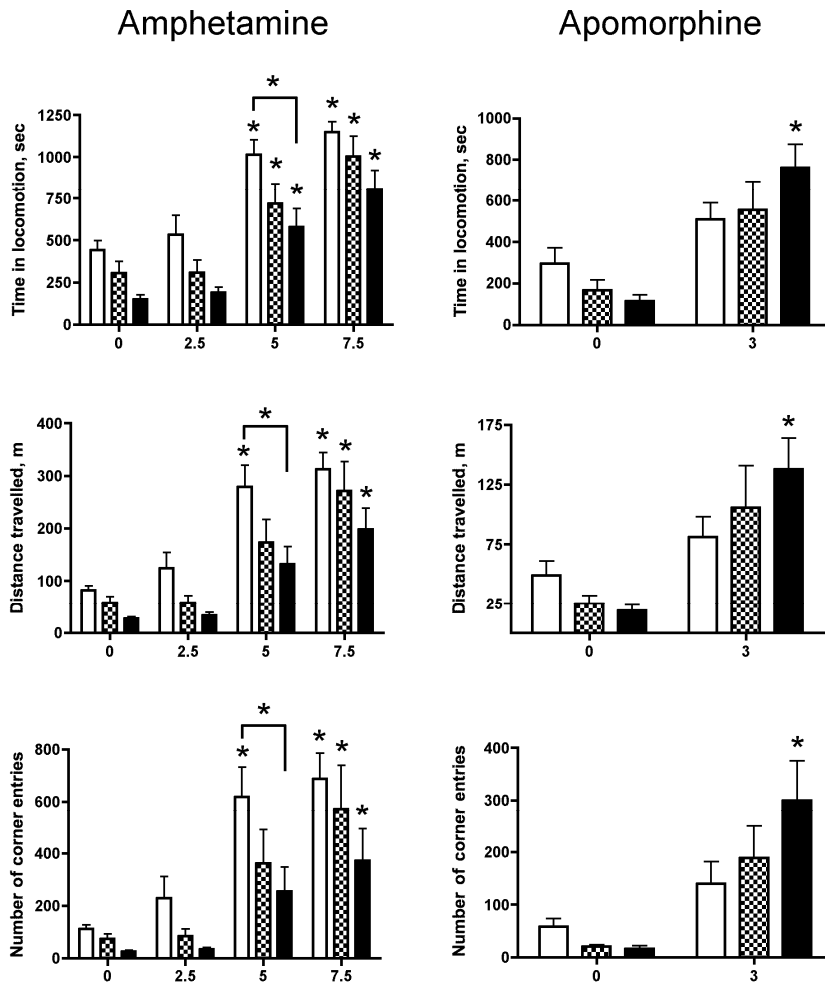


Figure 21. Differential sensitivity of *Wfs1*-deficient mice to the locomotor stimulatory effects of amphetamine (2.5, 5, 7.5 mg/kg) and apomorphine (3 mg/kg). White bars – wild-type mice, hatched bars – heterozygous *Wfs1*-deficient mice, black bars – homozygous *Wfs1*-deficient mice. (*) $p < 0.05$ (unless indicated otherwise, compared to saline-treated mice of respective genotype; Newman-Keuls test after significant repeated measures ANOVA). Number of animals in each group was 10.

3.8. Effect of short-term isolation on exploratory activity in light-dark test

The exploratory activity of non-isolated wild-type and homozygous *Wfs1*-deficient mice was not different in the dark/light box exploration test (Figure 22). By contrast, short-term isolation induced a significant suppression of exploratory behavior only in *Wfs1*-deficient mice. *Wfs1*-deficient mice made less transitions between the two compartments ($F(1, 42) = 8.40, p < 0.01$ (genotype); $F(1, 42) = 0.96, p = 0.33$ (isolation, between-subjects); $F(1, 42) = 2.99, p = 0.09$ (genotype x isolation)) and spent less time in the light compartment as compared to wild-type littermates ($F(1, 42) = 9.32, p < 0.01$ (genotype); $F(1, 42) = 3.41, p = 0.07$ (isolation, between-subjects); $F(1, 42) = 0.92, p = 0.34$ (genotype x isolation)).

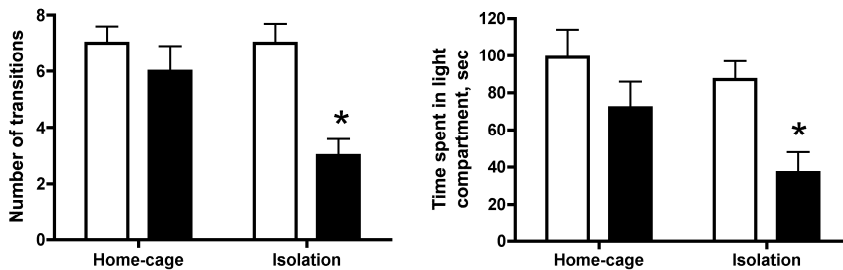


Figure 22. Anxiety-like behavior in *Wfs1*-deficient mice in light/dark exploration test. White bars – wild-type mice, black bars – homozygous *Wfs1*-deficient mice. (*) $p < 0.05$ (compared to isolated wild-type mice; Newman-Keuls test after significant two-way ANOVA). Number of animals in groups ranged from 11 to 12.

3.9. The effect of diazepam in elevated plus-maze

Vehicle-treated homozygous *Wfs1*-deficient mice displayed lower exploratory activity when compared to vehicle-treated wild-types (Figure 23). Specifically, the percentage of open arm entries and the number of head-dippings was significantly lower in *Wfs1*-deficient mice (Newman-Keuls test, $p < 0.05$). A similar, albeit not statistically significant, trend was observed for the number of open arm entries and time spent on open arms. Additionally, the number of incomplete attempts to enter the central platform, a measure of risk assessment behavior (Nelovkov *et al.*, 2006), was significantly higher in homozygous *Wfs1*-deficient mice when compared to wild-type littermates. Exploratory activity of wild-type mice was not affected by the administration of diazepam (1 mg/kg). In *Wfs1*-deficient mice, the administration of diazepam caused a robust anxiolytic-like effect as evidenced by increased number of open arm entries ($F(1, 60) = 0.01, p = 0.99$ (genotype); $F(1, 60) = 6.19, p < 0.01$ (treatment, between-subjects); $F(1, 60) = 3.72, p < 0.05$ (genotype x treatment)), increased time spent on open arms

($F(1, 60) = 0.46, p = 0.50$ (genotype); $F(1, 60) = 6.18, p < 0.01$ (treatment, between-subjects); $F(1, 60) = 2.75, p = 0.10$ (genotype x treatment)), increased percentage of open arm entries from total arm entries ($F(1, 60) = 0.18, p = 0.67$ (genotype); $F(1, 60) = 6.08, p < 0.05$ (treatment, between-subjects); $F(1, 60) = 4.65, p < 0.05$ (drug x treatment)), increased number of head-dippings ($F(1, 60) = 9.16, p < 0.01$ (genotype); $F(1, 60) = 3.44, p = 0.06$ (treatment, between-subjects); $F(1, 60) = 2.30, p = 0.13$ (genotype x treatment)) and decreased number of incomplete attempts to enter the central platform ($F(1, 60) = 2.08, p = 0.15$ (genotype); $F(1, 60) = 5.31, p < 0.05$ (treatment, between-subjects); $F(1, 60) = 1.28, p = 0.26$ (genotype x treatment)).

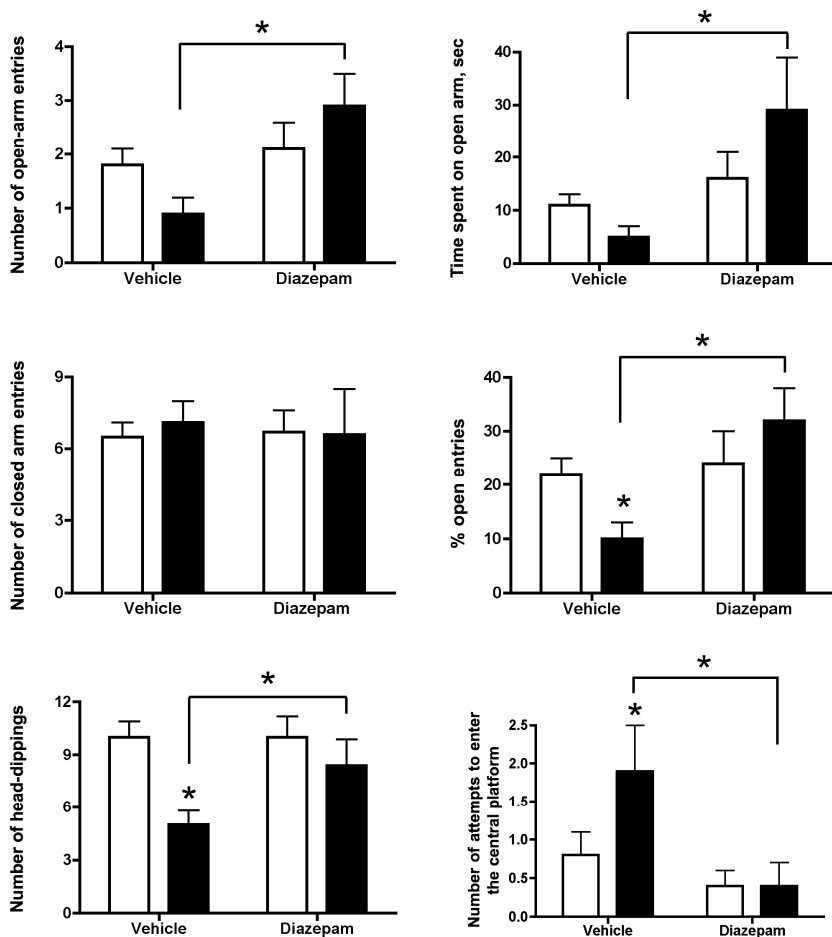


Figure 23. Anxiolytic effect of diazepam (1 mg/kg) on exploratory behavior of Wfs1-deficient mice in the elevated plus-maze. White bars – wild-type mice, black bars – homozygous Wfs1-deficient mice. (*) $p < 0.05$ (unless indicated otherwise, compared to vehicle-treated wild-type mice; Newman-Keuls test after significant two-way ANOVA). Number of animals in each group was 16.

3.10. Fear conditioning test

Homozygous Wfs1-deficient and wild-type mice exhibited comparably low freezing behavior in the pre-conditioning test (no freezing in wild-type, 2 freezing episodes in Wfs1-deficient mice). Both genotypes exhibited normal contextual memory after conditioning by increased freezing in the absence of the conditioned stimulus (Figure 24A). However, in the Wfs1-deficient mice, there was also a tendency towards the reduced number of rearings compared to wild-type littermates (Student's t-test, $p < 0.05$). When transferred to a new context, both, freezing behavior and rearing were similar to that observed in the pre-conditioning session (Figure 24B). Testing of cued fear by presenting the conditioned stimulus in the novel context produced a significant increase in freezing behavior ($F(1, 66) = 1.57$, $p = 0.21$ (genotype); $F(1, 66) = 152.1$, $p < 0.001$ (conditioned stimulus, within-subjects); $F(1, 66) = 0.42$, $p = 0.52$ (genotype x conditioned stimulus)) and a decrease in rearing ($F(1, 66) = 8.02$, $p < 0.01$ (genotype); $F(1, 66) = 30.6$, $p < 0.001$ (conditioned stimulus, within-subjects); $F(1, 66) = 10.3$, $p < 0.01$ (genotype x conditioned stimulus)) in both genotypes. Reduction in the number of rearings upon CS presentation was statistically significant only in wild-type mice ($p < 0.05$). While there was a tendency towards reduced rearing in Wfs1-deficient mice in the cued situation, floor-effect is a likely explanation of it not reaching statistical significance.

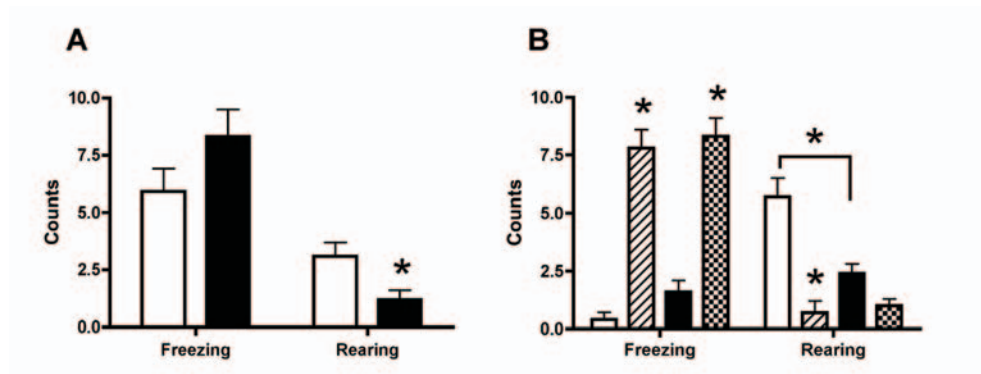


Figure 24. Contextual and cue-dependent responses in Wfs1-deficient mice in fear conditioning. **A.** Contextual fear. White bars – wild-type mice, black bars – homozygous Wfs1-deficient mice. (*) $p < 0.05$ (compared to wild-type mice, Student's t-test). **B.** Cued fear. White bars – wild-type mice in new context, striped bars – wild-type mice exposed to cued signal in new context, black bars – homozygous Wfs1-deficient mice in new context, hatched bars – homozygous Wfs1-deficient mice exposed to cued signal in new context. (*) $p < 0.05$ (unless indicated otherwise, compared to same mice in non-cued situation; Neuman-Keuls test after significant repeated measures ANOVA). Thirty-four wild-type and 33 Wfs1-deficient mice were used in this experiment.

3.12. Hyponeophagia test

Latency to start eating was significantly longer (Student's t-test, $p < 0.05$) in homozygous Wfs1-deficient mice (162 ± 8 sec; $n = 19$) when compared to wild-type littermates (135 ± 10 sec; $n = 19$).

3.13. Forced swimming test

Forced swimming did not reveal statistically significant differences between wild-type and homozygous Wfs1-deficient mice. For the following parameters the values (in seconds) for wild-type and Wfs1-deficient mice were, respectively: 39 ± 1.3 and 36 ± 2.4 (immobility), 5.2 ± 0.6 and 8.7 ± 2.4 (swimming), 3.9 ± 1.2 and 2.9 ± 1.3 (climbing).

3.14. Morris water maze test

Both, wild-type and homozygous Wfs1-deficient mice displayed significant learning effect as evidenced by preference for the target quadrant in probe trial on day 4 (Figure 25A) ($F(1, 148) = 0.001$, $p = 0.99$ (genotype); $F(3, 148) = 87.3$, $p < 0.001$ (quadrant, within-subjects); $F(3, 148) = 2.83$, $p < 0.05$ (genotype x quadrant)), and by gradual shortening of escape latencies to the hidden platform during the initial training ($F(1, 37) = 5.0$, $p < 0.05$ (genotype); $F(3, 111) = 73.6$, $p < 0.001$ (trial, within-subjects); $F(3, 111) = 1.88$, $p = 0.14$ (genotype x trial)). However, wild-type mice spent more time in the target quadrant than Wfs1-deficient littermates did ($p < 0.05$). Learning effect was also reflected in the gradual shortening of swimming distances over the training period (Figure 26) ($F(1, 37) = 0.42$, $p = 0.52$ (genotype); $F(3, 111) = 58.0$, $p < 0.001$ (trial, within-subjects); $F(3, 111) = 2.73$, $p < 0.05$ (genotype x trial)). Additionally, Wfs1-deficient mice displayed overall slower swimming speed ($F(1, 37) = 8.23$, $p < 0.01$ (genotype); $F(3, 111) = 6.0$, $p < 0.001$ (trial, within-subjects); $F(3, 111) = 0.19$, $p = 0.91$ (genotype x trial)). A significant learning effect was observed in both genotypes also after reversal training as evidenced by preference for the new target quadrant in probe trial on day 6 (Figure 25B).

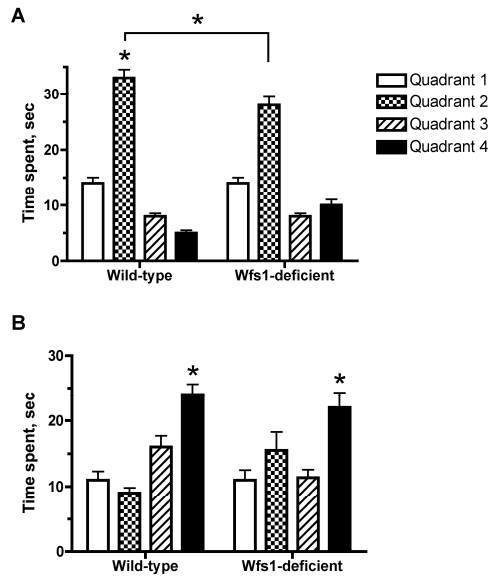


Figure 25. Spatial memory in Wfs1-deficient mice in Morris water maze: time spent in the four quadrants. **A.** Probe trial after initial training (day 4). (*) $p < 0.05$ (unless indicated otherwise, compared to time spent in quadrants 1, 3 and 4; Newman-Keuls test after significant two-way ANOVA). **B.** Probe trial after reversal training (day 6). (*) $p < 0.05$ (compared to time spent in quadrants 1, 2 and 3; Newman-Keuls test after significant two-way ANOVA). Nineteen wild-type and 20 homozygous Wfs1-deficient mice were used in the test.

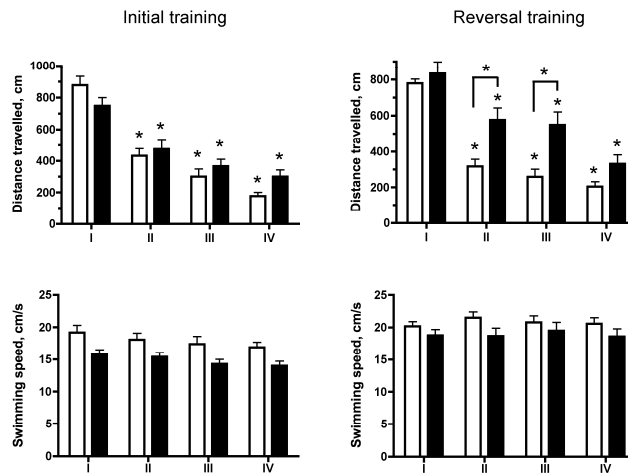


Figure 26. Morris water maze: distance travelled and swimming speed. White bars – wild-type mice, black bars – homozygous Wfs1-deficient mice. (*) $p < 0.05$ (unless indicated otherwise, compared to the first trial of respective genotype, Newman-Keuls test after significant repeated measures ANOVA). Nineteen wild-type and 20 homozygous Wfs1-deficient mice were used in the test.

However, in general, it took Wfs1-deficient mice significantly longer to find the platform (Figure 27) ($F(1, 37) = 15.5, p < 0.001$ (genotype); $F(3, 111) = 55.7, p < 0.001$ (trial, within-subjects); $F(3, 111) = 2.46, p = 0.067$ (genotype x trial)) and they covered longer distances when searching for it ($F(1, 37) = 11.4, p < 0.01$ (genotype); $F(3, 111) = 51.4, p < 0.001$ (trial, within-subjects); $F(3, 111) = 3.0, p < 0.05$ (genotype x trial)). There was an insignificant tendency towards slower swimming speed in Wfs1-deficient mice also during reversal training ($F(1, 37) = 2.18, p = 0.15$ (genotype); $F(3, 111) = 0.59, p = 0.63$ (trial, within-subjects); $F(3, 111) = 0.67, p = 0.57$ (genotype x trial)).

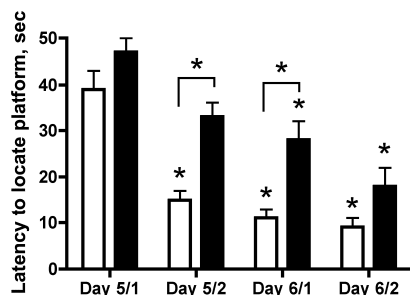


Figure 27. Escape latency in Wfs1-deficient mice during reversal training in Morris water maze. White bars – wild-type mice, black bars – homozygous Wfs1-deficient mice. (*) $p < 0.05$ (unless indicated otherwise, compared to the first trial of respective genotype; Newman-Keuls test after significant repeated measures ANOVA). Nineteen wild-type and 20 homozygous Wfs1-deficient mice were used in the test.

3.15. Active avoidance test

Both, wild-type and homozygous Wfs1-deficient mice learned the task of active avoidance without significant differences (Figure 28) ($F(1, 36) = 0.58, p = 0.45$ (genotype); $F(3, 108) = 12.2, p < 0.001$ (trial, within-subjects); $F(3, 108) = 0.05, p = 0.98$ (genotype x trial)).

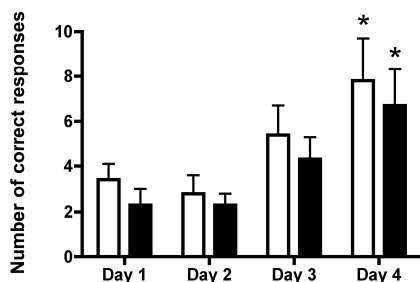


Figure 28. Conditioned responses in Wfs1-deficient mice in active avoidance test. White bars – wild-type mice, black bars – homozygous Wfs1-deficient mice. (*) $p < 0.05$ (compared to the first day of respective genotype, Newman-Keuls test after significant repeated measures ANOVA). Number of animals in each group was 19.

DISCUSSION

I. Wfs1 mRNA is induced in amygdaloid area of rats after cat odor-induced fear response

In Study 1 we found that during anxiety response a number of genes involved directly or indirectly in the synthesis of neuropeptides or neurotransmitters (e.g. carboxypeptidase E, tyrosine 3-monooxygenase/tryptophan 5-mono-oxygenase activation protein) and in signal transduction (Rho GTPase, neurochondrin, Ca/calmodulin-dependent protein kinase) were activated. Additionally, reverse subtraction in control animals identified several genes with apparently opposite expression dynamics in relation to these genes (e.g. nischarin, Rab geranyl-geranyl transferase). We identified a number of genes with unknown function as possibly involved in the regulation of anxiety response. One of the genes was *Wfs1* which was upregulated in the amygdaloid area of rats after cat odor-induced fear response. A subsequent study has demonstrated lower expression of *Wfs1* in the ventral striatum (nucleus accumbens and olfactory tubercle) and temporal lobe of C57BL/6 mice compared to 129Sv strain which was paralleled by increased anxiety-like behavior only in C57BL/6 mice after cat odor exposure (Raud *et al.*, 2007). While the results of these two studies are apparently at conflict the use of different species and different methods for mRNA expression measurements can explain divergence in the findings. cDNA RDA, for example, is at best a semi-quantitative method based on multiple subtractive hybridization steps of two pools of mRNA (Hubank and Schatz, 1999) while real-time quantitative PCR (as used in Raud *et al.*, 2007) is probably one of the most sensitive and accurate methods for mRNA quantification. Nonetheless, both of the studies support the notion that the fear response induced by cat odor might coincide with transcriptional regulation of *Wfs1* in brain regions involved in behavioral adaptation. The relevance of this finding to human central nervous system is supported the facts that around 60% of WS patients suffer from psychiatric symptoms (Swift *et al.*, 1990) and that WFS1 mutation carriers have a 7-fold increased risk of hospitalization for psychiatric illness (Swift and Swift, 2005). Notably, in the latter study, all eight mutation-positive close blood relatives of WS patients had been hospitalized for a major depression, a disorder characterized by impaired behavioral adaptation due to depressed mood, feelings of guilt and worthlessness, and inability to experience pleasure or joy (World Health Organization, 2004). WS carriers have also been reported with post-traumatic stress disorder, general anxiety disorder and suicide attempts (Swift *et al.*, 1998). Furthermore, an analysis of human WFS1 promoter has identified a strong activating region between nucleotides -49 and -233 bp and a negative regulatory region between -233 to -327 suggesting that there exist distinct molecular mechanisms for the up- and down-regulation of WFS1 expression (Ricketts *et al.*, 2006).

2. Wfs1 protein expression is enriched in basal forebrain structures involved in the regulation of behavioral adaptation

2.1. Technical considerations

In Study 2 we used a genetic targeting approach to replace amino acids 360–890 of Wfs1 protein with bacterial β -galactosidase. As a result, we obtained a Wfs1-deficient mouse strain expressing truncated Wfs1 protein fused to β -galactosidase reporter enzyme (Wfs1^{bgal/bgall} mice). The successful targeting of Wfs1 gene was confirmed by the absence of Wfs1C antibody staining in Wfs1^{bgal/bgall} mice and a virtually complete overlap of β -galactosidase immunoreactivity with Wfs1-positive neurons in the heterozygous mice (Fig. 9). Wfs1C antibody staining in wild-type mice revealed a high degree of overlap with X-Gal staining in Wfs1^{bgal/bgall} mice, indicating that β -galactosidase activity could be used as a marker for mapping Wfs1-expressing cells in Wfs1^{bgal/bgall} mice (Fig. 10). In contrast to Wfs1 immunoreactivity, which was evident in neuronal somata, proximal processes and nerve fibers of normal mice, X-Gal staining in Wfs1^{bgal/bgall} mice was almost exclusively found in the cytoplasm of the soma and proximal processes. This was somewhat unexpected, as the Wfs1 targeting construct included a nuclear localization signal (NLS) to target β -galactosidase into the nucleus, and suggests that N-terminal fusion with Wfs1 protein had masked the NLS. In rare cases, punctate X-Gal staining was seen in areas containing Wfs1 immunoreactive nerve fibers such as the substantia nigra, alveus, dorsal hippocampal commissure (Fig. 11I–K) and ventral part of lateral globus pallidus. Finally, weak Wfs1 immunoreactivity was found in several brain regions where X-Gal staining was not detected (see Table 8, for details). As the same regions were found to express Wfs1 mRNA according to the Allen Brain Atlas (Lein *et al.*, 2007), this discrepancy is likely due to the lower sensitivity of X-Gal staining in Wfs1^{bgal/bgall} mice.

2.2. Relationship of Wfs1 expression to the Extended Amygdala concept

Contemporary views of basal forebrain organization revolve around three distinct functional-anatomical macrosystems: the striatopallidum (Heimer and Wilson, 1975), the extended amygdala, and the hippocampal-septal system (Alheid and Heimer, 1988; Heimer, 2003); see Heimer and Van Hoesen (2006), for a critical discussion on the limbic system concept. In the present study, we detected a continuum of Wfs1-positive neurons spanning the forebrain, starting at the closely associated olfactory tubercle and nucleus accumbens, and stretching into the central nucleus of amygdala and caudal caudate putamen. This field is continuous via Wfs1 neurons found in the interstitial nucleus of the

posterior limb of anterior commissure and dorsolateral bed nucleus of stria terminalis. Owing to an overall similarity in connectivity and an extensive network of intrinsic connections, the neuroanatomical concept of central extended amygdala comprises central nucleus of amygdala, lateral bed nucleus of stria terminalis, central division of the supracapsular bed nucleus, interstitial nucleus of the posterior limb of anterior commissure and central sublentiform extended amygdala (de Olmos *et al.*, 2004). From the medial division of extended amygdala (medial amygdaloid nucleus, medial bed nucleus of the stria terminalis, medial division of the supracapsular bed nucleus, medial sublentiform extended amygdala), the central division is distinguished by close connections with the lateral, rather than medial, hypothalamus and with the parabrachial nucleus and solitary nuclear complex in the brainstem. Also, nucleus accumbens shell and to some extent the medial part of olfactory tubercle, have been shown to possess features reminiscent of the extended amygdala, while the core and lateral parts of the olfactory tubercle appear to be closely related to the adjacent striatum (Heimer, 2003). The notion that common molecular markers may be found along the central extended amygdala axis has been mentioned before, for example, on the basis of the distribution of GABA A receptor alpha-2-subunit and angiotensin II immunoreactivity (Alheid and Heimer, 1988; Kaufmann *et al.*, 2003). Our results lend support to the observation that the central nucleus of amygdala and lateral bed nucleus of stria terminalis share structural and functional similarities (Alheid, 2003; de Olmos and Heimer, 1999) as evidenced by a significantly higher Wfs1 expression level in the central nucleus of amygdala and dorsal part of lateral bed nucleus in comparison to all other basal forebrain structures. It must be noted, however, that Wfs1 expression in other subdivisions of the lateral bed nucleus was considerably lower. No Wfs1-expressing cells were found in the parabrachial nucleus and nucleus of the solitary tract which are the brainstem target areas of central extended amygdala. In striatopallidum, densely distributed Wfs1-positive neurons were observed in the core and shell regions of nucleus accumbens and in the olfactory tubercle while no Wfs1-expressing cells were detected in the ventral pallidum or medial and lateral globus pallidus. A striking division of caudate putamen into Wfs1-negative anterior and Wfs1-positive posterior parts was observed. A similar division has been documented, for example, in staining for c-lyn (Chen *et al.*, 1996) and reflects regional specialization or functional asymmetry across the rostro-caudal axis of the caudate putamen.

2.3. Relationship of Wfs1 immunoreactive nerve fibers to known projection pathways

In several brain regions, we found Wfs1 immunoreactivity in the nerve fibers. In the lateral hypothalamus, prominent Wfs1-positive fibers were found that extend from the ventral pallidum to the substantia nigra in the midbrain. According to several characteristics, these fibers likely represent the stria-

tonigral pathway originating from the nucleus accumbens (Gerfen, 2004). In addition to the dense labeling especially in the dorsomedial and dorsolateral parts of reticular substantia nigra, a much sparser distribution of Wfs1-positive fibers was identified in the compact part of substantia nigra and ventral tegmental area. The high density of Wfs1 immunoreactive fibers in the dorsomedial part of reticular substantia nigra relative to the compact subdivision and ventral tegmental area, indicates a relatively larger contribution of fibers from neurons located in the core of the nucleus accumbens rather than the shell. Thus in the rat, a bias for the core projection to innervate the substantia nigra-lateral mesencephalic tegmentum, and for the shell projection to reach primarily the ventral tegmental-paramedian tegmentum area has been noted (Heimer *et al.*, 1991). Additionally, (Berendse *et al.*, 1992) have observed prominent projections to the dorsomedial part of the reticular substantia nigra after anterograde tracer injections into strongly enkephalin immunoreactive areas surrounding the anterior commissure in the core of the nucleus accumbens. Together, these observations fit well with Wfs1 expression pattern in the nucleus accumbens, which appears to be higher in the core relative to the shell. Rostrally, in the subcommissural ventral pallidum, the striatofugal axons formed a dense network of very fine fibers which surrounded a roughly circular cluster of Wfs1 immunoreactive fascicles (bundles of labelled axons of passage). Similar fascicles have been observed by Heimer and co-workers (1991) in rostral ventral pallidum after injections of anterograde tracer into the core of the nucleus accumbens. In the rostral part of lateral globus pallidus, Wfs1-positive fibers were detected only ventrally and in the adjacent central sublenticular extended amygdala. More caudally, Wfs1-positive fibers occupied the whole extent of lateral globus pallidus and converged ventrally to form a large fiber bundle. This rostro-caudal gradient in Wfs1 expression in the nerve fibers of the lateral globus pallidus correlates with Wfs1 expression in the caudate putamen. Therefore, it is very likely that these fibers represent axons of Wfs1-positive neurons in the caudate putamen, as it would explain the apparent lack of Wfs1-positive fibers in the dorsal part of rostral lateral globus pallidus, because Wfs1 is not expressed in the bulk of the caudate putamen at this level except in the marginal zone. The fibers we observed in the ventral aspect of rostral lateral globus pallidus might in fact originate from the ventral striatofugal pathway. Mogenson and colleagues (1983) have reported a similar pattern of fiber labeling in the ventral globus pallidus and central sublenticular extended amygdala upon anterograde tracer injections into the nucleus accumbens of the rat.

2.4. Relationship of Wfs1 expression to Wolfram Syndrome

Our results provide neuroanatomical evidence consistent with the neurological and psychiatric symptoms characteristic of Wolfram syndrome patients. High expression of Wfs1 protein in the central extended amygdala and ventral striatum suggests a role in the regulation of emotional behavior especially in

relation to fear and anxiety. Fear and anxiety are evolutionarily conserved responses crucial for behavioral adaptation to environmental conditions. Maladaptive anxiety and fear are the core symptoms of such affective disorders as major depression and panic disorder. An implication of WFS1 dysfunction in psychiatric disorders has been previously suggested by frequent diagnosis of psychiatric disorders in Wolfram syndrome patients. Furthermore, Wolfram syndrome carriers have increased susceptibility to affective and anxiety disorders and a possible association of WFS1 haplotypes with major depressive disorder has been reported (Koido *et al.*, 2005; Swift and Swift, 2005; Swift *et al.*, 1990). We have previously identified an upregulation of Wfs1 mRNA in amygdaloid area of rats in response to cat odor induced fear response (Koks *et al.*, 2002).

Progressive optic atrophy and sensory-neural hearing-loss are characteristic neurological symptoms of Wolfram syndrome patients (Barrett *et al.*, 1995). We detected prominent Wfs1 expression at various levels of the mouse auditory pathway including lateral lemniscus, olivary complex, inferior colliculus and auditory cortex. Wfs1 expression has also been detected in mouse inner ear cells (Cryns *et al.*, 2003). Recently, a post-mortem study indicated an absence of inner and outer hair cells in the basal turns of the cochlea and focal atrophy of the stria vascularis in a WS patient that correlated well with high-frequency sensory neural hearing loss (Justin B. Hilson, personal communication). In the present study, no significant Wfs1 protein expression was detected in the central visual pathway. An apparent lack of Wfs1 expression in the central visual pathway is also supported by mRNA in situ hybridization data published by Allen Brain Atlas project. Since diabetic retinopathy is rare among Wolfram syndrome patients with poor visual acuity, neurological complications have been implicated (Barrett *et al.*, 1997; Seynaeve *et al.*, 1994). Numerous studies of Wolfram syndrome patients have revealed atrophy of the optic nerves, chiasm, tracts and the lateral geniculate nuclei (see Table 2) while degeneration of the cortical visual areas has not been reported. In addition, Wfs1 expression has been detected in retinal ganglion cells and optic nerve glia of cynomolgus monkey (*Macaca fascicularis*), suggesting a similar expression profile in humans (Yamamoto *et al.*, 2006). Altogether, the aforementioned results make it likely that the progressive loss of vision in WS patients is mainly due to peripheral causes such as the loss of retinal ganglion cells (Justin B. Hilson, personal communication).

Symptoms of hypothalamic dysfunction such as diabetes insipidus and growth retardation have been documented in Wolfram syndrome patients (Barrett *et al.*, 1995; Hansen *et al.*, 2005; Hofmann *et al.*, 1997; Soliman *et al.*, 1995). Specific expression of Wfs1 in compact part of dorsomedial hypothalamic nucleus that is the only brain region where glucagon-like peptide-2 (GLP-2) receptors are found, suggests a role in body weight regulation and feeding behavior (Tang-Christensen *et al.*, 2000). The pre-proglucagon derived peptides, glucagon-like peptide-1 (GLP-1) and GLP-2 are both involved in a wide variety of peripheral functions, such as glucose homeostasis, gastric

emptying, intestinal growth, insulin secretion as well as the regulation of food intake (Tang-Christensen *et al.*, 2001). *Wfs1* expression pattern in paraventricular and supraoptic nuclei suggests an enrichment in the magnocellular neurosecretory component of these structures. These magnocellular neurons synthesize neurohormones vasopressin and oxytocin. The hormones are transported to posterior pituitary and released in an action potential-dependent manner into the bloodstream in response to various stimuli ranging from perturbations in water balance and blood pressure to gastric distention and lactation (Armstrong, 2004). The functional importance of *WFS1* expression in the magnocellular neurosecretory system has been suggested by post-mortem examinations of Wolfram syndrome patients with diabetes insipidus revealing a loss of immunoreactivity for processed vasopressin in supraoptic and paraventricular nuclei (Gabreels *et al.*, 1998).

3. *Wfs1*-deficiency results in impaired behavioral adaptation in stressful environment

In Study 3 we analyzed the behavior of female *Wfs1*-deficient mice with [(129S6/SvEvTac x C57BL/6) x (129S6/SvEvTac x C57BL/6)] mixed background. *Wfs1* gene was invalidated by targeted disruption of exon 8, the principal coding exon, resulting in premature termination of *Wfs1* protein. Absence of *Wfs1* C-terminal immunostaining in *Wfs1*-deficient mice was demonstrated in Study 2. Functional disruption of *Wfs1* gene was confirmed by intolerance to glucose challenge, a finding consistently reported in *Wfs1*-deficient mice by other groups employing different strategies of *Wfs1* disruption (Ishihara *et al.*, 2004; Riggs *et al.*, 2005). In the present study, the effect of *Wfs1*-deficiency on behavior was studied only in young adult female mice due to their milder metabolic disturbances than observed in males and older mice.

The analysis of metabolic parameters in *Wfs1*-deficient female mice revealed lower body weight at four months of age by latest, and intolerance to intraperitoneal administration of glucose whereas no differences in baseline concentrations of blood glucose were found in non-fasted animals. The behavior of mutant mice did not differ from that of wild-type littermates in terms of motor performance in the rota-rod and forced swimming tests. Nevertheless, several measures of motor activity such as time spent in locomotion, distance travelled, number of rearing, and swimming speed were consistently diminished in *Wfs1*-deficient mice. In most cases, however, these effects were not statistically significant. Likewise, no obvious shortcomings in sensory functioning were evident in any of the behavioral tests. *Wfs1*-deficient mice appeared normal in heat-induced pain perception, were able to differentiate between brightly and dimly lit environments, developed intact responses to electric foot-shocks and a 10 kHz conditioned auditory stimulus, and were able to navigate by means of visual contextual cues in Morris water maze. No gross learning deficit was identified in *Wfs1*-deficient mice. Thus, learned responses to

conditioned fear-eliciting stimuli were intact, as well as spatial memory in Morris water maze as evidenced by preference for the target quadrant after initial and reversal training. However, in contrast to wild-type mice, finding the platform during reversal training took Wfs1-deficient mice significantly more time and they covered longer distances in doing so. Subtle impairments in reversal learning might indicate dysfunction in the hippocampal and/or prefrontal circuits. At least in humans and monkeys, impairments in reversal learning have been associated with orbitofrontal cortex dysfunction (Jentsch *et al.*, 2002; Waltz and Gold, 2007). In mice, hippocampal CA1 and CA3 regions have been implicated specifically in reversal learning (Havekes *et al.*, 2006). Notably, both prefrontal cortex and hippocampal CA1 region are enriched in Wfs1 protein and mRNA (Lein *et al.*, 2007; Study 2).

As a rule, in the present study, altered responses were established when Wfs1-deficient mice were exposed to novel environments or stressful manipulations. Increased behavioral inhibition of Wfs1-deficient mice in novel environment was apparent in hyponeophagia test where their latency to start eating was significantly longer than in wild-type littermates. When compared to wild-type mice, locomotor activity was significantly lower in Wfs1-deficient mice only in the more aversive bright environment as opposed to dim environment. Similarly, short-term social isolation of Wfs1-deficient mice induced significant anxiety-like behavior in light/dark exploration test when compared to non-isolated mice. In contrast, social isolation had no major impact on the behavior of wild-type mice in the test. The relatively higher sensitivity of Wfs1-deficient mice to environmental stressors was further supported by increased analgetic response after electric foot-shocks of intermediate intensity and a nearly three-fold higher plasma corticosterone concentration after handling and injection stress when compared to wild-type littermates. By contrast, we detected no difference in baseline corticosterone concentrations between wild-type and Wfs1-deficient mice. A higher level of anxiety in Wfs1-deficient mice was suggested by the administration of a moderate dose of diazepam (1 mg/kg) which had a robust anxiolytic-like effect on plus-maze behavior in Wfs1-deficient mice but not in the wild-type mice. Additionally, a subset of Wfs1-deficient mice produced spontaneous audible vocalizations which increased in loudness under stressful conditions and were suppressed by the administration of diazepam. Attribution of an increased anxiety response to explain the behavior of Wfs1-deficient mice is also supported by neuro-anatomical evidence indicating an enrichment of Wfs1 expression in the central extended amygdala and paraventricular hypothalamic nucleus (Becker *et al.*, 2008; Study 2). Rather than being a single anatomical entity, the extended amygdala concept stands for a network of basal ganglionic nuclei with similar connectivity and neurochemical properties forming a functional-anatomical macrostructure involved in the etiology of such neuropsychiatric disorders as generalized anxiety and depression (Alheid and Heimer, 1988; Heimer, 2003). The paraventricular hypothalamic nucleus, on the other hand, is involved in the endocrine regulation of stress response by controlling the activity of the

hypothalamic-pituitary-adrenocortical (HPA) axis, secretion of neurohypophysial peptides such as vasopressin and oxytocin, and by regulating autonomic centres in brainstem and spinal cord (Herman *et al.*, 2008).

Finally, pharmacological manipulation of the mesolimbic dopamine system by amphetamine and apomorphine indicated differential responsiveness of Wfs1-deficient mice to the psychomotor stimulant effects of these compounds. The stimulatory effect of amphetamine at intermediate and high doses was significantly weaker in Wfs1-deficient mice, probably indicating lower pre-synaptic release potential for dopamine in the mesolimbic pathway. Conversely, postsynaptic dopamine receptor agonist apomorphine induced significantly higher locomotor activation in Wfs1-deficient mice reflecting most likely postsynaptic upregulation of dopamine receptors in the mesolimbic area. As opposed to the present results, reduction in the effect of apomorphine has been demonstrated by Rowland *et al.* (1985) in hypoinsulinaemic mice displaying otherwise a similar behavioral profile in terms of lower basal locomotor activity (Merali *et al.*, 1988; Owens *et al.*, 2005; Sevak *et al.*, 2007) and resistance to the motor stimulatory properties of amphetamine and other related psychomotor stimulants (Marshall, 1978; Merali *et al.*, 1988; Rowland *et al.*, 1985). Hence, it is not likely that the behavioral phenotype of Wfs1-deficient mice is reducible to indirect effects of metabolic disturbances resulting from impaired stimulus-secretion coupling of insulin in the pancreatic β -cells. In mice, Wfs1 protein is expressed at high levels in the ventral striatum (nucleus accumbens and olfactory tubercle) and, to a lesser degree, in caudal part of caudate putamen while being undetectable in the more voluminous rostral part and dopaminergic neurons residing in ventral tegmental area and compact part of substantia nigra (Study 2). Hence, nucleus accumbens is the most obvious candidate for producing disturbances in mesolimbic dopaminergic transmission in Wfs1-deficient mice. Although mostly known as the brain structure mediating the reinforcing actions of addictive drugs (Koob and Le Moal, 2001) nucleus accumbens has been additionally implicated in the regulation of anxiety and stress response (Barrot *et al.*, 2002; Barrot *et al.*, 2005). In addition to high Wfs1 expression in neuronal perikarya in the core and shell regions of nucleus accumbens, there is a prominent Wfs1-rich projection from nucleus accumbens to reticular part of substantia nigra and less dense projections of unknown origin to the compact part of substantia nigra and ventral tegmental area (Study 2). Hypothetically, reduced activation of Wfs1-positive neurons in the nucleus accumbens leading to increased inhibitory tone on motor regions targeted by inhibitory efferents from reticular substantia nigra could account for behavioral inhibition apparent in Wfs1-deficient mice. Such a situation is plausible as Wfs1-deficiency has been shown to reduce stimulus-secretion coupling in pancreatic β -cells (Ishihara *et al.*, 2004; Takei *et al.*, 2006).

During the preparation of this manuscript a study from Kato and colleagues appeared, describing the behavioral phenotype and gene expression analysis of male mice with genetic ablation of the second exon of Wfs1 gene (Kato *et al.*, 2008). Behavioral alternations reported in these Wfs1-deficient mice are less

apparent than in the present study. Significant differences between homozygous Wfs1-deficient and wild type mice were established in terms of increased escape latencies during the conditioning phase in passive avoidance test and in the first block of trials on day 3 of active avoidance test, in terms of increased freezing during conditioning phase in fear conditioning test, and increased latency to find the platform during training in Morris water maze. Together, these results support the notion that Wfs1-deficient mice in that study had subtle impairments in behavioral activation in demanding situations. In addition to the almost negligible behavioral differences, no alterations in the body weight or other phenotypic parameters were reported. The markedly increased severity of phenotypic alterations in Wfs1-deficient mice in the present study could be due to several reasons. First, our Wfs1 targeting strategy spared amino acids 1–359 of Wfs1 protein whereas in the other knockout no N-terminal immunoreactivity of Wfs1 was retained (see Ishihara *et al.* (2004), for original description). Thus, in our mice, the functionality of Wfs1 protein is disrupted while its N-terminal cytoplasmic region is free to interact with its molecular partners possibly prohibiting the activation of compensatory pathways. Secondly, Ishihara *et al.* (2004) have demonstrated that the diabetogenic effect of Wfs1-deficiency is considerably weaker in C57BL/6 background when compared to F2 intercross bearing a more or less equal and random mix of 129S6/SvEvTac and C57BL/6 genetic material (Wolfer *et al.*, 2002). Our behavioral data indicates that the dependency of phenotypic severity on genetic background extends also to the central nervous system. This conclusion is expectable as the differential impact of 129S6-derived and C57BL/6 inbred genetic backgrounds on anxiety-like behavior is well known (Abramov *et al.*, 2008; Holmes *et al.*, 2003; Hovatta *et al.*, 2005). Differences in the observed behavioral phenotype can also be attributed to different research designs. In our lab we have established that long-term social isolation induces an anxiety-like state in female mice whereas increased aggressiveness and exploratory drive are observed in males (Abramov *et al.*, 2004). Kato *et al.* (2008) studied male mice housed individually for several days whereas in our experiments group-housed female mice were used. The order of experiments can also have an impact on the observed phenotype because a number of behavioral tests are sensitive to previous experience and/or handling. For example, plus-maze exposure is extremely sensitive to previous experience (Voikar, 2007). Unlike the present study, Kato *et al.* (2008) never performed plus-maze as the first test.

4. Concluding remarks and future prospects

The main contribution of the present study lies in demonstrating that Wfs1 protein is involved in the regulation of behavioral adaptation. By using animal models we showed that Wfs1 expression is inducible by cat odor-provoked fear response (Study 1), that Wfs1 expression is enriched in brain regions involved in the regulation of behavioral adaptation (Study 2), and that Wfs1-deficiency results in abnormally high anxiety, increased corticosterone response and lower exploratory activity in stressful situations (Study 3). In addition, Study 2 demonstrated that Wfs1 expression in the brain is remarkably concentrated into functionally related brain structures, e.g. central extended amygdala, ventral striatum, prefrontal cortex – behavioral adaptation; hypothalamic magnocellular neurosecretory system, arcuate nucleus – regulation of endocrine function; inferior colliculus, lateral lemniscus, primary auditory cortex – hearing; perirhinal, postrhinal and entorhinal cortices, parasubiculum – highly interconnected parahippocampal areas which relay polysensory information to the hippocampus (Burwell and Amaral, 1998; Furtak *et al.*, 2007), and that Wfs1 expression pattern in the central nervous system correlates with hearing impairment, diabetes insipidus and psychiatric symptoms found in WS patients. When investigating the effect of Wfs1-deficiency on mouse behavior and comparing it to a similar study by Kato *et al.* (2008) we found that the observed effects were often dependent on gender and genetic background of the mice. Thus, Wfs1-deficient males exhibited more severe glucose intolerance than females, and the behavioral phenotype of mice with mixed 129SV and C57BL/6 background was much more remarkable than in mice used by Kato *et al.* (2008) which had been backcrossed to C57BL/6 background. In essence, the significant contribution of background genetic factors to the phenotype associated with Wfs1-deficiency (fundamentally, gender is also a genetic factor) indicates that Wfs1 protein is involved in a flexible molecular network that possesses a high (but not complete) capacity for functional compensation.

Owing to its dynamic expression in fear-provoking situations and a potential capacity for up- and down-regulation by discrete transcriptional mechanisms, it is likely that the functional effects of Wfs1 protein are available in an on-demand fashion. Perhaps, Wfs1 protein might allow the cells to adapt to variations in external stimulation and to ensure stimulus-secretion coupling across a wide range of stimulus frequencies. Previously, WFS1 protein has been shown to positively modulate Ca^{2+} levels in the ER by increasing the rate of Ca^{2+} uptake (Takei *et al.*, 2006), and to have a dose-dependent positive effect on insulin secretion from pancreatic islets upon stimulation with different secretagogues. The smooth endoplasmic reticulum (SER) is a well characterized buffer and source of Ca^{2+} in somatic, axonal and dendritic compartments of neurons, and the functionality of the Ca^{2+} store is known to affect both the polarity and the spatial extent of Ca^{2+} -dependent shifts in synaptic efficacy (Bardo *et al.*, 2006). Remarkably, Study 2 revealed extensive distribution of Wfs1 protein in the dendrites of CA1 pyramidal neurons and axons originating from medium spiny

GABA-ergic projection neurons in the nucleus accumbens and posterior caudate putamen. By enhancing Ca^{2+} uptake into the SER WFS1 protein could alter the neuronal stimulus-response coupling and, hence, alter the responsiveness of neural pathways that involve brain structures enriched in WFS1 expression.

In conclusion, Wfs1 is likely to exert its effects at all levels of the central nervous system as Wfs1 protein is expressed in the neocortex, basal ganglia, hypothalamus, midbrain and brainstem. Furthermore, in the basal forebrain, high Wfs1 expression is seen in functionally antagonistic structures such as the central nucleus of amygdala and nucleus accumbens. Hence, Wfs1 is not likely to regulate only positive or negative affect – only pleasure or anxiety. Instead, its role seems to be in balancing the effects of functionally antagonistic brain structures in order to produce adaptive behavior across a variety of environmental contexts. High Wfs1 expression in the CA1 region of hippocampus and prefrontal cortex further substantiates such a conclusion. Hippocampus and prefrontal cortex can be seen as neural interfaces between previous experience and present reality which play an active role in the selection of appropriate behavioral and affective responses (Phillips *et al.*, 2003; Wager *et al.*, 2008). Additionally, cingulate cortex and insular cortex have been implicated in the regulation of affect and appear to be enriched in Wfs1 expression (Pezawas *et al.*, 2005; Phillips *et al.*, 2003). Perhaps high Wfs1 expression in brain regions regulating the affective component of behavior is not purely coincidental and, instead, is a result of functional connectivity between these structures. Further studies into Wfs1 function in the central nervous system should attempt to investigate this possibility. For example, correlating the expression dynamics of c-fos protein in anxiety- and fear-provoking situations in Wfs1-deficient mice and normal mice could reveal brain structures that display altered responsiveness in stressful situations upon Wfs1 ablation. The effect of the Wfs1-rich projection arising from ventral striatum on midbrain dopaminergic neurons could be studied further in Wfs1-deficient mice by in vivo microdialysis, striatal dopamine receptor binding measurements and highly selective antagonists in combination with indirect agonists. More direct evidence regarding the effects of Wfs1 could be sought by electrophysiological measurements of neuronal activity in Wfs1-deficient mice in brain regions which normally express high levels of Wfs1, and their projection areas.

Wfs1-deficient CA1 pyramidal neurons could make an ideal model for studying dendritic excitability and synaptic plasticity in neurons otherwise expressing high levels of Wfs1 protein in the dendrites, soma and possibly axons. On the molecular level, future research should aim at establishing correspondence between the structure and function of WFS1 protein. Evaluation of intracellular Ca^{2+} homeostasis, WFS1 protein turnover and ER-stress markers in a panel of naturally occurring WFS1 mutants with single amino acid substitutions could establish a correlation between the genotypes and phenotypes of patients with Wolfram Syndrome, low frequency sensory-neural hearing loss and psychiatric disorders.

Based on results obtained in the present study and from studies published elsewhere, it can be speculated that the principal role Wfs1 protein lies in increasing the exocytotic responsiveness of cells in situations which require rapid and high magnitude secretory responses. For example, pancreatic β -cells must respond quickly by releasing large amounts of insulin in response to transient rises in blood sugar concentration. Similarly, brain structures involved in the regulation of adaptive behaviors have to respond rapidly to relevant environmental stimuli such as the appearance of a predator or a desired food item. The fact that Wfs1 expression in the brain is anatomically highly variable to the degree of being virtually absent in a number of brain areas, speaks against its constitutive role in exocytotic processes. Instead, by increasing the filling state of ER with Ca^{2+} ions Wfs1 can enhance the exocytotic responsiveness of cells. The molecular mechanism by which Wfs1 increases Ca^{2+} concentration in the ER is still unknown and remains a focal topic for future research.

CONCLUSIONS

1. Cat odor-induced fear response in rats coincides with the induction of Wfs1 mRNA in the amygdaloid area. Additionally, a number genes involved directly or indirectly in the synthesis of neurotransmitters (e.g. carboxypeptidase E, tyrosine 3-monooxygenase/tryptophan 5-mono-oxygenase activation protein) and in signal transduction (Rho GTPase, neurochondrin, Ca/calmodulin-dependent protein kinase) were activated. Reverse subtraction in control animals identified several genes with opposite expression dynamics in relation to these genes (e.g. nischarin, Rab geranylgeranyl transferase).

2. Wfs1 protein is expressed in anatomically distinct clusters of neurons in all subdivisions of mouse central nervous system including the neocortex, hippocampus, basal ganglia, hypothalamus, thalamus, midbrain, cerebellum and brainstem. Wfs1 expression is enriched in brain structures related to (1) behavioral adaptation – amygdaloid complex, bed nucleus of stria terminalis, the core and shell fields of nucleus accumbens, the prefrontal cortex and the CA1 field of hippocampus; (2) hearing – inferior colliculus, lateral lemniscus, primary auditory cortex; (3) the regulation of endocrine function – supraoptic and paraventricular hypothalamic nuclei, the arcuate nucleus; (4) cortical regions related to hippocampal function – perirhinal, postrhinal and entorhinal cortices, parasubiculum. Two functional-anatomical macrosystems – the central extended amygdala (central nucleus of amygdala, interstitial nucleus of posterior limb of anterior commissure and lateral bed nucleus of stria terminalis) and ventral striatum (nucleus accumbens and olfactory tubercle) form a continuous field of Wfs1-enriched neurons spanning the basal forebrain. Wfs1 expression pattern in the mouse brain correlates with hearing loss, diabetes insipidus and psychiatric symptoms found in Wolfram Syndrome patients.

3. In mice, Wfs1-deficiency does not produce obvious shortcomings in sensory functioning as evidenced by normal heat-induced pain perception, normal discrimination between brightly and dimly lit environments, intact responses to electric foot-shocks and a 10 kHz conditioned auditory stimulus, and preserved ability to navigate by means of visual contextual cues in Morris water maze. Likewise, no gross motor deficits were established in rota-rod test, motility box, forced swimming and Morris water maze tests. Wfs1-deficiency resulted in higher anxiety response in stressful situations as indicated by increased eating latency in hyponeophagia test, lower exploration in brightly lit motility box, anxiety-like behavior in dark-light box test after short-term social isolation, a nearly three-fold higher plasma corticosterone concentration after handling and injection stress, and higher sensitivity to a moderate dose of diazepam in the plus-maze test. Additionally, a subset of Wfs1-deficient mice produced spontaneous audible vocalizations which increased in loudness under stressful conditions and were suppressed by the administration of diazepam. Wfs1-deficient mice display altered pharmacological responsiveness of the mesolimbic

dopamine pathway as evidenced by differential sensitivity to amphetamine and apomorphine. The stimulatory effect of amphetamine at intermediate and high doses was significantly weaker in *Wfs1*-deficient mice, probably indicating lower presynaptic release potential for dopamine in the mesolimbic pathway. Conversely, postsynaptic dopamine receptor agonist apomorphine induced significantly higher locomotor activation in *Wfs1*-deficient mice reflecting most likely postsynaptic upregulation of dopamine receptors in the mesolimbic area.

REFERENCES

1. Abramov U, Puussaar T, Raud S, Kurrikoff K, Vasar E. 2008. Behavioural differences between C57BL/6 and 129S6/SvEv strains are reinforced by environmental enrichment. *Neurosci Lett* 443(3):223–227.
2. Abramov U, Raud S, Koks S, Innos J, Kurrikoff K, Matsui T, Vasar E. 2004. Targeted mutation of CCK(2) receptor gene antagonises behavioural changes induced by social isolation in female, but not in male mice. *Behavioural brain research* 155(1):1–11.
3. Alheid GF. 2003. Extended amygdala and basal forebrain. *Ann N Y Acad Sci* 985:185–205.
4. Alheid GF, Heimer L. 1988. New perspectives in basal forebrain organization of special relevance for neuropsychiatric disorders: the striatopallidal, amygdaloid, and corticopetal components of substantia innominata. *Neuroscience* 27(1):1–39.
5. Amr S, Heisey C, Zhang M, Xia XJ, Shows KH, Ajlouni K, Pandya A, Satin LS, El-Shanti H, Shiang R. 2007. A homozygous mutation in a novel zinc-finger protein, ERIS, is responsible for Wolfram syndrome 2. *American journal of human genetics* 81(4):673–683.
6. Armstrong W. 2004. Hypothalamic supraoptic and paraventricular nuclei. In: Paxinos G, editor. *The Rat Nervous System*. 3rd ed. San Diego, London: Elsevier Academic Press. p 369–388.
7. Arvidsson U, Riedl M, Elde R, Meister B. 1997. Vesicular acetylcholine transporter (VACHT) protein: a novel and unique marker for cholinergic neurons in the central and peripheral nervous systems. *J Comp Neurol* 378(4):454–467.
8. Asherson P, Mant R, Williams N, Cardno A, Jones L, Murphy K, Collier DA, Nanko S, Craddock N, Morris S, Muir W, Blackwood B, McGuffin P, Owen MJ. 1998. A study of chromosome 4p markers and dopamine D5 receptor gene in schizophrenia and bipolar disorder. *Mol Psychiatry* 3(4):310–320.
9. Bacanu SA, Bulik CM, Klump KL, Fichter MM, Halmi KA, Keel P, Kaplan AS, Mitchell JE, Rotondo A, Strober M, Treasure J, Woodside DB, Sonpar VA, Xie W, Bergen AW, Berrettini WH, Kaye WH, Devlin B. 2005. Linkage analysis of anorexia and bulimia nervosa cohorts using selected behavioral phenotypes as quantitative traits or covariates. *Am J Med Genet B Neuropsychiatr Genet* 139B(1): 61–68.
10. Bardo S, Cavazzini MG, Emptage N. 2006. The role of the endoplasmic reticulum Ca²⁺ store in the plasticity of central neurons. *Trends in pharmacological sciences* 27(2):78–84.
11. Barrett TG, Bunday SE, Fielder AR, Good PA. 1997. Optic atrophy in Wolfram (DIDMOAD) syndrome. *Eye* 11 (Pt 6):882–888.
12. Barrett TG, Bunday SE, Macleod AF. 1995. Neurodegeneration and diabetes: UK nationwide study of Wolfram (DIDMOAD) syndrome. *Lancet* 346(8988):1458–1463.
13. Barrot M, Olivier JD, Perrotti LI, DiLeone RJ, Berton O, Eisch AJ, Impey S, Storm DR, Neve RL, Yin JC, Zachariou V, Nestler EJ. 2002. CREB activity in the nucleus accumbens shell controls gating of behavioral responses to emotional stimuli. *Proc Natl Acad Sci U S A* 99(17):11435–11440.
14. Barrot M, Wallace DL, Bolanos CA, Graham DL, Perrotti LI, Neve RL, Chambliss H, Yin JC, Nestler EJ. 2005. Regulation of anxiety and initiation of sexual behavior

- by CREB in the nucleus accumbens. *Proc Natl Acad Sci U S A* 102(23):8357–8362.
15. Becker JAJ, Katia Befort Y, Blad C, Filliol D, Ghate A, Dembele D, Thibault C, Koch M, Muller J, Lardenois A, Poch O, Kieffer BL. 2008. Transcriptome analysis identifies genes with enriched expression in the mouse central extended amygdala. *Neuroscience In Press*, Accepted Manuscript.
 16. Belzung C, El Hage W, Moindrot N, Griebel G. 2001. Behavioral and neurochemical changes following predatory stress in mice. *Neuropharmacology* 41(3): 400–408.
 17. Berendse HW, Groenewegen HJ, Lohman AH. 1992. Compartmental distribution of ventral striatal neurons projecting to the mesencephalon in the rat. *J Neurosci* 12(6):2079–2103.
 18. Berton, F., Vogel, E., and Belzung, C. 1998. Modulation of mice anxiety in response to cat odor as a consequence of predators diet. *Physiol Behav* 65(2): 247–254.
 19. Beshpalova IN, Van Camp G, Bom SJ, Brown DJ, Cryns K, DeWan AT, Erson AE, Flothmann K, Kunst HP, Kurnool P, Sivakumaran TA, Cremers CW, Leal SM, Burmeister M, Lesperance MM. 2001. Mutations in the Wolfram syndrome 1 gene (WFS1) are a common cause of low frequency sensorineural hearing loss. *Hum Mol Genet* 10(22):2501–2508.
 20. Blackwood DH, He L, Morris SW, McLean A, Whitton C, Thomson M, Walker MT, Woodburn K, Sharp CM, Wright AF, Shibasaki Y, St Clair DM, Porteous DJ, Muir WJ. 1996. A locus for bipolar affective disorder on chromosome 4p. *Nat Genet* 12(4):427–430.
 21. Blanchard, D.C., Markham, C., Yang, M., Hubbard, D., Madarang, E., and Blanchard, R.J. 2003. Failure to produce conditioning with low-dose trimethylthiazoline or cat feces as unconditioned stimuli. *Behav Neurosci* 117(2): 360–368.
 22. Bretz GW, Baghdassarian A, Graber JD, Zacherle BJ, Norum RA, Blizzard RM. 1970. Coexistence of diabetes mellitus and insipidus and optic atrophy in two male siblings. Studies and review of literature. *The American journal of medicine* 48(3): 398–403.
 23. Burwell RD, Amaral DG. 1998. Cortical afferents of the perirhinal, postrhinal, and entorhinal cortices of the rat. *J Comp Neurol* 398(2):179–205.
 24. Cano A, Rouzier C, Monnot S, Chabrol B, Conrath J, Lecomte P, Delobel B, Boileau P, Valero R, Procaccio V, Paquis-Flucklinger V, Vialettes B. 2007. Identification of novel mutations in WFS1 and genotype-phenotype correlation in Wolfram syndrome. *Am J Med Genet A* 143A(14):1605–1612.
 25. Chen S, Bing R, Rosenblum N, Hillman DE. 1996. Immunohistochemical localization of Lyn (p56) protein in the adult rat brain. *Neuroscience* 71(1):89–100.
 26. Christoforou A, Le Hellard S, Thomson PA, Morris SW, Tenesa A, Pickard BS, Wray NR, Muir WJ, Blackwood DH, Porteous DJ, Evans KL. 2007. Association analysis of the chromosome 4p15-p16 candidate region for bipolar disorder and schizophrenia. *Mol Psychiatry* 12(11):1011–1025.
 27. Crawley J, Goodwin FK. 1980. Preliminary report of a simple animal behavior model for the anxiolytic effects of benzodiazepines. *Pharmacology, biochemistry, and behavior* 13(2):167–170.
 28. Cremers CW, Wijdeveld PG, Pinckers AJ. 1977. Juvenile diabetes mellitus, optic atrophy, hearing loss, diabetes insipidus, atonia of the urinary tract and bladder, and other abnormalities (Wolfram syndrome). A review of 88 cases from the literature

- with personal observations on 3 new patients. *Acta paediatrica Scandinavica*(264):1–16.
29. Cryan JF, Markou A, Lucki I. 2002. Assessing antidepressant activity in rodents: recent developments and future needs. *Trends in pharmacological sciences* 23(5):238–245.
 30. Cryns K, Thys S, Van Laer L, Oka Y, Pfister M, Van Nassauw L, Smith RJ, Timmermans JP, Van Camp G. 2003. The WFS1 gene, responsible for low frequency sensorineural hearing loss and Wolfram syndrome, is expressed in a variety of inner ear cells. *Histochem Cell Biol* 119(3):247–256.
 31. de Olmos JS, Beltramino CA, Alheid GF. 2004. Amygdala and Extended Amygdala of the Rat: A Cytoarchitectonical, Fibroarchitectonical, and Chemoarchitectonical Survey. In: Paxinos G, editor. *The Rat Nervous System*. 3rd ed. San Diego; London: Elsevier Academic Press. p 510–636.
 32. de Olmos JS, Heimer L. 1999. The concepts of the ventral striatopallidal system and extended amygdala. *Ann N Y Acad Sci* 877:1–32.
 33. Dielenberg RA, Carrive P, McGregor IS. 2001. The cardiovascular and behavioral response to cat odor in rats: unconditioned and conditioned effects. *Brain Res* 897(1–2):228–237.
 34. Domenech E, Gomez-Zaera M, Nunes V. 2004. Study of the WFS1 gene and mitochondrial DNA in Spanish Wolfram syndrome families. *Clinical genetics* 65(6):463–469.
 35. El-Shanti H, Lidral AC, Jarrah N, Druhan L, Ajlouni K. 2000. Homozygosity mapping identifies an additional locus for Wolfram syndrome on chromosome 4q. *American journal of human genetics* 66(4):1229–1236.
 36. Ewald H, Flint T, Kruse TA, Mors O. 2002. A genome-wide scan shows significant linkage between bipolar disorder and chromosome 12q24.3 and suggestive linkage to chromosomes 1p22–21, 4p16, 6q14–22, 10q26 and 16p13.3. *Mol Psychiatry* 7(7):734–744.
 37. Fonseca SG, Fukuma M, Lipson KL, Nguyen LX, Allen JR, Oka Y, Urano F. 2005. WFS1 is a novel component of the unfolded protein response and maintains homeostasis of the endoplasmic reticulum in pancreatic beta-cells. *J Biol Chem* 280(47):39609–39615.
 38. Fraser FC, Gunn T. 1977. Diabetes mellitus, diabetes insipidus, and optic atrophy. An autosomal recessive syndrome? *Journal of medical genetics* 14(3):190–193.
 39. Fukuoka, H., Kanda, Y., Ohta, S., and Usami, S. 2007. Mutations in the WFS1 gene are a frequent cause of autosomal dominant nonsyndromic low-frequency hearing loss in Japanese. *J Hum Genet* 52(6): 510–515.
 40. Furtak SC, Wei SM, Agster KL, Burwell RD. 2007. Functional neuroanatomy of the parahippocampal region in the rat: the perirhinal and postrhinal cortices. *Hippocampus* 17(9):709–722.
 41. Gabreels BA, Swaab DF, de Kleijn DP, Dean A, Seidah NG, Van de Loo JW, Van de Ven WJ, Martens GJ, Van Leeuwen FW. 1998. The vasopressin precursor is not processed in the hypothalamus of Wolfram syndrome patients with diabetes insipidus: evidence for the involvement of PC2 and 7B2. *J Clin Endocrinol Metab* 83(11):4026–4033.
 42. Galluzzi P, Filosomi G, Vallone IM, Bardelli AM, Venturi C. 1999. MRI of Wolfram syndrome (DIDMOAD). *Neuroradiology* 41(10):729–731.
 43. Genis D, Davalos A, Molins A, Ferrer I. 1997. Wolfram syndrome: a neuropathological study. *Acta neuropathologica* 93(4):426–429.

44. Gerfen CR. 2004. Basal Ganglia. In: Paxinos G, editor. *The Rat Nervous System*. 3rd ed. San Diego; London: Elsevier Academic Press. p 458–509.
45. Hadidy AM, Jarrah NS, Al-Till MI, El-Shanti HE, Ajlouni KM. 2004. Radiological findings in Wolfram syndrome. *Saudi medical journal* 25(5):638–641.
46. Hampton RY. 2000. ER stress response: getting the UPR hand on misfolded proteins. *Curr Biol* 10(14):R518–521.
47. Handley SL, Mithani S. 1984. Effects of alpha-adrenoceptor agonists and antagonists in a maze-exploration model of 'fear'-motivated behaviour. *Naunyn-Schmiedeberg's archives of pharmacology* 327(1):1–5.
48. Hansen L, Eiberg H, Barrett T, Bek T, Kjaersgaard P, Tranebjærg L, Rosenberg T. 2005. Mutation analysis of the WFS1 gene in seven Danish Wolfram syndrome families; four new mutations identified. *Eur J Hum Genet* 13(12):1275–1284.
49. Hattori H, Inada H, Tanaka K, Niihira S, Seto T, Matsuoka O, Isshiki G. 1998. [Auditory brainstem responses (ABR) in patients with Wolfram syndrome]. *No to hattatsu* 30(5):387–393.
50. Havekes R, Nijholt IM, Luiten PG, Van der Zee EA. 2006. Differential involvement of hippocampal calcineurin during learning and reversal learning in a Y-maze task. *Learning & memory* (Cold Spring Harbor, NY) 13(6):753–759.
51. Hebb, A.L., Zacharko, R.M., Dominguez, H., Trudel, F., Laforest, S., and Drolet, G. 2002. Odor-induced variation in anxiety-like behavior in mice is associated with discrete and differential effects on mesocorticolimbic cholecystokinin mRNA expression. *Neuropsychopharmacology* 27(5): 744–755.
52. Heimer L. 2003. A new anatomical framework for neuropsychiatric disorders and drug abuse. *Am J Psychiatry* 160(10):1726–1739.
53. Heimer L, Van Hoesen GW. 2006. The limbic lobe and its output channels: implications for emotional functions and adaptive behavior. *Neurosci Biobehav Rev* 30(2):126–147.
54. Heimer L, Wilson RD. 1975. The subcortical projections of allocortex: similarities in the neuronal associations of the hippocampus, the piriform cortex and the neocortex. In: Santini M, editor. *Golgi Centennial Symposium Proceedings*. New York: Raven Press. p 177–193.
55. Heimer L, Zahm DS, Churchill L, Kalivas PW, Wohltmann C. 1991. Specificity in the projection patterns of accumbal core and shell in the rat. *Neuroscience* 41(1): 89–125.
56. Herman JP, Flak J, Jankord R. 2008. Chronic stress plasticity in the hypothalamic paraventricular nucleus. *Progress in brain research* 170:353–364.
57. Hofmann M, Boehmer H, Zumbach M, Borcea V, Grauer A, Kasperk C, Heilmann P, Ziegler R, Wahl P, Nawroth PP. 1997. [The Wolfram syndrome: diabetes mellitus, hypacusis, optic atrophy and short stature in STH deficiency]. *Dtsch Med Wochenschr* 122(4):86–90.
58. Hofmann S, Philbrook C, Gerbitz KD, Bauer MF. 2003. Wolfram syndrome: structural and functional analyses of mutant and wild-type wolframin, the WFS1 gene product. *Hum Mol Genet* 12(16):2003–2012.
59. Holmes A, Lit Q, Murphy DL, Gold E, Crawley JN. 2003. Abnormal anxiety-related behavior in serotonin transporter null mutant mice: the influence of genetic background. *Genes, brain, and behavior* 2(6):365–380.
60. Hovatta I, Tennant RS, Helton R, Marr RA, Singer O, Redwine JM, Ellison JA, Schadt EE, Verma IM, Lockhart DJ, Barlow C. 2005. Glyoxalase 1 and glutathione reductase 1 regulate anxiety in mice. *Nature* 438(7068):662–666.

61. Hubank M, Schatz DG. 1999. cDNA representational difference analysis: a sensitive and flexible method for identification of differentially expressed genes. *Methods in enzymology* 303:325–349.
62. Inoue H, Tanizawa Y, Wasson J, Behn P, Kalidas K, Bernal-Mizrachi E, Mueckler M, Marshall H, Donis-Keller H, Crock P, Rogers D, Mikuni M, Kumashiro H, Higashi K, Sobue G, Oka Y, Permutt MA. 1998. A gene encoding a transmembrane protein is mutated in patients with diabetes mellitus and optic atrophy (Wolfram syndrome). *Nat Genet* 20(2):143–148.
63. Ishihara H, Takeda S, Tamura A, Takahashi R, Yamaguchi S, Takei D, Yamada T, Inoue H, Soga H, Katagiri H, Tanizawa Y, Oka Y. 2004. Disruption of the WFS1 gene in mice causes progressive beta-cell loss and impaired stimulus-secretion coupling in insulin secretion. *Hum Mol Genet* 13(11):1159–1170.
64. Ito S, Sakakibara R, Hattori T. 2007. Wolfram syndrome presenting marked brain MR imaging abnormalities with few neurologic abnormalities. *Ajnr* 28(2):305–306.
65. Jakobsson J, Rosenqvist N, Marild K, D VA, Lundberg C. 2006. Evidence for disease-regulated transgene expression in the brain with use of lentiviral vectors. *Journal of neuroscience research* 84(1):58–67.
66. Jentsch JD, Olausson P, De La Garza R, 2nd, Taylor JR. 2002. Impairments of reversal learning and response perseveration after repeated, intermittent cocaine administrations to monkeys. *Neuropsychopharmacology* 26(2):183–190.
67. Kakiuchi C, Ishiwata M, Hayashi A, Kato T. 2006. XBP1 induces WFS1 through an endoplasmic reticulum stress response element-like motif in SH-SY5Y cells. *J Neurochem* 97(2):545–555.
68. Karasik A, O'Hara C, Srikanta S, Swift M, Soeldner JS, Kahn CR, Herskowitz RD. 1989. Genetically programmed selective islet beta-cell loss in diabetic subjects with Wolfram's syndrome. *Diabetes Care* 12(2):135–138.
69. Kato T, Ishiwata M, Yamada K, Kasahara T, Kakiuchi C, Iwamoto K, Kawamura K, Ishihara H, Oka Y. 2008. Behavioral and gene expression analyses of Wfs1 knockout mice as a possible animal model of mood disorder. *Neuroscience research* 61(2):143–158.
70. Kaufmann WA, Humpel C, Alheid GF, Marksteiner J. 2003. Compartmentation of alpha 1 and alpha 2 GABA(A) receptor subunits within rat extended amygdala: implications for benzodiazepine action. *Brain Res* 964(1):91–99.
71. Kawano J, Tanizawa Y, Shinoda K. 2008. Wolfram syndrome 1 (Wfs1) gene expression in the normal mouse visual system. *J Comp Neurol* 510(1):1–23.
72. Kellner M, Strian F, Fassbender K, Kennerknecht I, Klein R. 1994. DIDMOAD (Wolfram) syndrome. *Br J Psychiatry* 164(1):132.
73. Kesner Y, Zohar J, Merenlender A, Gispan I, Shalit F, Yadid G. 2007. WFS1 gene as a putative biomarker for development of post-traumatic syndrome in an animal model. *Mol Psychiatry*.
74. Khanim F, Kirk J, Latif F, Barrett TG. 2001. WFS1/wolframin mutations, Wolfram syndrome, and associated diseases. *Human mutation* 17(5):357–367.
75. Kinsley BT, Firth RG. 1992. The Wolfram syndrome: a primary neurodegenerative disorder with lethal potential. *Irish medical journal* 85(1):34–36.
76. Kinsley BT, Swift M, Dumont RH, Swift RG. 1995. Morbidity and mortality in the Wolfram syndrome. *Diabetes Care* 18(12):1566–1570.
77. Koido K, Koks S, Nikopensius T, Maron E, Altmae S, Heinaste E, Vabrit K, Tammekivi V, Hallast P, Kurg A, Shlik J, Vasar V, Metspalu A, Vasar E. 2005. Polymorphisms in wolframin (WFS1) gene are possibly related to increased risk for mood disorders. *Int J Neuropsychopharmacol* 8(2):235–244.

78. Koks S, Planken A, Luuk H, Vasar E. 2002. Cat odour exposure increases the expression of wolframin gene in the amygdaloid area of rat. *Neurosci Lett* 322(2): 116–120.
79. Koob GF, Le Moal M. 2001. Drug addiction, dysregulation of reward, and allostasis. *Neuropsychopharmacology* 24(2):97–129.
80. Kustanovich V, Ishii J, Crawford L, Yang M, McGough JJ, McCracken JT, Smalley SL, Nelson SF. 2004. Transmission disequilibrium testing of dopamine-related candidate gene polymorphisms in ADHD: confirmation of association of ADHD with DRD4 and DRD5. *Mol Psychiatry* 9(7):711–717.
81. Lein ES, Hawrylycz MJ, Ao N, Ayres M, Bensinger A, Bernard A, Boe AF, Boguski MS, Brockway KS, Byrnes EJ, Chen L, Chen L, Chen TM, Chin MC, Chong J, Crook BE, Czaplinska A, Dang CN, Datta S, Dee NR, Desaki AL, Desta T, Diep E, Dolbeare TA, Donelan MJ, Dong HW, Dougherty JG, Duncan BJ, Ebbert AJ, Eichele G, Estin LK, Faber C, Facer BA, Fields R, Fischer SR, Fliss TP, Frensley C, Gates SN, Glattfelder KJ, Halverson KR, Hart MR, Hohmann JG, Howell MP, Jeung DP, Johnson RA, Karr PT, Kawal R, Kidney JM, Knapik RH, Kuan CL, Lake JH, Laramée AR, Larsen KD, Lau C, Lemon TA, Liang AJ, Liu Y, Luong LT, Michaels J, Morgan JJ, Morgan RJ, Mortrud MT, Mosqueda NF, Ng LL, Ng R, Orta GJ, Overly CC, Pak TH, Parry SE, Pathak SD, Pearson OC, Puchalski RB, Riley ZL, Rockett HR, Rowland SA, Royall JJ, Ruiz MJ, Sarno NR, Schaffnit K, Shapovalova NV, Sivisay T, Slaughterbeck CR, Smith SC, Smith KA, Smith BI, Sotdt AJ, Stewart NN, Stumpf KR, Sunkin SM, Sutram M, Tam A, Teemer CD, Thaller C, Thompson CL, Varnam LR, Visel A, Whitlock RM, Wohnoutka PE, Wolkey CK, Wong VY, Wood M, Yaylaoglu MB, Young RC, Youngstrom BL, Yuan XF, Zhang B, Zwingman TA, Jones AR. 2007. Genome-wide atlas of gene expression in the adult mouse brain. *Nature* 445(7124):168–176.
82. Leiva-Santana C, Carro-Martinez A, Monge-Argiles A, Palao-Sanchez A. 1993. [Neurologic manifestations in Wolfram's syndrome]. *Revue neurologique* 149(1): 26–29.
83. Leonardo ED, Hen R. 2006. Genetics of affective and anxiety disorders. *Annual review of psychology* 57:117–137.
84. Lesperance MM. 2008. WFS1 Gene Mutation and Polymorphism Database.
85. Lesperance MM, Hall JW, 3rd, Bess FH, Fukushima K, Jain PK, Ploplis B, San Agustin TB, Skarka H, Smith RJ, Wills M, et al. 1995. A gene for autosomal dominant nonsyndromic hereditary hearing impairment maps to 4p16.3. *Hum Mol Genet* 4(10):1967–1972.
86. Lister RG. 1987. The use of a plus-maze to measure anxiety in the mouse. *Psychopharmacology* 92(2):180–185.
87. Marshall JF. 1978. Further analysis of the resistance of the diabetic rat to d-amphetamine. *Pharmacology, biochemistry, and behavior* 8(3):281–286.
88. Mathis S, Paquis V, Mesnage V, Balaboi I, Gil R, Gilbert B, Neau JP. 2007. [Wolfram's syndrome presenting as a cerebellar ataxia]. *Revue neurologique* 163(2):197–204.
89. McIlwain KL, Merriweather MY, Yuva-Paylor LA, Paylor R. 2001. The use of behavioral test batteries: effects of training history. *Physiology & behavior* 73(5): 705–717.
90. Medlej R, Wasson J, Baz P, Azar S, Salti I, Loiselet J, Permutt A, Halaby G. 2004. Diabetes mellitus and optic atrophy: a study of Wolfram syndrome in the Lebanese population. *J Clin Endocrinol Metab* 89(4):1656–1661.

91. Merali Z, Ahmad Q, Veitch J. 1988. Behavioral and neurochemical profile of the spontaneously diabetic Wistar BB rat. *Behavioural brain research* 29(1–2):51–60.
92. Millipore. 2008a. Mouse monoclonal anti-tyrosine hydroxylase antibody clone LNC1 MAB318 Product Information.
93. Millipore. 2008b. Rabbit anti-Met-enkephalin polyclonal antibody AB5026 Product Information.
94. Mogenson GJ, Swanson LW, Wu M. 1983. Neural projections from nucleus accumbens to globus pallidus, substantia innominata, and lateral preoptic-lateral hypothalamic area: an anatomical and electrophysiological investigation in the rat. *J Neurosci* 3(1):189–202.
95. Mtanda AT, Cruysberg JR, Pinckers AJ. 1986. Optic atrophy in Wolfram syndrome. *Ophthalmic paediatrics and genetics* 7(3):159–165.
96. Mullen RJ, Buck CR, Smith AM. 1992. NeuN, a neuronal specific nuclear protein in vertebrates. *Development (Cambridge, England)* 116(1):201–211.
97. Nanko S, Yokoyama H, Hoshino Y, Kumashiro H, Mikuni M. 1992. Organic mood syndrome in two siblings with Wolfram syndrome. *Br J Psychiatry* 161:282.
98. Nelovkov A, Areda T, Innos J, Koks S, Vasar E. 2006. Rats displaying distinct exploratory activity also have different expression patterns of gamma-aminobutyric acid- and cholecystokinin-related genes in brain regions. *Brain Res* 1100(1):21–31.
99. O'Neill MJ, Sinclair AH. 1997. Isolation of rare transcripts by representational difference analysis. *Nucleic acids research* 25(13):2681–2682.
100. Osman AA, Saito M, Makepeace C, Permutt MA, Schlesinger P, Mueckler M. 2003. Wolframin expression induces novel ion channel activity in endoplasmic reticulum membranes and increases intracellular calcium. *J Biol Chem* 278(52):52755–52762.
101. Owens WA, Sevak RJ, Galici R, Chang X, Javors MA, Galli A, France CP, Daws LC. 2005. Deficits in dopamine clearance and locomotion in hypoinsulinemic rats unmask novel modulation of dopamine transporters by amphetamine. *J Neurochem* 94(5):1402–1410.
102. Pakdemirli E, Karabulut N, Bir LS, Sermez Y. 2005. Cranial magnetic resonance imaging of Wolfram (DIDMOAD) syndrome. *Australasian radiology* 49(2):189–191.
103. Paley RG, Tunbridge RE. 1956. Primary optic atrophy in diabetes mellitus. *Diabetes* 5(4):295–296.
104. Pastorian K, Hawel L, 3rd, Byus CV. 2000. Optimization of cDNA representational difference analysis for the identification of differentially expressed mRNAs. *Analytical biochemistry* 283(1):89–98.
105. Paylor R, Nguyen M, Crawley JN, Patrick J, Beaudet A, Orr-Urtreger A. 1998. Alpha7 nicotinic receptor subunits are not necessary for hippocampal-dependent learning or sensorimotor gating: a behavioral characterization of Acra7-deficient mice. *Learning & memory (Cold Spring Harbor, NY)* 5(4–5):302–316.
106. Pellow S, Chopin P, File SE, Briley M. 1985. Validation of open:closed arm entries in an elevated plus-maze as a measure of anxiety in the rat. *Journal of neuroscience methods* 14(3):149–167.
107. Pezawas L, Meyer-Lindenberg A, Drabant EM, Verchinski BA, Munoz KE, Kolachana BS, Egan MF, Mattay VS, Hariri AR, Weinberger DR. 2005. 5-HTTLPR polymorphism impacts human cingulate-amygdala interactions: a genetic susceptibility mechanism for depression. *Nature neuroscience* 8(6):828–834.

108. Phillips ML, Drevets WC, Rauch SL, Lane R. 2003. Neurobiology of emotion perception I: The neural basis of normal emotion perception. *Biol Psychiatry* 54(5):504–514.
109. Quirk GJ, Beer JS. 2006. Prefrontal involvement in the regulation of emotion: convergence of rat and human studies. *Current opinion in neurobiology* 16(6):723–727.
110. Raud S, Sutt S, Plaas M, Luuk H, Innos J, Philips MA, Koks S, Vasar E. 2007. Cat odor exposure induces distinct changes in the exploratory behavior and Wfs1 gene expression in C57Bl/6 and 129Sv mice. *Neurosci Lett* 426(2):87–90.
111. Ricketts C, Zatyka M, Barrett T. 2006. The characterisation of the human Wolfram syndrome gene promoter demonstrating regulation by Sp1 and Sp3 transcription factors. *Biochimica et biophysica acta* 1759(7):367–377.
112. Riggs AC, Bernal-Mizrachi E, Ohsugi M, Wasson J, Fatrai S, Welling C, Murray J, Schmidt RE, Herrera PL, Permutt MA. 2005. Mice conditionally lacking the Wolfram gene in pancreatic islet beta cells exhibit diabetes as a result of enhanced endoplasmic reticulum stress and apoptosis. *Diabetologia* 48(11):2313–2321.
113. Rose FC, Fraser GR, Friedmann AI, Kohnner EM. 1966. The association of juvenile diabetes mellitus and optic atrophy: clinical and genetical aspects. *The Quarterly journal of medicine* 35(139):385–405.
114. Rowland N, Joyce JN, Bellush LL. 1985. Stereotyped behavior and diabetes mellitus in rats: reduced behavioral effects of amphetamine and apomorphine and reduced in vivo brain binding of [3H]spiroperidol. *Behavioral neuroscience* 99(5):831–841.
115. Roy, V., Belzung, C., Delarue, C., and Chapillon, P. 2001. Environmental enrichment in BALB/c mice: effects in classical tests of anxiety and exposure to a predatory odor. *Physiol Behav* 74(3): 313–320.
116. Saiz A, Vila N, Munoz JE, Marti MJ, Graus F, Tolosa E. 1995. [Wolfram's syndrome: correlation of clinical signs and neurological images]. *Neurologia (Barcelona, Spain)* 10(2):107–109.
117. Scolding NJ, Kellar-Wood HF, Shaw C, Shneerson JM, Antoun N. 1996. Wolfram syndrome: hereditary diabetes mellitus with brainstem and optic atrophy. *Annals of neurology* 39(3):352–360.
118. Sevak RJ, Owens WA, Koek W, Galli A, Daws LC, France CP. 2007. Evidence for D2 receptor mediation of amphetamine-induced normalization of locomotion and dopamine transporter function in hypoinsulinemic rats. *J Neurochem* 101(1):151–159.
119. Seynaeve H, Vermeiren A, Leys A, Dralands L. 1994. Four cases of Wolfram syndrome: ophthalmologic findings and complications. *Bull Soc Belge Ophtalmol* 252:75–80.
120. Shannon P, Becker L, Deck J. 1999. Evidence of widespread axonal pathology in Wolfram syndrome. *Acta neuropathologica* 98(3):304–308.
121. Shindler K, Roth K. 1996. Double immunofluorescent staining using two unconjugated primary antisera raised in the same species. *J Histochem Cytochem* 44(11):1331–1335.
122. Simsek E, Simsek T, Tekgul S, Hosal S, Seyrantepe V, Aktan G. 2003. Wolfram (DIDMOAD) syndrome: a multidisciplinary clinical study in nine Turkish patients and review of the literature. *Acta Paediatr* 92(1):55–61.
123. Soliman AT, Bappal B, Darwish A, Rajab A, Asfour M. 1995. Growth hormone deficiency and empty sella in DIDMOAD syndrome: an endocrine study. *Arch Dis Child* 73(3):251–253.

124. Strom TM, Hortnagel K, Hofmann S, Gekeler F, Scharfe C, Rabl W, Gerbitz KD, Meitinger T. 1998. Diabetes insipidus, diabetes mellitus, optic atrophy and deafness (DIDMOAD) caused by mutations in a novel gene (wolframin) coding for a predicted transmembrane protein. *Hum Mol Genet* 7(13):2021–2028.
125. Sunkin SM, Hohmann JG. 2007. Insights from spatially mapped gene expression in the mouse brain. *Hum Mol Genet* 16 Spec No. 2:R209–219.
126. Swift M, Swift RG. 2005. Wolframin mutations and hospitalization for psychiatric illness. *Mol Psychiatry* 10(8):799–803.
127. Swift RG, Perkins DO, Chase CL, Sadler DB, Swift M. 1991. Psychiatric disorders in 36 families with Wolfram syndrome. *Am J Psychiatry* 148(6):775–779.
128. Swift RG, Polymeropoulos MH, Torres R, Swift M. 1998. Predisposition of Wolfram syndrome heterozygotes to psychiatric illness. *Mol Psychiatry* 3(1):86–91.
129. Swift RG, Sadler DB, Swift M. 1990. Psychiatric findings in Wolfram syndrome homozygotes. *Lancet* 336(8716):667–669.
130. Takahashi LK, Nakashima BR, Hong H, Watanabe K. 2005. The smell of danger: a behavioral and neural analysis of predator odor-induced fear. *Neurosci Biobehav Rev* 29(8):1157–1167.
131. Takeda K, Inoue H, Tanizawa Y, Matsuzaki Y, Oba J, Watanabe Y, Shinoda K, Oka Y. 2001. WFS1 (Wolfram syndrome 1) gene product: predominant sub-cellular localization to endoplasmic reticulum in cultured cells and neuronal expression in rat brain. *Hum Mol Genet* 10(5):477–484.
132. Takei D, Ishihara H, Yamaguchi S, Yamada T, Tamura A, Katagiri H, Maruyama Y, Oka Y. 2006. WFS1 protein modulates the free Ca(2+) concentration in the endoplasmic reticulum. *FEBS Lett* 580(24):5635–5640.
133. Tang-Christensen M, Larsen PJ, Thulesen J, Romer J, Vrang N. 2000. The proglucagon-derived peptide, glucagon-like peptide-2, is a neurotransmitter involved in the regulation of food intake. *Nat Med* 6(7):802–807.
134. Tang-Christensen M, Vrang N, Larsen PJ. 2001. Glucagon-like peptide containing pathways in the regulation of feeding behaviour. *Int J Obes Relat Metab Disord* 25 Suppl 5:S42–47.
135. Ueda K, Kawano J, Takeda K, Yujiri T, Tanabe K, Anno T, Akiyama M, Nozaki J, Yoshinaga T, Koizumi A, Shinoda K, Oka Y, Tanizawa Y. 2005. Endoplasmic reticulum stress induces Wfs1 gene expression in pancreatic beta-cells via transcriptional activation. *Eur J Endocrinol* 153(1):167–176.
136. Voikar V. 2007. Evaluation of Methods and Applications for Behavioural Profiling of Transgenic Mice. Helsinki: University of Helsinki.
137. Voikar V, Vasar E, Rauvala H. 2004. Behavioral alterations induced by repeated testing in C57BL/6J and 129S2/Sv mice: implications for phenotyping screens. *Genes, brain, and behavior* 3(1):27–38.
138. Wager TD, Davidson ML, Hughes BL, Lindquist MA, Ochsner KN. 2008. Prefrontal-subcortical pathways mediating successful emotion regulation. *Neuron* 59(6):1037–1050.
139. Waltz JA, Gold JM. 2007. Probabilistic reversal learning impairments in schizophrenia: further evidence of orbitofrontal dysfunction. *Schizophrenia research* 93(1–3):296–303.
140. Wolf ME, LeWitt PA, Bannon MJ, Dragovic LJ, Kapatos G. 1991. Effect of aging on tyrosine hydroxylase protein content and the relative number of dopamine nerve terminals in human caudate. *J Neurochem* 56(4):1191–1200.

141. Wolfer DP, Crusio WE, Lipp HP. 2002. Knockout mice: simple solutions to the problems of genetic background and flanking genes. *Trends in neurosciences* 25(7):336–340.
142. Wolfram DJ, Wagener HP. 1938. Diabetes mellitus and simple optic atrophy among siblings: report of four cases. *Mayo Clinic proceedings*(13):715–718.
143. World Health Organization. 2004. *International Statistical Classification of Diseases and Related Health Problems: Tenth Revision*. Geneva: WHO.
144. Yamada T, Ishihara H, Tamura A, Takahashi R, Yamaguchi S, Takei D, Tokita A, Satake C, Tashiro F, Katagiri H, Aburatani H, Miyazaki J, Oka Y. 2006. WFS1-deficiency increases endoplasmic reticulum stress, impairs cell cycle progression and triggers the apoptotic pathway specifically in pancreatic beta-cells. *Hum Mol Genet* 15(10):1600–1609.
145. Yamaguchi S, Ishihara H, Tamura A, Yamada T, Takahashi R, Takei D, Katagiri H, Oka Y. 2004. Endoplasmic reticulum stress and N-glycosylation modulate expression of WFS1 protein. *Biochem Biophys Res Commun* 325(1):250–256.
146. Yamamoto H, Hofmann S, Hamasaki DI, Yamamoto H, Kreczmanski P, Schmitz C, Parel JM, Schmidt-Kastner R. 2006. Wolfram syndrome 1 (WFS1) protein expression in retinal ganglion cells and optic nerve glia of the cynomolgus monkey. *Exp Eye Res* 83(5):1303–1306.
147. Yang MS, Chen CC, Cheng YY, Tyan YS, Wang YF, Lee SK. 2005. Imaging characteristics of familial Wolfram syndrome. *Journal of the Formosan Medical Association = Taiwan yi zhi* 104(2):129–132.
148. Young TL, Ives E, Lynch E, Person R, Snook S, MacLaren L, Cater T, Griffin A, Fernandez B, Lee MK, King MC. 2001. Non-syndromic progressive hearing loss DFNA38 is caused by heterozygous missense mutation in the Wolfram syndrome gene WFS1. *Hum Mol Genet* 10(22):2509–2514.
149. Zatyka M, Ricketts C, da Silva Xavier G, Minton J, Fenton S, Hofmann-Thiel S, Rutter GA, Barrett T. 2007. Sodium-potassium ATPase beta 1 subunit is a molecular partner of Wolframin, an endoplasmic reticulum (ER) protein involved in ER stress. *Hum Mol Genet* 17(2):190–200.

APPENDIX I

REPORTED MUTATIONS IN WFS1 GENE (adapted from [1])

Disease	Type	Patient ID	Location	Description	aa change	Reference
WS	insertion	Family WS12	E-3	c.409_424dup16	V142fsX251	[2] ^b
WS	insertion	Family WS13	E-3	c.409_424dup16	V142fsX251	[2] ^b
WS	insertion	Family WS16	E-3	c.409_424dup16	V142fsX251	[2] ^b
WS	insertion	Family WS18	E-3	c.409_424dup16	V142fsX251	[2] ^b
WS	insertion	Family WS20	E-3	c.409_424dup16	V142fsX251	[2] ^b
WS	insertion		E-3	c.409_424dup16	V142fsX251	[3]
WS	insertion	Family WS22	E-3	c.409_424dup16	V142fsX251	[4]
WS	insertion	Family WS24	E-3	c.409_424dup16	V142fsX251	[4]
WS	insertion	Family WS26	E-3	c.409_424dup16	V142fsX251	[4]
WS	insertion	Family 7	E-3	c.409_424dup16	V142fsX251	[5] ^d
WS	insertion	Family WS9	E-3	c.409_424dup16	V142fsX251	[6]
WS	insertion	Family 16	E-3	c.409_424dup16	V142fsX251	[6]
WS	missense	Family WS12	E-4	c.328T>A	Y110N	[6]
WS	missense	Family WS2	E-4	c.376G>A	A126T	[2]
WS	nonsense	Family 7	E-4	c.387G>A	W129X	[5]
WS	missense	1	E-4	c.397G>A	A133T	[7]
WS	missense	Family WS12	E-4	c.397G>A	A133T	[6]
WS	missense	EE32	E-4	c.397G>A	A133T	[8]
WS	nonsense	Family B	E-4	c.406C>T	Q136X	[9]
WS	insertion	Family WS2	E-4	c.409_424dup16	V142fsX251	[2] ^b
WS	insertion	WS5	E-4	c.409_424dup16	V142fsX251	[10]
WS	missense	LIB4	E-4	c.490G>A	G107E	[11]
WS	Splice	13775	I-4	IVS4+1G>A	Splice	[12]
WS	Splice	WF1	I-4	IVS4+1G>A	Splice	[13]
WS	missense	5461	E-5	c.505G>A	E169K	[9]
WS	nonsense	EE31	E-5	c.580C>T	Q194X	[8]
WS	missense	Family 56	E-5	c.631G>A	D211N	[1]
WS	missense	641	E-5	c.631G>A	D211N	[1]
WS	missense	WF5	E-5	c.631G>A	D211N	[13]
WS	deletion	10	E-5	c.532_537del6	K178_A179del	[14]
WS	deletion	13076	E-5	c.599delT	L200fs286X	[12]
WS	deletion	13070	E-5	c.599delT	L200fs286X	[12]
WS	missense		E-5	c.530G>C	R177P	[15]
WS	nonsense	2	E-6	c.670C>T	Q224X	[7]
WS	nonsense	13062	E-6	c.676C>T	Q226X	[12]
WS	deletion	WS10	E-6	c.639_642delGGCG	A214fsX285	[10]
WS	Splice	Family WS10	I-7	IVS7+1G>A	Splice	[6]
WS	nonsense	7944	E-8	c.817G>T	E273X	[9]
WS	nonsense	4815	E-8	c.817G>T	E273X	[9]
WS	nonsense	WS21	E-8	c.873C>A	Y291X	[4]
WS	nonsense	Family WS7	E-8	c.873C>A	Y291X	[6]
WS	Missense	7944	E-8	c.874C>T	P292S	[9]
WS	missense	5461	E-8	c.887T>G	I296S	[9]

APPENDIX 1. REPORTED MUTATIONS IN WFS1 GENE (continued)

Disease	Type	Patient ID	Location	Description	aa change	Reference
WS	nonsense	Family J	E-8	c.906C>A	Y302X	[9]
WS	missense	EE33	E-8	c.937C>T	H313Y	[8]
WS	missense	MORL10	E-8	c.968A>G	H323R	[1]
WS	missense	WS11	E-8	c.1037C>T	P346L	[10] ^d
WS	nonsense	13885	E-8	c.1096C>T	Q366X	[12]
WS	nonsense	13073	E-8	c.1096C>T	Q366X	[12]
WS	nonsense	WS3	E-8	c.1096C>T	Q366X	[10]
WS	nonsense		E-8	c.1096C>T	Q366X	[16]
WS	nonsense	14	E-8	c.1112G.A	W371X	[14]
WS	nonsense	Family WS4	E-8	c.1113G>A	W371X	[6]
WS	Nonsense	2	E-8	c.1113G.A	W371X	[17]
WS	Missense	WS11	E-8	c.1280T>G	I427S	[10]
WS	Missense	Family E	E-8	c.1309G>C	G437R	[9]
WS	Missense	Family 4	E-8	c.1328G>T	S443I	[18]
WS	Missense	Family WS8	E-8	c.1371G>T	R457S	[6]
WS	Nonsense	Family H	E-8	c.1433G>A	W478X	[9]
WS	Nonsense	Family F	E-8	c.1433G>A	W478X	[9]
WS	Nonsense	5514	E-8	c.1433G>A	W478X	[9]
WS	Nonsense	3	E-8	c.1456C>T	Q486X	[14]
WS	Missense	Family WS-5	E-8	c.1511C>T	P504L	[19]
WS	Missense	Family WS7	E-8	c.1511C>T	P504L	[2] ^b
WS	Missense		E-8	c.1511C>T	P504L	[1]
WS	Missense	Family 9	E-8	c.1511C>T	P504L	[5]
WS	Missense	Family WS11	E-8	c.1511C>T	P504L	[6]
WS	Missense	18	E-8	c.1514G>A	C505Y	[14]
WS	Missense	Family 1	E-8	c.1517T>G	L506R	[5]
WS	Nonsense	13073	E-8	c.1558C>T	Q520X	[12]
WS	Nonsense	Family WS15	E-8	c.1558C>T	Q520X	[2] ^b
WS	Nonsense	Family WS1	E-8	c.1558C>T	Q520X	[6]
WS	Nonsense	WS2	E-8	c.1558C>T	Q520X	[10]
WS	Nonsense	WS6	E-8	c.1558C>T	Q520X	[10]
WS	Nonsense	13	E-8	c.1584C>G	Y528X	[14]
WS	Nonsense	2	E-8	c.1602C>G	Y534X	[14]
WS	Nonsense	W1050	E-8	c.1620G>A	W540X	[1]
WS	Missense	1	E-8	c.1628T>G	L543R	[14]
WS	Missense	EE32	E-8	c.1628T>G	L543R	[8]
WS	Missense	1	E-8	c.1637T>A	V546D	[14]
WS	Missense	19	E-8	c.1637T>A	V546D	[14]
WS	Missense	10	E-8	c.1673G>A	R558H	[14]
WS	missense	Family 3	E-8	c.1673G>A	R558H	[5]
WS	missense	WS9	E-8	c.1673G>A	R558H	[10]
WS	missense	WS8	E-8	c.1672C>T	R558C	[10]
WS	missense	17	E-8	c.1816G>C	V606L	[14]
WS	missense	WF5	E-8	c.180C>G	P607R	[13]
WS	nonsense	Family 6	E-8	c.1838G>A	W613X	[5]

APPENDIX 1. REPORTED MUTATIONS IN WFS1 GENE (continued)

Disease	Type	Patient ID	Location	Description	aa change	Reference
WS	nonsense	Family 56	E-8	c.1839G>A	W613X	[1]
WS	missense		E-8	c.1885C>T	R629W	[20]
WS	missense	Family WS14	E-8	c.1944G>A	R629W	[6]
WS	missense	2	E-8	c.1944G>A	R629W	[17]
WS	nonsense	Family WS-4	E-8	c.1944G>A	W648X	[19]
WS	nonsense	Family D	E-8	c.1944G>A	W648X	[9]
WS	nonsense	Family WS15	E-8	c.1980C>G	Y660X	[6]
WS	nonsense	Family T	E-8	c.1999C>T	Q667X	[9]
WS	nonsense		E-8	c.1999C>T	Q667X	[3]
WS	nonsense	WS7	E-8	c.1999C>T	Q667X	[10]
WS	nonsense	Family H	E-8	c.2002C>T	Q668X	[9]
WS	missense	13076	E-8	c.2006A>G	Y669C	[12]
WS	missense	Family 3	E-8	c.2051C>T	A684V	[18] ^a
WS	missense	Family 81	E-8	c.2051C>T	A684V	[1]
WS	missense	5461	E-8	c.2068T>C	C690R	[9]
WS	missense	Family WS-4	E-8	c.2084G>T	G695V	[19]
WS	missense	3328	E-8	c.2100G>T	W700C	[9]
WS	missense	Family 4	E-8	c.2100G>T	W700C	[5]
WS	nonsense	Family 5	E-8	c.2099G>A	W700X	[6]
WS	missense		E-8	c.2149G>A	E717K	[1]
WS	missense	Family WS-3	E-8	c.2171C>T	P724L	[19]
WS	missense	Family J	E-8	c.2206G>A	G736S	[9]
WS	missense	Family WS6	E-8	c.2206G>A	G736S	[6]
WS	missense	WS25	E-8	c.2206G>C	G736R	[4] ^b
WS	nonsense	3328	E-8	c.2254G>T	E752X	[9]
WS	nonsense	1519	E-8	c.254G>T	E752X	[9]
WS	nonsense	Family 4	E-8	c.254G>T	E752X	[5]
WS	missense	Family 2	E-8	c.2327A>T	E776V	[5]
WS	missense	Family WS19	E-8	c.2338G>C	G780R	[2]
WS	missense	19	E-8	c.2378G>C	R793P	[14]
WS	missense	Family WS4	E-8	c.2452C>T	R818C	[2]
WS	missense	Family 8	E-8	c.2452C>T	R818C	[5] ^c
WS	nonsense	13062	E-8	c.2455C>T	Q819X	[12]
WS	missense	WS3	E-8	c.2513C>T	P838L	[10]
WS	missense	Family 52	E-8	c.2578C>G	H860D	[5]
WS	nonsense	Family 3	E-8	c.2590G>T	E864X	[5]
WS	missense	Family 148	E-8	c.2590G>A	E864K	[21]
WS	nonsense	Family WS13	E-8	c.2601G>A	W867X	[6]
WS	missense	MORL11	E-8	c.2602CC>G	R868G	[1]
WS	missense	1709	E-8	c.2654C>T	P885L	[9]
WS	deletion	Family 9	E-8	c.862–1357del1254	delexon8	[5]
WS	deletion	WS5	E-8	c.877delC	L293fsX303	[10]
WS	deletion	Family WS5	E-8	c.1046–1048delTCT	F350del	[2]

APPENDIX 1. REPORTED MUTATIONS IN WFS1 GENE (continued)

Disease	Type	Patient ID	Location	Description	aa change	Reference
WS	deletion		E-8	c.1052–1055delACCT	Y351fsX356	[1]
WS	deletion	5514	E-8	c.1060_1062delTTC	F354del	[9]
WS	deletion	Family WS17	E-8	c.1060_1062delTTC	F354del	[2]
WS	deletion	WS8	E-8	c.1060_1062delTTC	F345del	[10]
WS	deletion	Family 2	E-8	c.1230_1233delCTCT	V412fsX440	[18] ^a
WS	deletion	Family 3	E-8	c.1230_1233delCTCT	V412fsX440	[18] ^a
WS	deletion	15	E-8	c.1230_1233delCTCT	V412fsX440	[14]
WS	deletion	WF4	E-8	c.1230_1233delCTCT	V412fsX440	[13]
WS	deletion	Family WS16	E-8	c.1230_1233delCTCT	V412fsX440	[6]
WS	deletion	MORL12	E-8	c.1230_1233delCTCT	V412fsX440	[1]
WS	deletion	Family WS7	E-8	c.1232_1233delCT	S411fsX541	[6]
WS	deletion		E-8	c.1240_1242delTTC	F414del	[1]
WS	deletion	Family WS6	E-8	c.1240_1242delTTC	F414del	[6]
WS	deletion	Family S	E-8	c.1243_1245delGTC	V415del	[9]
WS	deletion	Family 1	E-8	c.1243_1245delGTC	V415del	[5]
WS	deletion	Family 15	E-8	c.1243_1245delGTC	V415del	[6]
WS	deletion	EE35	E-8	c.1243_1245delGTC	V415del	[8]
WS	deletion	Family 81	E-8	c.1243_1245delGTC	V415del	[1]
WS	deletion		E-8		F417del	[22]
WS	deletion	Family 1	E-8	c.1362_1377del16	Y454X	[18] ^b
WS	deletion	Family 5	E-8	c.1362_1377del16	Y454X	[18] ^b
WS	deletion	4	E-8	c.1362_1377del16	Y454X	[14]
WS	deletion	5	E-8	c.1362_1377del16	Y454X	[14]
WS	deletion	6	E-8	c.1362_1377del16	Y454X	[14]
WS	deletion	7	E-8	c.1362_1377del16	Y454X	[14]
WS	deletion	8	E-8	c.1362_1377del16	Y454X	[14]
WS	deletion	9	E-8	c.1362_1377del16	Y454X	[14]
WS	deletion	11	E-8	c.1362_1377del16	Y454X	[14]

APPENDIX 1. REPORTED MUTATIONS IN WFS1 GENE (continued)

Disease	Type	Patient ID	Lo- cation	Description	aa change	Refe- rence
WS	deletion	14	E-8	c.1362_1377del16	Y454X Y454_L459del	[14]
WS	deletion		E-8	c.1362_1377del16	_fsX454	[23]
WS	deletion	5516	E-8	c.1380_1388del9	V461_V463del	[12]
WS	deletion	Family WS14	E-8	c.1401_1403delGCT	L468del	[6]
WS	deletion	WS4	E-8	c.1507_1529del13nt	V503fsX517	[10]
WS	deletion	15	E-8	c.1546_1548delTTC	F516del	[14]
WS	deletion	WF3	E-8	c.1522_1536del15	Y508_L512del	[13]
WS	deletion	WF4	E-8	c.1522_1536del15	Y508_L512del	[13]
WS	deletion		E-8	c.1522_1523delTA	Y508fsX421	[24]
WS	deletion	13781	E-8	c.1523_1524delAT	Y508fsX541	[12]
WS	deletion	3	E-8	c.1523_1524delAT	Y508fsX541	[14]
WS	deletion	WF6	E-8	c.1525_1537del13	Y509fsX517	[13]
WS	deletion	Family D	E-8	c.1549delC	R517fsX521	[9]
WS	deletion	Family W	E-8	c.1549delC	R517fsX521 del538_542fsX	[9]
WS	deletion		E-8	c.1611_1624del14	537	[9]
WS	deletion	18	E-8	c.1620_1622delGTG	W540del	[14]
WS	deletion	Family WS2	E-8	c.1620_1622delGTG	W540del	[6]
WS	deletion	Family WS3	E-8	c.1698_1703del6	L567_F568del	[6]
WS	deletion	Family E	E-8	c.1699_1704delCTCTTT	L567_F568del	[9]
WS	deletion	Family 17	E-8	c.1775_1776delTG	L592fsX604	[6]
WS	deletion	Ws23	E-8	c.1949_1950delAT	Y650fsX710	[4]
WS	deletion	4	E-8	c.2262_2263delCT	C755fsX757	[7]
WS	deletion	Family I	E-8	c.2433delA c.2638_2643delGACTT	S812fs861X	[9]
WS	deletion	Family 2	E-8	C	D880_F881del	[25]
WS	deletion	Family WS-1	E-8	c.2642_2643delTC	F883fsX938	[19]
WS	deletion	Family 5	E-8	c.2642_2643delTC	F883fsX938	[5]
WS	deletion	ER76	E-8	c.2646_2649delTTTC	F993fsX950	[8]

APPENDIX 1. REPORTED MUTATIONS IN WFS1 GENE (continued)

Disease	Type	Patient ID	Location	Description	aa change	Reference
WS	deletion	Family T	E-8	c.2648_2651delTC TT	F883fsX950	[9]
WS	deletion	Family W	E-8	c.2648_2651delTC TT	F883fsX950	[9]
WS	deletion	3328	E-8	c.2648_2651delTC TT	F883fsX950	[9]
WS	deletion	1945	E-8	c.2648_2651delTC TT	F883fsX950	[9]
WS	deletion		E-8	c.2648_2651delTC TT	F883fsX950	[26]
WS	deletion	Family 5	E-8	c.2648_2651delTC TT	F883fsX950	[6]
WS	deletion	EE34	E-8	c.2649delC	F883fsX951	[8]
WS	deletion	WS7	E-8	c.2649delC	F884fsX951	[10], 57
WS	insertion	ER76	E-8	c.937- 941dupCACTG	L315fsX360	[8]
WS	insertion	1	E-8	c.1029insC	344fsX395	[17]
WS	insertion	Family 8	E-8	c.1032_1033ins9	344_345insAFF	[5] ^c
WS	insertion		E-8	c.1032_1033ins9	344_345insAFF	[27]
WS	insertion	Family 1	E-8	c.1038_1039insC c.1109_1110insAA	L347fsX396	[25]
WS	insertion		E-8	GGC c.1440_1441insCT	A371fsX443	[28]
WS	insertion	Family WS-6	E-8	GAAGG	L481fsX544	[19]
WS	insertion	4815	E-8	c.1504_1505ins24	ins8aa	[9]
WS	insertion	WF2	E-8	c.1581_1582insC	Y528fsX542	[13]
WS	insertion	WS2	E-8	c.1813_1814insA	S605fsX711 N721_M722dup8	[10]
WS	insertion	12131	E-8	c.2164_2165dup24	aa N721_M722dup8	[12] ^a
WS	insertion	16	E-8	c.2164_2165dup24	aa	[14]
WS	insertion	Family WS11	E-8	c.2224_2225insT	C742fsX758	[6]
WS	insertion	Family 2	E-8	c.2315_2316insT	Y773fsX776	[25]
WS	insertion	16	E-8	c.2504_2505insC	K836fsX939	[14]
WS	missense	LIB1	E-8	c.1552C>G	T416S	[11]
WS	missense	LIB1	E-8	c.2694C>T	L842F	[11]
WS	missense	LIB13	E-8	c.1752T>G	Y528D	[11]
WS	frameshift	LIB7	E-8	c.2106del8	F646fsX708	[11]
WS	missense	LIB12	E-8	c.2238T>G	C690G	[11]
WS	missense	LIB14	E-8	c.2289G>A	V707I	[11]
WS	frameshift	LIB2	E-8	c.2819delC c.2637_2639delAT	F884fsX951	[11]
WS	deletion	LIB6	E-8	C	I823del	[11]
WS	frameshift		E-8	c.2716_2717ins22	T857fs946X	[11]
WS	frameshift		E-8	c.1354del16	P451fsX515	[15]

APPENDIX 1. REPORTED MUTATIONS IN WFS1 GENE (continued)

Disease	Type	Patient ID	Location	Description	aa change	Reference
WS	deletion	Family WS9	E-8	c.1661_1687del27	L554_G562 del	[6]
Type2 diabetes	missense	CM000448	E-8		R653C	[29]
Type1 diabetes	missense	CM000447	E-8		H611R	[29]
Type1 diabetes	missense	CM000449	E-8		I720V	[29]
Type1 diabetes	missense	CM000446	E-8		R456H	[29]
Suicide	missense		E-8	c.977C>T	A326V	[30]
Suicide	missense		E-8	c.1181A>T	E394V	[30]
Suicide	missense		E-8	c.1495C>T	L499F	[30]
Suicide	frameshift		E-8	c.1522–1523delTA	Y508fsX421	[24]
Suicide	missense		E-8	c.1597C>T	P533S	[30]
Suicide	missense		E-8	c.1964A>G	E655G	[30]
Suicide	missense		E-8	c.2012C>T	A671V	[30]
Suicide	missense		E-8	c.2053C>T	R685C	[30]
Schizoph., M. depres.	missense		E-8	c.1294C>G	L432V	[31], [30]
Schizoph., Bipolar	missense		E-8	c.2452C>T	R818C	[31], [2], [30]
Schizoph.	missense		E-8	c.935T>G	M312R	[31]
Schizoph.	missense		E-8	c.1554G>A	M518I	[31]
Schizoph.	missense		E-8	c.1672C>T	R558C	[31]
Schizoph.	missense		E-8	c.2312A>G	D771G	[31]
Schizoph.	missense		E-8	c.2314C>T	R772C	[31]
Schizoph.	missense		E-8	c.2356G>A	G786S	[31]
Schizoph.	missense		E-8	c.2596G>A	D866N	[31]
Major Depression	missense		E-8	c.1277G>A	C426Y	[31]
Major Depression	missense		E-8	c.1756G>A	A586T	[31]
Major Depression	missense		E-8	c.2149G>A	E717K	[31]
LFSNHL	missense		E-5	c.482G>A	R161Q	[32]
LFSNHL	missense	MP16	E-5	c.577A>C	K193Q	[33]
LFSNHL	missense	MORL6	E-5	c.577A>C	K193Q	[1]
LFSNHL	missense	MORL3	E-8	c.1371G>T	R457S	[1]
LFSNHL	missense	MORL7	E-8	c.1554G>A	M518I	[1]
LFSNHL	missense	MORL4	E-8	c.1669C>T	L557F	[1]
LFSNHL	missense	MORL8	E-8	c.1805C>T	A602V	[1]
LFSNHL	missense	Family #1	E-8	c.1846G>T	A616S	[34]
LFSNHL	missense	MORL5	E-8	c.1871T>C	V624A	[1]
LFSNHL	missense		E-8	c.1901A>C	K634T	[35]
LFSNHL	missense		E-8	c.2005T>C	Y669H	[36]
LFSNHL	missense	Family Dutch III	E-8	c.2021G>A	G674E	[33]

APPENDIX 1. REPORTED MUTATIONS IN WFS1 GENE (CONTINUED)

Disease	Type	Patient ID	Location	Description	aa change	Reference
LFSNHL	Missense	Family Dutch IV	E-8	c.2021G>T	G674V	[33]
LFSNHL	Missense	Family#69	E-8	c.2033G>T	W678L	[1]
LFSNHL	Missense	Family T	E-8	c.2096C>T	T699M	[37]
LFSNHL	Missense	Family U27	E-8	c.2096C>T	T699M	[33]
LFSNHL	Missense		E-8	c.2096C>T	T699M	[32]
LFSNHL	Missense	Family MR	E-8	c.2115G>C	K705N	[38]
LFSNHL	Missense	Family W	E-8	c.2146G>A	A716T	[37]
LFSNHL	Missense	Family#35	E-8	c.2146G>A	A716T	[37]
LFSNHL	Missense	Family C	E-8	c.2146G>A	A716T	[39]
LFSNHL	Missense	MORL9	E-8	c.2146G>A	A716T	[1]
LFSNHL	Missense	Family#70	E-8	c.2146G>A	A716T	[1]
LFSNHL	Missense	Family#1	E-8	c.2146G>A	A716T	[40]
LFSNHL	Missense		E-8	c.2209G>A	E737K	[34]
LFSNHL	Missense		E-8	c.2311G>C	D771H	[41]
LFSNHL	Missense	Family#21	E-8	c.2335G>A	V779M	[37]
LFSNHL	Missense	Family M	E-8	c.2419A>C	S807R	[33]
LFSNHL	Missense	Family#59	E-8	c.2486T>C	L829P	[37]
LFSNHL	Missense	MORL1	E-8	c.2486T>C	L829P	[1]
LFSNHL	Missense	MORL2	E-8	c.2486T>C	L829P	[1]
LFSNHL	Missense	Family#19	E-8	c.2492G>A	G831D	[37]
LFSNHL	Missense	Family #4150	E-8	c.2492G>A	G831D	[33]
LFSNHL	Missense	TMDU#34	E-8	c.2530G>A	A844T	[42]
LFSNHL	Missense		E-8	c.2576G>C	R859P	[41]
LFSNHL	Missense		E-8	c.2576G>A	R859Q	[43]
LFSNHL	Missense	Family #2	E-8	c.2590G>A	E864K	[40]
LFSNHL	Missense	Family #3	E-8	c.2590G>A	E864K	[40]
LFSNHL	Missense	Family # 3	E-8	c.2596G>A	D866N	[34]
LFSNHL	Deletion	Family A	E-8	c.2300_2302delTCA	Idel767	[33]
LFSNHL	Missense		E-8	c.2054G>C	R685P	[44]
Bipolar Affective disorder	Missense		E-8	c.1321G>A	V441M	[31]
	Missense	CM993371	E-8		A559T	[45]

^a: Described as probable neutral changes. However, since they are absent in the control chromosomes and they affect the conserved amino acid, it is possible that it represents a mutation rather than polymorphisms.

^b: Originally described as G736A.

^c: Described as mutation in a family with homozygous 344insAFF mutation.

^d: Manuscript lists nucleotide numbering as 1067

APPENDIX 1. REPORTED MUTATIONS IN WFS1 GENE (CONTINUED)

REFERENCES FOR APPENDIX 1

1. Lesperance, M.M. 2008. WFS1 Gene Mutation and Polymorphism Database. Available from: http://www.khri.med.umich.edu/research/lesperance_lab/low_freq.php.
2. Gomez-Zaera, M., Strom, T.M., Rodriguez, B., Estivill, X., Meitinger, T., and Nunes, V. 2001. Presence of a major WFS1 mutation in Spanish Wolfram syndrome pedigrees. *Mol Genet Metab* 72(1): 72–81.
3. Pennings, R.J., Huygen, P.L., van den Ouweland, J.M., Cryns, K., Dikkeschei, L.D., Van Camp, G., and Cremers, C.W. 2004. Sex-related hearing impairment in Wolfram syndrome patients identified by inactivating WFS1 mutations. *Audiol Neurotol* 9(1): 51–62.
4. Domenech, E., Gomez-Zaera, M., and Nunes, V. 2004. Study of the WFS1 gene and mitochondrial DNA in Spanish Wolfram syndrome families. *Clin Genet* 65(6): 463–469.
5. Smith, C.J., Crock, P.A., King, B.R., Meldrum, C.J., and Scott, R.J. 2004. Phenotype-genotype correlations in a series of wolfram syndrome families. *Diabetes Care* 27(8): 2003–2009.
6. Giuliano, F., Bannwarth, S., Monnot, S., Cano, A., Chabrol, B., Vialettes, B., Delobel, B., and Paquis-Flucklinger, V. 2005. Wolfram syndrome in French population: characterization of novel mutations and polymorphisms in the WFS1 gene. *Hum Mutat* 25(1): 99–100.
7. Khanim, F., Kirk, J., Latif, F., and Barrett, T.G. 2001. WFS1/wolframin mutations, Wolfram syndrome, and associated diseases. *Hum Mutat* 17(5): 357–367.
8. Hansen, L., Eiberg, H., Barrett, T., Bek, T., Kjaersgaard, P., Tranebjærg, L., and Rosenberg, T. 2005. Mutation analysis of the WFS1 gene in seven Danish Wolfram syndrome families; four new mutations identified. *Eur J Hum Genet* 13(12): 1275–1284.
9. Hardy, C., Khanim, F., Torres, R., Scott-Brown, M., Seller, A., Poulton, J., Collier, D., Kirk, J., Polymeropoulos, M., Latif, F., and Barrett, T. 1999. Clinical and molecular genetic analysis of 19 Wolfram syndrome kindreds demonstrating a wide spectrum of mutations in WFS1. *Am J Hum Genet* 65(5): 1279–1290.
10. Cano, A., Rouzier, C., Monnot, S., Chabrol, B., Conrath, J., Lecomte, P., Delobel, B., Boileau, P., Valero, R., Procaccio, V., Paquis-Flucklinger, V., and Vialettes, B. 2007. Identification of novel mutations in WFS1 and genotype-phenotype correlation in Wolfram syndrome. *Am J Med Genet A* 143A(14): 1605–1612.
11. Zalloua, P.A., Azar, S.T., Delepine, M., Makhoul, N.J., Blanc, H., Sanyoura, M., Lavergne, A., Stankov, K., Lemainque, A., Baz, P., and Julier, C. 2008. WFS1 mutations are frequent monogenic causes of juvenile-onset diabetes mellitus in Lebanon. *Hum Mol Genet*.
12. Strom, T.M., Hortnagel, K., Hofmann, S., Gekeler, F., Scharfe, C., Rabl, W., Gerbitz, K.D., and Meitinger, T. 1998. Diabetes insipidus, diabetes mellitus, optic atrophy and deafness (DIDMOAD) caused by mutations in a novel gene (wolframin) coding for a predicted transmembrane protein. *Hum Mol Genet* 7(13): 2021–2028.

APPENDIX 1. REPORTED MUTATIONS IN WFS1 GENE (CONTINUED)

13. van den Ouweland, J.M., Cryns, K., Pennings, R.J., Walraven, I., Janssen, G.M., Maassen, J.A., Veldhuijzen, B.F., Arntzenius, A.B., Lindhout, D., Cremers, C.W., Van Camp, G., and Dikkeschei, L.D. 2003. Molecular characterization of WFS1 in patients with Wolfram syndrome. *J Mol Diagn* 5(2): 88–95.
14. Colosimo, A., Guida, V., Rigoli, L., Di Bella, C., De Luca, A., Briuglia, S., Stuppia, L., Salpietro, D.C., and Dallapiccola, B. 2003. Molecular detection of novel WFS1 mutations in patients with Wolfram syndrome by a DHPLC-based assay. *Hum Mutat* 21(6): 622–629.
15. Zenteno, J.C., Ruiz, G., Perez-Cano, H.J., and Camargo, M. 2008. Familial Wolfram syndrome due to compound heterozygosity for two novel WFS1 mutations. *Mol Vis* 14: 1353–1357.
16. Flipsen-ten Berg, K., van Hasselt, P.M., Eleveld, M.J., van der Wijst, S.E., Hol, F.A., de Vroede, M.A., Beemer, F.A., Hochstenbach, P.F., and Poot, M. 2007. Unmasking of a hemizygous WFS1 gene mutation by a chromosome 4p deletion of 8.3 Mb in a patient with Wolf-Hirschhorn syndrome. *Eur J Hum Genet* 15(11): 1132–1138.
17. Hofmann, S., Philbrook, C., Gerbitz, K.D., and Bauer, M.F. 2003. Wolfram syndrome: structural and functional analyses of mutant and wild-type wolframin, the WFS1 gene product. *Hum Mol Genet* 12(16): 2003–2012.
18. Tessa, A., Carbone, I., Matteoli, M.C., Bruno, C., Patrono, C., Patera, I.P., De Luca, F., Lorini, R., and Santorelli, F.M. 2001. Identification of novel WFS1 mutations in Italian children with Wolfram syndrome. *Hum Mutat* 17(4): 348–349.
19. Inoue, H., Tanizawa, Y., Wasson, J., Behn, P., Kalidas, K., Bernal-Mizrachi, E., Mueckler, M., Marshall, H., Donis-Keller, H., Crock, P., Rogers, D., Mikuni, M., Kumashiro, H., Higashi, K., Sobue, G., Oka, Y., and Permutt, M.A. 1998. A gene encoding a transmembrane protein is mutated in patients with diabetes mellitus and optic atrophy (Wolfram syndrome). *Nat Genet* 20(2): 143–148.
20. Kadayifci, A., Kepekci, Y., Coskun, Y., and Huang, Y. 2001. Wolfram syndrome in a family with variable expression. *Acta Medica (Hradec Kralove)* 44(3): 115–118.
21. Eiberg, H., Hansen, L., Kjer, B., Hansen, T., Pedersen, O., Bille, M., Rosenberg, T., and Tranebjaerg, L. 2006. Autosomal dominant optic atrophy associated with hearing impairment and impaired glucose regulation caused by a missense mutation in the WFS1 gene. *J Med Genet* 43(5): 435–440.
22. Fang, Q.C., Jia, W.P., Zhang, R., Li, Q., Hu, C., Shao, X.Y., Chai, H.Q., Lu, H.J., and Xiang, K.S. 2005. [A novel mutation of WFS1 gene in Chinese patients with Wolfram syndrome]. *Zhonghua Yi Xue Za Zhi* 85(35): 2468–2471.
23. Lombardo, F., Chiurazzi, P., Hortnagel, K., Arrigo, T., Valenzise, M., Meitinger, T., Messina, M.F., Salzano, G., Barberi, I., and De Luca, F. 2005. Clinical picture, evolution and peculiar molecular findings in a very large pedigree with Wolfram syndrome. *J Pediatr Endocrinol Metab* 18(12): 1391–1397.
24. Aluclu, M.U., Bahceci, M., Tuzcu, A., Arkan, S., and Gokalp, D. 2006. A new mutation in WFS1 gene (C.1522–1523delTA, Y508fsX421) may be responsible for early appearance of clinical features of Wolfram syndrome and suicidal behaviour. *Neuro Endocrinol Lett* 27(6): 691–694.
25. Eller, P., Foger, B., Gander, R., Sauper, T., Lechleitner, M., Finkenstedt, G., and Patsch, J.R. 2001. Wolfram syndrome: a clinical and molecular genetic analysis. *J Med Genet* 38(11): E37.

APPENDIX 1. REPORTED MUTATIONS IN WFS1 GENE (CONTINUED)

26. Sam, W., Qin, H., Crawford, B., Yue, D., and Yu, S. 2001. Homozygosity for a 4-bp deletion in a patient with Wolfram syndrome suggesting possible phenotype and genotype correlation. *Clin Genet* 59(2): 136–138.
27. Inukai, K., Awata, T., Inoue, K., Kurihara, S., Nakashima, Y., Watanabe, M., Sawa, T., Takata, N., and Katayama, S. 2005. Identification of a novel WFS1 mutation (AFF344–345ins) in Japanese patients with Wolfram syndrome. *Diabetes Res Clin Pract* 69(2): 136–141.
28. Nakamura, A., Shimizu, C., Nagai, S., Taniguchi, S., Umetsu, M., Atsumi, T., Wada, N., Yoshioka, N., Ono, Y., Tanizawa, Y., and Koike, T. 2006. A novel mutation of WFS1 gene in a Japanese man of Wolfram syndrome with positive diabetes-related antibodies. *Diabetes Res Clin Pract* 73(2): 215–217.
29. Awata, T., Inoue, K., Kurihara, S., Ohkubo, T., Inoue, I., Abe, T., Takino, H., Kanazawa, Y., and Katayama, S. 2000. Missense variations of the gene responsible for Wolfram syndrome (WFS1/wolframin) in Japanese: possible contribution of the Arg456His mutation to type 1 diabetes as a nonautoimmune genetic basis. *Biochem Biophys Res Commun* 268(2): 612–616.
30. Crawford, J., Zielinski, M.A., Fisher, L.J., Sutherland, G.R., and Goldney, R.D. 2002. Is there a relationship between Wolfram syndrome carrier status and suicide? *Am J Med Genet* 114(3): 343–346.
31. Torres, R., Leroy, E., Hu, X., Katrivanou, A., Gourzis, P., Papachatzopoulou, A., Athanassiadou, A., Beratis, S., Collier, D., and Polymeropoulos, M.H. 2001. Mutation screening of the Wolfram syndrome gene in psychiatric patients. *Mol Psychiatry* 6(1): 39–43.
32. Tranebjaerg, L., Hansen, L., Bille, M., Eiberg, H., Fagerheim, T., Munk-Nielsen, L., Sanggaard, K., Thyssen, F., and Parving, A., Low frequency hearing impairment due to GJB2 and WFS1 mutations shows unrecognized genetic heterogeneity, in *Molecular Biology of Hearing & Deafness*. 2004: Bethesda, MD.
33. Cryns, K., Pfister, M., Pennings, R.J., Bom, S.J., Flothmann, K., Caethoven, G., Kremer, H., Schattelman, I., Koln, K.A., Toth, T., Kupka, S., Blin, N., Nurnberg, P., Thiele, H., van de Heyning, P.H., Reardon, W., Stephens, D., Cremers, C.W., Smith, R.J., and Van Camp, G. 2002. Mutations in the WFS1 gene that cause low-frequency sensorineural hearing loss are small non-inactivating mutations. *Hum Genet* 110(5): 389–394.
34. Liu, Y.H., Ke, X.M., and Xiao, S.F. 2005. [Heterogenous mutations of Wolfram syndrome I gene responsible for low frequency nonsyndromic hearing loss]. *Zhonghua Er Bi Yan Hou Tou Jing Wai Ke Za Zhi* 40(10): 764–768.
35. Komatsu, K., Nakamura, N., Ghadami, M., Matsumoto, N., Kishino, T., Ohta, T., Niikawa, N., and Yoshiura, K. 2002. Confirmation of genetic homogeneity of nonsyndromic low-frequency sensorineural hearing loss by linkage analysis and a DFNA6/14 mutation in a Japanese family. *J Hum Genet* 47(8): 395–399.
36. Tsai, H.T., Wang, Y.P., Chung, S.F., Lin, H.C., Ho, G.M., and Shu, M.T. 2007. A novel mutation in the WFS1 gene identified in a Taiwanese family with low-frequency hearing impairment. *BMC Med Genet* 8: 26.
37. Bespalova, I.N., Van Camp, G., Bom, S.J., Brown, D.J., Cryns, K., DeWan, A.T., Erson, A.E., Flothmann, K., Kunst, H.P., Kurnool, P., Sivakumaran, T.A., Cremers, C.W., Leal, S.M., Burmeister, M., and Lesperance, M.M. 2001. Mutations in the Wolfram syndrome 1 gene (WFS1) are a common cause of low frequency sensorineural hearing loss. *Hum Mol Genet* 10(22): 2501–2508.

APPENDIX 1. REPORTED MUTATIONS IN WFS1 GENE (CONTINUED)

38. Kunz, J., Marquez-Klaka, B., Uebe, S., Volz-Peters, A., Berger, R., and Rausch, P. 2003. Identification of a novel mutation in WFS1 in a family affected by low-frequency hearing impairment. *Mutat Res* 525(1–2): 121–124.
39. Young, T.L., Ives, E., Lynch, E., Person, R., Snook, S., MacLaren, L., Cater, T., Griffin, A., Fernandez, B., Lee, M.K., and King, M.C. 2001. Non-syndromic progressive hearing loss DFNA38 is caused by heterozygous missense mutation in the Wolfram syndrome gene WFS1. *Hum Mol Genet* 10(22): 2509–2514.
40. Fukuoka, H., Kanda, Y., Ohta, S., and Usami, S. 2007. Mutations in the WFS1 gene are a frequent cause of autosomal dominant nonsyndromic low-frequency hearing loss in Japanese. *J Hum Genet* 52(6): 510–515.
41. Gurtler, N., Kim, Y., Mhatre, A., Schlegel, C., Mathis, A., Daniels, R., Shelton, C., and Lalwani, A.K. 2005. Two families with nonsyndromic low-frequency hearing loss harbor novel mutations in Wolfram syndrome gene 1. *J Mol Med* 83(7): 553–560.
42. Noguchi, Y., Yashima, T., Hatanaka, A., Uzawa, M., Yasunami, M., Kimura, A., and Kitamura, K. 2005. A mutation in Wolfram syndrome type 1 gene in a Japanese family with autosomal dominant low-frequency sensorineural hearing loss. *Acta Otolaryngol* 125(11): 1189–1194.
43. Hildebrand, M.S., Sorensen, J.L., Jensen, M., Kimberling, W.J., and Smith, R.J. 2008. Autoimmune disease in a DFNA6/14/38 family carrying a novel missense mutation in WFS1. *Am J Med Genet A* 146A(17): 2258–2265.
44. Bramhall, N.F., Kallman, J.C., Verrall, A.M., and Street, V.A. 2008. A novel WFS1 mutation in a family with dominant low frequency sensorineural hearing loss with normal VEMP and EcochG findings. *BMC Med Genet* 9: 48.
45. Furlong, R.A., Ho, L.W., Rubinsztein, J.S., Michael, A., Walsh, C., Paykel, E.S., and Rubinsztein, D.C. 1999. A rare coding variant within the wolframin gene in bipolar and unipolar affective disorder cases. *Neurosci Lett* 277(2): 123–126.

APPENDIX 2

METABOLIC PARAMETERS OF HOMOZYGOUS WFS1-DEFICIENT MICE

The data represents homozygous Wfs1-deficient mice on F2 and F5 generation C57BL/6 backcrossed genetic background (del2exon-F2xB6 and del2exon-F5xB6, respectively) from Ishihara *et al.* (2004) (study A), and pancreas-specific homozygous Wfs1-deficient mice on 129SvJ genetic background (del8exon-129SvJ) from Riggs *et al.* (2005) (study B).

Phenotype	State	Strain	Age (weeks)	Study
Non-fasting blood glucose	High	del2exon-F2xB6	36	A
Non-fasting blood glucose	Normal	del2exon-F5xB6	36	A
Glucose tolerance	Impaired	del2exon-F5xB6	17	A
Fasting (6h) plasma insulin	Normal	del2exon-F5xB6	17	A
Non-fasting plasma insulin	Normal	del2exon-F5xB6	24	A
Non-fasting plasma insulin	50% lower	del2exon-F5xB6	36	A
Sensitivity to i.p. insulin	High	del2exon-F5xB6	19	A
Islet number	50% lower	del2exon-F5xB6	14–17	A
Insulin content per islet	16% lower	del2exon-F5xB6	14–17	A
Glucose: islet insulin secretion	23% lower	del2exon-F5xB6	14–17	A
Carbachol: islet insulin secretion	26% lower	del2exon-F5xB6	14–17	A
Glucose: β -cell cytosolic Ca ²⁺	36% lower	del2exon-F5xB6	14–17	A
Pancreas insulin content	30% lower	del2exon-F5xB6	2	A
Pancreas insulin content	60% lower	del2exon-F5xB6	36	A
insulin-positive area : pancreas	Mild decrease	del2exon-F5xB6	8	A
insulin-positive area : pancreas	Marked decrease	del2exon-F5xB6	36	A
insulin-positive area : pancreas	Gross decrease	del2exon-F2xB6	24	A
glucagon-positive area : pancreas	Marked increase	del2exon-F5xB6	36	A
glucagon-positive area : pancreas	Marked increase	del2exon-F2xB6	24	A
Pancreatic glucagon content	2.4-fold increase	del2exon-F5xB6	36	A
TUNEL-positive cells in pancreas	Normal	del2exon-F5xB6		A
activated-caspase 3-positive cells in pancreas	Normal	del2exon-F5xB6		A
islet DNA-fragmentation after 3 days of 5 mM glucose	Normal	del2exon-F5xB6		A

APPENDIX 2. METABOLIC PARAMETERS OF HOMOZYGOUS WFS1-DEFICIENT MICE (CONTINUED)

Phenotype	State	Strain	Age (weeks)	Study
islet DNA-fragmentation after 3 days of 25 mM glucose	1.6-fold higher	del2exon-F5xB6		A
islet DNA-fragmentation after tunicamycin (2 µg/mL)	2.2-fold higher	del2exon-F5xB6		A
islet DNA-fragmentation after thapsigargin (2 µM)	2.4-fold higher	del2exon-F5xB6		A
islet DNA-fragmentation after TNF- alfa IFN-gamma	Normal	del2exon-F5xB6		A
Body weight	Low	del8exon-129SvJ	24	B
Fasting blood glucose	Normal	del8exon-129SvJ	24	B
Fasting plasma insulin	Normal	del8exon-129SvJ	24	B
Fasting glucose:insulin ratio	High	del8exon-129SvJ	12	B
Non-fasting blood glucose	High	del8exon-129SvJ	24	B
Non-fasting plasma insulin	Low	del8exon-129SvJ	12	B
Non-fasting glucose:insulin ratio	High	del8exon-129SvJ	12	B
Glucose tolerance	Mild impairment	del8exon-129SvJ	12	B
Glucose tolerance	Significant impairment	del8exon-129SvJ	16	B
Plasma insulin after i.p glucose	2-fold lower	del8exon-129SvJ	12	B
Islet architecture	Disrupted	del8exon-129SvJ	12	B
Pancreas weight	Normal	del8exon-129SvJ	24	B
Beta-cell: pancreas ratio	Low	del8exon-129SvJ	24	B
Beta-cell mass	Low	del8exon-129SvJ	24	B
activated-caspase 3-positive cells in pancreas	2.5-fold higher	del8exon-129SvJ	24	B
BRDU-positive cells in pancreas	Normal	del8exon-129SvJ	24	B
Hspa5 (BiP) expression	High	del8exon-129SvJ	24	B
Ddit3 expression	Insignif. higher	del8exon-129SvJ	24	B

APPENDIX 3

TABLE OF ABBREVIATIONS USED IN FIGURES 9–14

3	oculomotor nucleus	GI	granular insular cortex
4V	fourth ventricle	HDB	horizontal diagonal band
7	facial nucleus	I	intercalated nuclei of amygdala
ac	anterior commissure	IC	inferior colliculus
AcbC	nucleus accumbens core	ILL	intermediate nucleus of lateral lemniscus
AcbSh	nucleus accumbens shell	Ins	insular cortex
AI	agranular insular cortex	IPAC	interstitial nucleus of posterior limb of anterior commissure
alv	alveus	LaDL	lateral nucleus of amygdala, dorsolateral
AP	area postrema	LaVL	lateral nucleus of amygdala, ventrolateral
APir	amygdalopiriform transition area	LEnt	lateral entorhinal cortex
AStr	amygdalostratial transition area	LGP	lateral globus pallidus
Au	auditory cortex	LH	lateral hypothalamus
AVC	anteroventral cochlear nucleus	LSD	dorsal nucleus of lateral septum
AVPe	anteroventral periventricular hypothalamic nucleus	LSO	lateral superior olive
BLA	basolateral amygdaloid nucleus	LSt	lateral stripe of striatum
BLP	basolateral amygdaloid nucleus, posterior	LVe	lateral vestibular nucleus
BSA	bovine serum albumin	M	motor cortex
BSTIA	intraamygdaloid division of bed nucleus of stria terminalis	MCPO	magnocellular preoptic nucleus
BSTLD	dorsal part of lateral bed nucleus of stria terminalis	Med	medial cerebellar nucleus
BSTLP	lateral nucleus of bed nucleus of stria terminalis, posterior	MGP	medial globus pallidus
BSTS	supracapsular part of bed nucleus of stria terminalis	Mo5	motor trigeminal nucleus
BSTSL	supracapsular part of bed nucleus of stria terminalis, lateral	MVe	medial vestibular nucleus
CA1	CA1 field of hippocampus	MVeMC	medial vestibular nucleus, mediocaudal
CeA	central nucleus of amygdala	MZ	marginal zone
CeC	central nucleus of amygdala, capsular division	opt	optic nerve
CeL	central nucleus of amygdala, lateral division	Orb	orbital cortex
CeM	central nucleus of amygdala, medial division	PaS	parasubiculum
CeMPV	central nucleus of amygdala, medial posteroventral division	Pe	periventricular hypothalamic nucleus
Cg	cingulate cortex	PFC	prefrontal cortex
CIC	central nucleus of inferior colliculus	Pir	piriform cortex
CPu	caudate putamen	PLCo	posterolateral cortical amygdaloid nucleus
CxA	cortex amygdala transition zone	PnO	pontine reticular nucleus, oral
dhc	dorsal hippocampal commissure	POR	postrhinal cortex
DMC	dorsomedial hypothalamic nucleus, compact part	Pr5	principal trigeminal nucleus
Ect	entorhinal cortex	Prh	perirhinal cortex
fi	fimbria	PVLM	lateral magnocellular division of paraventricular hypothalamic nucleus
FrA	frontal association cortex	PVMM	medial magnocellular division of paraventricular hypothalamic nucleus
		Py	pyramidal layer of CA1
		RPO	rostral periolivary region

RTh	reticular thalamic nucleus	SolDM	nucleus of the solitary tract, dorsomedial
S1	primary somatosensory cortex	SolM	nucleus of the solitary tract, medial
S2	secondary somatosensory cortex	SON	supraoptic nucleus
SCO	subcommissural organ	SPO	superior paraolivary nucleus
SGI	superficial glial layer of cochlear nucleus	st	stria terminalis
SLEAc	sublenticular extended amygdala, central	Tu	olfactory tubercle
SNC	substantia nigra, compact	VCP	ventral cochlear nucleus, posterior
SNR	substantia nigra, reticular	VLL	ventral nucleus of lateral lemniscus
SolC	nucleus of the solitary tract, central	VmArc	ventromedial arcuate nucleus
		VP	ventral pallidum
		VTA	ventral tegmental area

SUMMARY IN ESTONIAN

Wfs1 valgu levik kesknärvisüsteemis ja selle mõju käitumisele

Sissejuhatus

Nii inimestel kui paljudel teistel loomadel on emotsioonide tajumine oluliseks kohanemiskäitumise osaks. Emotsioonid annavad meist väljaspool toimuvatele sündmustele hinnangu, mille tulemusena tekib organismi valmisolek nendele reageerimiseks. Pea kõik psühhiaatrilised häired on seotud häiretega emotsionaalses käitumises, millega kaasnevad kohanemisraskused argieluga. Emotsionaalse käitumise geneetiliste tegurite uurimine on viimastel aastakümnetel muutunud suureks uurimisvaldkonnaks, mis peamiselt loomkatsete abil püüab tuvastada geene, mida saaks rakendada psühhiaatriliste häirete ravimisihtmärkideks. Osaliselt tänu käesoleva töö tulemustele on üheks uueks kandidaadiks Wfs1 (Wolfram syndrome locus 1) geen, mis on oma nime saanud seoses ühe päriliku haigusega. Wolfram'i sündroomi (edaspidi WS) kirjeldasid esmakordselt Wolfram ja Wagener (1938). WS'i esinemissagedus üldpopulatsioonis on hinnanguliselt 1/770 000 inimese kohta (Barrett, Bunday jt., 1995). Suhkrudiabeet ja nägemise halvenemine ilmnevad patsientidel esimesel elukümnenndil, millele võivad teisel kümnendil lisanduda magediabeet ja kuulmislangus (Barrett, Bunday jt., 1995; Hansen, Eiberg jt., 2005). WS haigetel on leitud hulgaliselt muid sümptomeid, mistõttu seda haigust nimetatakse kliiniliselt pleiomorfseks (mitmetahulise ja kohati varieeruva kliinilise pildiga haigus). Swift, Perkins jt. (1991) on näidanud, et veerandil Wolfram'i sündroomiga patsientidest esineb raskeid psühhiaatrilisi sümptomeid. Haiged surevad keskmiselt 30 aasta vanustena neuroloogiliste või kusetrakti komplikatsioonide tõttu (Barrett, Bunday jt., 1995; Kinsley, Swift jt., 1995). Hoolimata WS'i väikesest esinemissagedusest on Wfs1 mutatsioonide mõju potentsiaalselt oluline ka üldpopulatsiooni mastaabis, kuna Wfs1 mutatsioonide kandjaid (inimesi, kellel on ainult üks Wfs1 alleel mutantne) on hinnanguliselt umbes 1% ja neil on märgatavalt suurem risk sattuda haiglasse psühhiaatriliste häirete tõttu (Swift ja Swift, 2005). Wfs1 valgu funktsioon molekulaarsel tasandil ei ole veel täpselt selge. Praeguseks hetkeks on teada, et tema puudumine põhjustab (1) glükoosi poolt stimuleeritud insuliini vabanemise vähenemist pankrease beetarakkudest (Ishihara, Takeda jt., 2004), (2) suurendab beetarakkude suremust programmeeritud rakusurma (apoptoosi) vahendusel (Riggs, Bernal-Mizrachi jt., 2005; Yamada, Ishihara jt., 2006), (3) vähendab kaltsiumiioonide kontsentratsiooni endoplasmaatilises retiikulumis (Takei, Ishihara jt., 2006) ja (4) suurendab endoplasmaatilise retiikulumi stressi peegeldavate markergeenide ekspressiooni (Riggs, Bernal-Mizrachi jt., 2005; Yamada, Ishihara jt., 2006).

Eesmärgid

1. Emotsionaalse käitumise regulatsiooniga seotud kandidaatgeenide tuvastamine rottidel kassi lõhna poolt tekitatud hirmureaktsiooni mudelis (uurimus 1).
2. Wfs1 valgu (üks tuvastatud kandidaatidest) leviku kirjeldamine hiire ajus (uurimus 2).
3. Wfs1 valgu puudulikkusega hiireliini loomine ja nende käitumusliku fenotüübi iseloomustamine (uurimused 2 ja 3).

Katseloomad ja meetodid

Kasutati isaseid Wistar liini rotte (uurimus 1) ning C57BL/6 ja 129S6/SvEvTac segataustaga Wfs1-puudulikkusega hiiri (uurimused 2 ja 3) ja nende metsik-tüüpi pesakonnakaaslasid.

cDNA subtraktiivne hübridisatsioon

Emotsionaalse käitumise regulatsiooniga seotud geenid tuvastati rottide oimugast (sisaldas mandelkeha kompleksi) cDNA subtraktiivse hübridisatsiooni meetodil (cDNA RDA). Kassilõhnale eksponeeritud (tester) ja mitte-eksponeeritud rottide (driver) ajukoest eraldati RNA, millest sünteesiti cDNA. Mõlemad cDNA populatsioonid fragmenteeriti DpnI restriktasiga ja saadud fragmentidele ligeeriti erineva järjestusega adapterid. Adapteritega fragmendid denatueeriti ja driver ning tester cDNA populatsioonid hübridiseeriti omavahel. Seejärel viidi läbi polümeraasi ahelreaktsioon (PCR) tester populatsiooni spetsiifiliste praimeritega, et võimendada tester populatsioonis ülesindatud cDNA fragmente. Saadud produktid kloonieeriti, sekveneeriti ning tuvastati DNA joondamisalgoritmi NIX abil.

Wfs1-beetagalaktosidaas liitvalku ekspresseerivate hiirte loomine

Hiire genoomsest klonoteegist (genoomi katvate DNA fragmentide kogu) otsiti üles Wfs1 geeni sisaldav kloon ja subkloneeriti sealt DNA fragment, mis sisaldab introneid 6–7 ja eksoneid 7–8. Selle fragmendi sees asendati 8-ndat eksonit kodeeriv osa bakteriaalset beeta-galaktosidaasi kodeeriva DNA fragmendiga. Saadud DNA-konstruktile lisati positiivset ja negatiivset selektsiooni võimaldavad kodeerivad järjestused. Saadud DNA-konstrukt elektroporeeriti hiire embrüonaalsetesse tüvirakkudesse rakuliinist W4. Homoloogilise rekombinatsiooni tulemusena muutusid mõned nendest rakkudest heterosügootseteks Wfs1-lookuses, kuna ühel kromosoomil oli Wfs1 geeni 8 ekson asendunud

beetagalaktosidaasi kodeeriva DNA-järjestusega. Sellised rakud tuvastati kasutades Wfs1 geeni 8. eksoni-spetsiifilist polümeraasi ahelreaktsiooni (PCR) ja PCR-produkti sekveneerimist. Heterosügootne rakukloon paljundati ja süstiti normaalsesse blastotsüsti staadiumis embrüotesse (umbes 8-rakuline embrüo). Sündinud kimäärsed hiired (hiired, kelle koed sisaldasid lisaks normaalse genoomiga rakkudele erineval määral mutantse Wfs1 geeniga rakke) ristati normaalsete hiirtega ja nende järglastel tuvastati mutatsiooni edasikandumine Wfs1 8. eksoni-spetsiifilise PCR reaktsiooniga. Nii tuvastatud heterosügootsete hiirte ristamisel saadi homosügootsed hiired, kellel olid mõlemad Wfs1 geeni alleelid mutantsed (st. sisaldasid Wfs1 8-nda eksoni asemel beetagalaktosidaasi kodeerivat järjestust). Kokku kasutati käesoleva töö läbiviimiseks 21 hiirt, kellest 9 olid homosügootsed Wfs1-beetagalaktosidaas hiired, 2 heterosügootsed Wfs1-beetagalaktosidaas hiired ja 10 normaalsed hiired. Kõik loomadega läbiviidud protseduurid olid kooskõlas EÜ direktiiviga 86/609/EEC ja nende läbiviimiseks oli olemas Põllumajandusministeeriumi loomkatse komisjoni luba (nr. 39, 7 oktoober 2005).

Wfs1 antikeha loomine

Hiire Wfs1 valgu vastane antikeha loodi jänestest, keda immuniseeriti peptiidiga, mis vastab Wfs1 valgu viimasele 13-le aminohappele. Immuniseeriti 4 korra kahekuuliste intervallidega, 10 päeva pärast viimast immuniseerimist võeti jänestelt verd ja eraldati vere seerum, mida kasutati Wfs1 valgu värvimiseks hiire kudedel.

Kudede töötlemine ja värvimine

Homosügootsete Wfs1-beetagalaktosidaasi ekspresseerivate hiirteaju lõigud värviti X-Gal meetodil. Beetagalaktosidaasi ensümaatilise aktiivsuse toimel muutub värvusetu X-Gal ühend sinist värvi ühendiks, mis sadeneb koelõikudel beetagalaktosidaasi sisaldavatesse piirkondadesse. Nii saab sellistel hiirtel markeerida Wfs1 valgu ekspressioonimustrit. Normaalsetel hiirtel värviti Wfs1 valk spetsiifilise antikehaga, mis selle külge seostub. Antikeha külge seoti omakorda sekundaarne antikeha, mis oli liidetud fluorestseeruva värviga ning muutis reaktsiooni tulemused mikroskoobis jälgitavaks.

Peamised tulemused

Esimeses uurimuses tuvastasime mitmete närviülekandega seotud geenide ülekspressiooni rottide mandelkehas vastusena kassi lõhna poolt tekitatud hirmureaktsioonile. Üheks hirmureaktsiooni tulemusena ülekspresseerunud geeniks oli Wfs1, millele keskendusid edasised uurimused. Wfs1 antikeha

värving hiire aju ja X-Gal värving beeta-galaktosidaas reportergeeni ekspresseerivatel hiirtel tuvastasid Wfs1 valgu ekspressiooni spetsiifilistes anatoomilistes piirkondades. Eriti tugev oli Wfs1 ekspressioon mandelkeha tsentraalses tuumas, *nucleus accumbens*'is (naalduv tuum), haisteköbrateses, süngituum laterodorsaalses osas, hipokampuse CA1 piirkonnas, parasubiikulumis, peririnaalkoores, insulaarkoores, prefrontaalkoores jne. Anatoomilis-funktsionaalselt oli Wfs1 ülesindatud aju basaaltuumades, mis osalevad emotsionaalse käitumise regulatsioonis (tsentraalne laiendatud mandelkeha, ventraalne juttkeha, hipokampus), kuulmisega seotud ajuosades (primaarne kuulmiskoor, lateraalne lemniskus, alumine nelikküngastik) ja ajuripatsit innerveerivates hüpotaalamuse struktuurides (paraventrikulaartuum, supraoptiline tuum, *nucleus arcuatus*). Wfs1-puudulikud hiired olid metsiktüüpi hiirtega võrreldes väiksema keha-kaaluga ja neil oli vähenenud tolerantsus glükoosile. Kuni neljandik Wfs1-puudulikkusega hiirtest tõi kuuldavale siutsumise-laadseid häälotsusi, mis väibusid pärast diasepaami manustamist. Käitumise analüüs ei tuvastanud märgatavaid motoorika ja sensoorse tundlikkuse häireid. Reeglina ilmnes normist erinev käitumine stressirikastes olukordades (intensiivne valgus, sotsiaalne isolatsioon, süstimine). Suurenenud ärevuselaadne käitumine ilmnes Wfs1-puudulikkusega hiirtel hüponeofaagia testis, intensiivse valgustusega uudistamistestis (*motility box*) ja pime-valge testis pärast sotsiaalset isolatsiooni. Lisaks ilmnes nendel hiirtel suurenenud analgeesia pärast elektrišokke ja kolm korda suurem plasma kortikosterooni kontsentratsioon pärast süstimist ja käsitlemist eksperimentaatori poolt. Stressivabas situatsioonis oli Wfs1-puudulikkusega hiirte vere plasma kortikosterooni kontsentratsioon normaalne. Diasepaami keskmine annus omas pluss-puuri Wfs1-puudulikele hiirtele anksiolüütilist toimet, kuid mitte metsiktüüpi hiirtele. Mesolimbilise dopamiinisüsteemi farmakoloogiline uurimine tuvastas amfetamiini nõrgenenud mõju motoorika aktivatsioonile ja suurenenud tundlikkuse apomorfiinile.

Järeldused

1. Kassi lõhna poolt põhjustatud hirmureaktsiooniga kaasneb rottidel Wfs1 mRNA ekspressiooni suurenemine mandelkehas. Lisaks oli suurenenud mitmete närviülekandega ja rakusisese signaaliülekandega seotud geenide ekspressioon (kaarboksüpeptidaas E, türosiin 3-monooksügenaasi aktiveeriv valk, Rho GTPaas, Ca-kalmoduliin-sõltuv kinaas jt.).

2. Wfs1 valk on ekspresseerunud spetsiifilistes anatoomilistes struktuurides kõigis suuremates aju osades – ajukoores, hipokampuses, basaaltuumades, hüpotaalamuses, taalamuses, keskajus, väikeajus ja ajutüves. Wfs1 ekspressioon on eriti tugev (1) kohanemiskäitumise regulatsiooniga seotud struktuurides – mandelkeha kompleks, süngituum, naalduv tuum, prefrontaalkoor, hipokampuse CA1 piirkond; (2) kuulmisega seotud struktuurides – alumine nelikküngastik, lateraalne lemniskus, primaarne kuulmiskoor; (3) endokriinfunktsiooni regulat-

siooniga seotud struktuurides – supraoptiline tuum, paraventrikulaartuum, *nucleus arcuatus*; (4) hipokampuse talitlusega seotud ajukoore osad – peririnaalkoor, postrinaalkoor, entorinaalkoor, parasubiikulum. Wfs1 on kõrgelt ekspresseerunud kahes funktsioonaal-anatoomilises makrostruktuuris: laiendatud tsentraalses amügdalas ja ventraalses juttkehas. Wfs1 ekspressiooni muster hiire ajus korreleerub kuulmiskahjustuse, magediabeedi ja psühiaatriliste sümptomite esinemisega Wolframi sündroomiga patsientidel.

3. Wfs1 funktsiooni puudumine ei tekita märgatavaid sensoorseid häireid, kuna Wfs1-puudulikel hiirtel on normaalne valutundlikkus, normaalne eristusvõime intensiivselt ja hämaralt valgustatud keskkonna vahel, nad reageerivad 10 kHz helisignaale ja suudavad Morrise veepuuris nähtavate märkide abil teed leida. Samuti on nendel hiirtel normaalselt arenenud motoorsed võimed rota-rod testis, liikumisaktiivsust mõõtvast tests, sundujumistestis ja Morrise veepuuris. Wfs1-puudulikkus põhjustas hiirtel suurenenud ärevuse stressitekitavas keskkonnas, mis väljendus pikenenud söömislatentsina hüponeofaagia testis, väiksema uudistamisaktiivsusega intensiivse valgusega liikumisaktiivsuse testis, ärevuslaadse käitumisena hele-tume puuris pärast lühiajalist sotsiaalset isolatsiooni, kolm korda suurenenud kortikosterooni vastusena pärast süstimist ja käsitlemist, ja diasepaami suurenenud anksiolüütilise toimega plusspuuris. Kuni neljandik Wfs1-puudulikkusega hiirtest tõi kuuldavale spontaanseid hääletsusi, mis vaibusid pärast diasepaami manustamist. Wfs1-puudulikel hiirtel on muutunud mesolimbilise dopamiinisüsteemi tundlikkus. Amfetamiini mootorikat stimuleeriv toime oli keskmises ja suures doosis nõrgem kui metsiktüüpi hiirtel. Sellele vastupidiselt põhjustas apomorfiini manustamine oluliselt suuremat mootorika aktivatsiooni kui metsiktüüpi hiirtel.

ACKNOWLEDGEMENTS

I would like to thank my supervisors Sulev Kõks and Eero Vasar for support and guidance, and peer-reviewers Anti Kalda ja Ursel Soomets for comments on the manuscript. I am grateful to my colleagues at the Department of Physiology for warm and inspiring atmosphere. Most of all, i would like to express deep gratitude to my parents, brothers, Erle and friends for being so wonderful.

ORIGINAL PUBLICATIONS

CURRICULUM VITAE

Hendrik Luuk

Date and place of birth 12.12.1978, Tartu
Citizenship Estonian
Marital status single
Address, phone, e-mail Ravila 19, Biomeedikum, r3090
Tartu 50411
tel 737 4335
hendrik.luuk@ut.ee
Affiliation Department of Physiology, University of Tartu

Education

1986–1997 Miina Härma Grammar School
1997–2002 Psychology, BSc (2002)
2002–2004 Developmental Biology, MSc (2004)
2004–2009 Ph.D. studies in Neuroscience

Career

2003–2004 Department of Physiology, lab assistant
2004–2005 Department of Physiology, referent
2005–2006 Department of Physiology, research fellow
2007–2008 Institute of Technology, University of Tartu, research fellow
2008–2012 Department of Physiology, research fellow

Awards

2008 3rd prize in Estonian Scientific Research Contest for
Ph.D. Students

Practical courses

- Hanseatic Students' Days of Science – video microscopy and fluorescent visualisation of cytoskeleton (Rostock, Germany, 2001)
- Mass spectrometry and 2DGE workshop lead by Curt T. Reimann (Lund, Sweden) (Tartu, Estonia, 2003)
- Behavioral Studies in Drug Discovery (Kuopio, Finland, 2003)
- Competence course on Laboratory Animal Science (Tartu, 2009)

Research

Functional analysis of genes involved in the regulation of emotional behavior. Nine publications have appeared in international peer-review journals.

List of publications

1. **Luuk H**, Plaas M, Raud S, Innos J, Sütt S, Lasner H, Abramov U, Kurrikoff K, Kõks S, Vasar E. 2008. Wfs1-deficient mice display impaired behavioural adaptation in stressful environment. *Behav Brain Res*. 2008 Nov 11. [Epub ahead of print]
2. Philips MA, Vikesaa J, **Luuk H**, Jønson L, Lilleväli K, Rehfeld JF, Vasar E, Kõks S, Nielsen FC. 2008. Characterization of MYG1 gene and protein: subcellular distribution and function. *Biol Cell*. 2008 Nov 18. [Epub ahead of print]
3. Plaas M, Karis A, Innos J, Rebane E, Baekelandt V, Vaarmann A, **Luuk H**, Vasar E, Koks S. 2008. Alpha-synuclein A30P point-mutation generates age-dependent nigrostriatal deficiency in mice. *J Physiol Pharmacol*. 59(2): 205–16.
4. **Luuk H**, Koks S, Plaas M, Hannibal J, Rehfeld JF, Vasar E. 2008. Distribution of Wfs1 protein in the central nervous system of the mouse and its relation to clinical symptoms of the Wolfram syndrome. *J Comp Neurol*. 509(6):642–60.
5. Raud S, Sütt S, Plaas M, **Luuk H**, Innos J, Philips MA, Kõks S, Vasar E. 2007. Cat odor exposure induces distinct changes in the exploratory behavior and Wfs1 gene expression in C57Bl/6 and 129Sv mice. *Neurosci Lett*. 426(2):87–90.
6. Kingo K, Philips MA, Aunin E, **Luuk H**, Karelson M, Rätsep R, Silm H, Vasar E, Kõks S. 2006. MYG1, novel melanocyte related gene, has elevated expression in vitiligo. *J Dermatol Sci*. 44(2):119–22.
7. Kõks S, **Luuk H**, Nelovkov A, Areda T, Vasar E. 2004. A screen for genes induced in the amygdaloid area during cat odor exposure. *Genes Brain Behav*. 3(2):80–9.
8. Rünkorg K, Veraksits A, Kurrikoff K, **Luuk H**, Raud S, Abramov U, Matsui T, Bourin M, Kõks S, Vasar E. 2003. Distinct changes in the behavioural effects of morphine and naloxone in CCK2 receptor-deficient mice. *Behav Brain Res*. 44(1–2):125–35.
9. Kõks S, Planken A, **Luuk H**, Vasar E. 2002. Cat odour exposure increases the expression of wolframin gene in the amygdaloid area of rat. *Neurosci Lett*. 322(2):116–20.

CURRICULUM VITAE

Hendrik Luuk

Sünniaeg ja -koht	12.12.1978, Tartu
Kodakondsus	Eesti
Perekonnaseis	vallaline
Aadress, telefon, e-post	Ravila 19, Biomeedikum, r3090 Tartu 50411 tel 737 4335 hendrik.luuk@ut.ee
Praegune töökoht	TÜ Füsioloogia instituut

Haridus

1986–1997	Miina Härma Gümnaasium
1997–2002	TÜ Sotsiaalteaduskond, psühholoogia eriala, BSc (2002)
2002–2004	TÜ Bioloogia ja Geograafia teaduskond, arengubioloogia eriala, MSc (2004)
2004–2009	TÜ Arstiteaduskond, neuroteaduste doktoriõpe, doktorant

Teenistuskäik

2003–2004	TÜ Füsioloogia instituut, preparaator
2004–2005	TÜ Füsioloogia instituut, referent
2005–2006	TÜ Füsioloogia instituut, erakorraline teadur
2007–2008	TÜ Tehnoloogiainstituut, biotehnoloogia erakorraline teadur
2008–2012	TÜ Füsioloogia instituut, teadur

Tunnustused

2008	Õpilaste teadustööde riiklik konkurss, doktoriõpe 3. auhind
------	---

Erialane enesetäiendus

- Hanseatic Students' Days of Science – video microscopy and fluorescent visualisation of cytoskeleton (Rostock, Germany, 2001)
- Mass spectrometry and 2DGE workshop lead by Curt T. Reimann (Lund, Sweden) (Tartu, Estonia, 2003)
- Behavioral Studies in Drug Discovery (Kuopio, Finland, 2003)
- Katseloomateaduse kursus (Tartu, 2009)

Teadustöö

Emotsionaalse käitumise regulatsiooniga seotud geenide funktsionaalne analüüs. Rahvusvahelise levikuga eelretsenseeritavates väljaannetes on ilmunud 9 publikatsiooni.

Teadustööde loetelu

1. **Luuk H**, Plaas M, Raud S, Innos J, Sütt S, Lasner H, Abramov U, Kurrikoff K, Kõks S, Vasar E. 2008. Wfs1-deficient mice display impaired behavioural adaptation in stressful environment. *Behav Brain Res*. 2008 Nov 11. [Epub ahead of print]
2. Philips MA, Vikesaa J, **Luuk H**, Jønson L, Lilleväli K, Rehfeld JF, Vasar E, Kõks S, Nielsen FC. 2008. Characterization of MYG1 gene and protein: subcellular distribution and function. *Biol Cell*. 2008 Nov 18. [Epub ahead of print]
3. Plaas M, Karis A, Innos J, Rebane E, Baekelandt V, Vaarmann A, **Luuk H**, Vasar E, Koks S. 2008. Alpha-synuclein A30P point-mutation generates age-dependent nigrostriatal deficiency in mice. *J Physiol Pharmacol*. 59(2): 205–16.
4. **Luuk H**, Koks S, Plaas M, Hannibal J, Rehfeld JF, Vasar E. 2008. Distribution of Wfs1 protein in the central nervous system of the mouse and its relation to clinical symptoms of the Wolfram syndrome. *J Comp Neurol*. 509(6):642–60.
5. Raud S, Sütt S, Plaas M, **Luuk H**, Innos J, Philips MA, Kõks S, Vasar E. 2007. Cat odor exposure induces distinct changes in the exploratory behavior and Wfs1 gene expression in C57Bl/6 and 129Sv mice. *Neurosci Lett*. 426(2):87–90.
6. Kingo K, Philips MA, Aunin E, **Luuk H**, Karelson M, Rätsep R, Silm H, Vasar E, Kõks S. 2006. MYG1, novel melanocyte related gene, has elevated expression in vitiligo. *J Dermatol Sci*. 44(2):119–22.
7. Kõks S, **Luuk H**, Nelovkov A, Areda T, Vasar E. 2004. A screen for genes induced in the amygdaloid area during cat odor exposure. *Genes Brain Behav*. 3(2):80–9.
8. Rünkorg K, Veraksits A, Kurrikoff K, **Luuk H**, Raud S, Abramov U, Matsui T, Bourin M, Kõks S, Vasar E. 2003. Distinct changes in the behavioural effects of morphine and naloxone in CCK2 receptor-deficient mice. *Behav Brain Res*. 44(1–2):125–35.
9. Kõks S, Planken A, **Luuk H**, Vasar E. 2002. Cat odour exposure increases the expression of wolframin gene in the amygdaloid area of rat. *Neurosci Lett*. 322(2):116–20.

DISSERTATIONES NEUROSCIENTIAE UNIVERSITATIS TARTUENSIS

1. **Sirli Raud.** Cholecystokinin₂ receptor deficient mice: changes in function of GABA-ergic system. Tartu, 2005.
2. **Kati Koido.** Single-nucleotide polymorphism profiling of 22 candidate genes in mood and anxiety disorders. Tartu, 2005.
3. **Dzhamilja Safiulina.** The studies of mitochondria in cultured cerebellar granule neurons: characterization of mitochondrial function, volume homeostasis and interaction with neurosteroids. Tartu, 2006.
4. **Tarmo Areda.** Behavioural and neurogenetic study of mechanisms related to cat odour induced anxiety in rodents. Tartu, 2006.
5. **Aleksei Nelovkov.** Behavioural and neurogenetic study of molecular mechanisms involved in regulation of exploratory behaviour in rodents. Tartu, 2006.
6. **Annika Vaarmann.** The studies on cystatin B deficient mice: neurochemical and behavioural alterations in animal model of progressive myoclonus epilepsy of Unverricht-Lundborg type. Tartu, 2007.
7. **Urho Abramov.** Sex and environmental factors determine the behavioural phenotype of mice lacking CCK₂ receptors: implications for the behavioural studies in transgenic lines. Tartu, 2008.

